



This is to certify that the

thesis entitled

ALKALI METAL ANIONS AND 'ELECTRIDES' VIA CRYPTANDS AND CROWNS: SOME OPTICAL AND MAGNETIC PROPERTIES

presented by

Michael Garrison DaGue

has been accepted towards fulfillment
of the requirements for
PhD
degree in
Chemistry

Date July 12, 1979

O-7639



OVERDUE FINES ARE 25¢ PER DAY PER ITEM

Return to book drop to remove this checkout from your record.

ALKALI METAL ANIONS AND 'ELECTRIDES' VIA CRYPTANDS AND CROWNS: SOME OPTICAL AND MAGNETIC PROPERTIES

Ву

Michael Garrison DaGue

A DISSERTATION

Submitted to
Michigan State University
in partial fulfillment of the requirements
for the degree of

DOCTOR OF PHILOSOPHY

Department of Chemistry

ABSTRACT

ALKALI METAL ANIONS AND 'ELECTRIDES' VIA CRYPTANDS AND CROWNS: SOME OPTICAL AND MAGNETIC PROPERTIES

Вy

Michael Garrison DaGue

Evaporation of methylamine or ammonia solutions containing alkali metal and a cation-complexing agent (cryptand or crown) results in the formation of blue or gold-colored solids. Some solids have been studied with optical transmission spectroscopy, ESR, and magnetic susceptibility.

Evaporation of these solutions yields thin, solvent-free films for optical study. Methylamine solutions of the well-characterized compound (Na⁺C222)Na⁻ where C222 is N(CH₂CH₂OCH₂CH₂OCH₂CH₂)₃N give films which are gold-colored by reflected light and blue by transmitted light. The spectrum shows absorptions at 15,400 cm⁻¹ (assigned to Na⁻) and 24,500 cm⁻¹ with a high-energy shoulder (18,900 cm⁻¹) on the former peak. Methylamine-potassium-C222 solutions with a metal to complexing agent mole ratio, R, of 2 give film spectra with a peak at 11,900 cm⁻¹ (assigned to K⁻). Similar solutions of rubidium and cesium give peaks at 11,600 cm⁻¹ and 10,500 cm⁻¹, assigned

to Rb and Cs, respectively. The band positions for M in the solvent-free solid films agree well with M band positions in ethylenediamine solution.

Spectra of films formed from R=1 methylamine solutions of potassium and C222 show a single band at 7400 cm $^{-1}$ (assigned to the trapped electron, e_{t}^{-}). This solid may represent a new class of compounds, electrides, in which the balancing charge for the cation is a trapped electron. Spectra of films from K-C222 methylamine solutions with R between 1 and 2 show both K $^{-}$ and e_{t}^{-} bands.

Optical spectra of films from R=0.5 cesium-18-Crown-6 methylamine solutions show only one band at 6500 cm $^{-1}$, assigned to trapped electrons. This solid gives a single ESR line at g=2.0022 with a width of 0.36 G at 214 K. Susceptibility measurements indicate about $(22\pm3)\%$ of the cesium atoms present contribute to the observed paramagnetism.

Films from ammonia solution were also studied. It is generally agreed that the spherically symmetric alkali metal anion, M, does not exist in ammonia. However, absorptions assigned to Na, K, Rb, and Cs are observed optically in solvent-free R=2 films from ammonia solution. In the ammonia solution, there is presumably some uncomplexed metal cation which acts as an efficient electron trap, forming M as ammonia is removed during film formation. By exposing the solvent-free film to ammonia vapor, the solvent-free films were converted to "damp" or "wet" solvent-containing films (depending on the degree of final

ammonia content). The solvent-free film spectrum of $(Na^{\dagger}C222)Na^{\dagger}$ shows the typical Na absorption band and a small e_{t}^{\dagger} peak. The wet film contains only the electron band and no Na band.

Sodium-ammonia solutions were used to form a film consisting of flecks of metal. No absorption bands were seen. The blue film resulting from wetting the metal flecks with ammonia gives an absorption spectrum - a plasma edge - typical of conduction electrons. Several systems studied give dry and/or wet film spectra similar to the plasma edge observed for concentrated metal-ammonia solutions. These include solvent-free and wet films from Li-C211 R=2 and K-C222 R=1 solutions.

The solid (K⁺C222)e⁻ from ammonia shows a single ESR line at g=2.0023 with a linewidth of 0.4 to 0.6 G at 4-5 K, narrowing to 0.1 to 0.4 G at 181 K. The optical spectrum and a single sample microwave conductivity indicate that this solid is metallic. ESR spectra indicate that not over 1% of the total potassium was present as potassium metal.

The properties of these solids indicate the existence of three classes of compounds. The first class consists of salts of the alkali metal anions and is now well established. The second class consists of electride salts, in which the balancing charge for the complexed cation is an electron which is locally trapped. While definitive proof of this assignment is not yet available, it is consistent with all measurements to date. The third

class appears to consist of an expanded metal in which the cation is (K⁺C222). Mixtures of these three classes also appear to exist. The electride salt and expanded metal can occur together and, in some cases, appear to be interconvertible. Electrides and the corresponding expanded metals were first studied in detail in this work. If the assignments are verified, the expanded metal studied is a new example in that class and the electride represents a new class of compounds.

to Beverly

ACKNOWLEDGEMENTS

I am grateful to Professor James Dye for his enthusiasm and guidance during this work. I would like to thank other members, past and present, of Dr. Dye's research group for their many helpful suggestions and discussions. In particular, thanks go to Michael R. Yemen, J. Steven Landers, and Dr. Harlan L. Lewis for their collaborative efforts in these studies. Professors G. T. Babcock, J. A. Cowen, and M. Robert kindly allowed use or time on their laboratory equipment for magnetic studies. The M.S.U. glassblowers, Keki Mistry, Andrew Seer, and Jerry DeGroot, have given excellent service and technical advice.

I am grateful to Professors J. L. Dye and Jean-Marie Lehn for the opportunity to work in the latter's laboratory with Dr. Dye during his 1975-76 sabbatical leave.

My wife and I are grateful to those who made our stay in France pleasant.

I appreciate having received teaching and research assistantships financed by the State of Michigan and the U.S. Government, respectively.

Finally, I thank Beverly B. DaGue and my parents for their encouragement during this work.

TABLE OF CONTENTS

																					Page
LIST C)F FI	GURI	ES.	• •	•	•	•		•	•		•	•	•	•		•	•			vi vii
KEY TO) SEL	LECT	ED S	YMB	JLS	A	ND	AC	CRC	NY	M	S	•	•	•	•	•	•	•	•	х
I.	INTR	RODUC	CTIO	N.	•			•	•	•	ı	•	•		•	•	•	•	•	•	1
			1 - A													•		•	•		2 7
		Meta																			
		Alka Use	of														ıts	•	•	•	16
			lut:													•	•	•	•	•	18
II.	EXPE	ERIMI	ENTA	L.	•	•			•	•		•	•	•	•	•	•	•	•		25
	Α.	Reag	gent	s.	•														•	•	25
		1.	So1	ven	ts	•					,										25
		2.	Met																		27
			Com																		30
			Mis																		31
	В.		ss A																		31
	C.	Grad	sel	ppa.	Ц	ah	Ve	201	11177			• c +	· om	•	•	•	•	•	•	•	32
	D.																				32
			rt A															•	•	•	32
	Ε.	Samp	ole	rre	par	al	101	1 8	HIO	. 1	. 11	Sι	Ιu	me	11 (.aı	L				33
		16	Chn: Gen	lque	· .	•	• •	4	•	•	· ~	•	• •	•	•	•	•	•	•	•	
		1.	Gen	era.	1 1	re	paı	rat	:1ν	e	1	еc	nn	10	lue	•	•	•	•	•	33
		2.	Opt ESR	ica.	1 5	pe	ctı	ra.	•	•	,	•	•	•	•	•	•	•	•	•	38
		3.	ESR	Sai	mp1	.е	Pre	epa	ıra	ti	.01	n	an	d							4.7
		_	I	ıstı	cum	en:	tat	io	n.	. •		•	•	•	•	•	•	•	•	•	43
		4.	Mag	net	ic	Su	sce	ept	it	i1	li	ty	:	F	ar	ac	lay	•			
			Τe	echr	niq	ue	•		•	•	,	•	•	•	•	•	•	•	•	•	44
III.	OPTI	CAL	SPE	CTR	A				,												
	Α.	Fi1r	ns f	rom	Me	th	v 1 a	ami	ine			_	_	_						_	50
			Res	_			-								_			•	Ī	Ī	50
		2.	Dis			-	-			-		-	-	•	٠	•	•	•	•	•	59
	В.		ns f										•	•	•	•	•	•	•	•	64
	υ.	1.										•	•	•	•	•	•	•	•	•	64
		2.	Sod Wet											n	th	· ie	•	•	•	•	04
				bsei		-															69
		3.	Pot																•	•	72
		4.	Rub																•	•	76
		5.	Ces															•	•	٠	79

																	Page
	С.	7.	Cesi Lith ary	ium-	Cry	ptai	nd (2	, 1,	1)	Fi:	1 m s	·		•	•		85
IV.	MAGN	NETIC	STU	DIES	5												
		1. 2. ESR. 1. 2.	Back Resu a. b.	grou ilts (Na [†] Soli Soli Soli Soli Soli	and C22 ds d following the contract of the con	Dis 2) Na from rom ions 	scus: n K-(Cs- scus: Cs- n K-(Ba-(Sio: C22 18C: Sio: 18C	n	=1 =0 ==0 ==1 ==1			iti	on		• • • • • • • • • • • • • • • • • • • •	115
	С.		nary												•	•	115
V.		RMODY K		C ST	TABI	LIT	OF	(N	a [†] C		2)N				•	•	120
VI.	CONC	CLUSI	ONS	AND	SUG	GES	rion	S F	OR	FU'	TUI	RE	WC	RK		•	123
	A. B.	Conc Sugg	lusi gesti	ons.	for	 Fu	 ture	Wo	 rk.	•	•		•	•	•		123 124
RIRIIO	CDAI	риv															126

LIST OF TABLES

Table		Page
1	Peak positions in metal-EDA solutions	9
2	Solvent dependence of the optical band shift of the K monomer from e_{solv}	14
3	Comparison of alkali metal anion peak positions in solid films from methylamine and in metal-EDA solutions	52
4	Summary of peak positions in optical spectra of films	87
5	Temperature-dependent susceptibility of the residue from Cs-18C6 R=0.5 methylamine solutions	101
6	Parameters in fitting of 4.7 K potassium-rich (K+C222)e ESR spectrum	114

LIST OF FIGURES

Figure	•	Page
1	Optical spectra of alkali metal-EDA solutions	8
2	Models for species of stoichiometry M^- . A fourth structure is the spherically symmetric alkali metal anion M^- with an s^2 configuration	13
3	Molecular structure of 18-Crown-6 and cryptand(2,2,2)	17
4	Selectivity and stability of cryptand(2,2,2) complexes with alkali metal cations in 95% methanol	19
5	Structure of (Na ⁺ C222)Na ⁻ based on x-ray study	23
6	Vacuum bottle with sidearm for alkali metal distillation	26
7	Apparatus for distribution of alkali metal under vacuum	29
8	Apparatus for preparation of (Na ⁺ C222)Na ⁻ crystals	34
9	Vacuum tee use	36
10	Apparatus for preparation of films for optical spectroscopy	40
11	Apparatus for preparation of magnetic susceptibility samples	47
12	Spectra of films prepared by evaporation of methylamine solutions which contain M ⁺ C and M ⁻ : from left to right (peak positions) M = Cs, Rb, K, Na, respectively. The arrows indicate the position of the absorption maxima for the corresponding anions in ethylenediamine	51

Figure		Page
	Baseline-corrected normalized spectra of the sodium anion under various conditions: solid line, (Na ⁺ C)Na ⁻ film from methylamine; dashed line, (K ⁺ C)Na ⁻ film from methylamine; dotted line, Na ⁻ in ethylenediamine	53
14	Spectra of films produced by evaporation of methylamine from solutions containing cryptand(2,2,2) and various relative amounts of potassium: spectra of films produced from solutions containing progressively lower concentrations of solvated electrons and higher concentrations of K ⁻ are in the order A,B,C	5.5
	Spectra of films produced by evaporation of methylamine solutions containing cryptand(2,2,2 and various relative amounts of rubidium anions and solvated electrons (solid and dashed lines). The dotted line spectrum is from a film prepared from a sodium borosilicate glass apparatus; the solution presumably contained some Na) 5 0
16	Film spectrum from a methylamine $R=0.5$ solution of Cs and 18C6	58
	Spectra of sodium-C222 films from ammonia. A - dry film, R=2; B - dry film, R=1; C - wet film, R=2. The wet film spectrum with R=1 is essentially the same as C	65
18	Wet film spectra of Na(A) and K(B) obtained by condensing ammonia onto dry metal films produced by evaporation of metal-ammonia solutions	71
19	Spectra of K-C222 films from ammonia with R=2. A - dry film, B - damp film, D - wet film, C - intermediate film	73
20	Spectra of K-C222 films from ammonia with R=1. A - initial dry film, B - dry "annealed" film, C - wet film	74
21	Spectra of Rb-C222 films from ammonia with R=2. A - dry film, B - damp film, C - wet film	77
22	Spectra of Rb-C222 films from ammonia with R=1. A - initial dry film, B - film A after 40 minutes. C - wet film	78

Figure			Page
23	Spectra of Cs-C222 films from ammonia with R=2. A - dry film, B - damp film	•	80
24	Spectra of Cs-C222 films from ammonia with R=2. A - wet film, B - same film 5 minutes after freezing bulk solution, C - 37 minutes after freezing bulk solution	•	81
25	Spectrum of Cs-C222 wet film from ammonia with R=2	•	83
26	Spectra of Cs-C222 and Cs-18C6 dry films. A - Cs-C222 film, R=2, from methylamine; B - Cs-C222 film, R=2, from ammonia; C - Cs-18C6 film, R=0.5, from ammonia	•	84
27	Spectra of lithium-C211 films from ammonia with R=2. A - dry film, B - damp film, C - wet film	•	86
28	General temperature behavior of some dia- magnetic and paramagnetic susceptibilities .		94
29	$1/\chi_M^{corr}$ vs. T for the residue from Cs-18C6 R=0.5 methylamine solutions		100
30	ESR spectra for cryptand-rich (K ⁺ C222)e ⁻ from 4.5 K to 55 K	•	106
31	ESR spectra for cryptand-rich (K ⁺ C222)e ⁻ from 113 to 193 K	•	107
32	ESR spectra for potassium-rich (K ⁺ C222)e ⁻ from 4.7 K to 77 K	•	111
33	ESR spectra for potassium-rich (K ⁺ C222)e ⁻ from 133 to 193 K		112
34	Fitting of the 4.7 K potassium-rich (K ⁺ C222)e ⁻ ESR spectrum with Gaussian-Lorentzian lineshapes	•	113
35	Area under the ESR absorption spectrum vs. 1/T from 4.2 to 77 K for the solid from a Ba-C222 R=1 solution	•	116

SELECTED SYMBOLS AND ACRONYMS

a cation-anion distance (in A)

A Angstroms, 10⁻¹⁰ m

C222 cryptand(2,2,2)

18C6 18-crown-6

ctts charge transfer to solvent

CTTS ctts

EDA ethylenediamine

 e_{solv}^{-} solvated electron

 e_{t}^{-} trapped electron

f_z vertical force

k Boltzmann constant

M alkali metal monomer

M⁺ alkali metal cation

M alkali metal anion

(M⁺C222) a cation, M⁺, complexed by C222

 M^+C (M^+C222)

MAS metal-ammonia solution

MPM mole percent metal

n/V number of electrons per unit volume

R mole ratio of metal to complexing agent

T_F Fermi temperature

THF	tetrahydrofuran
λ	wavelength
$\overline{\nu}$	wavenumber (cm ⁻¹)
х _g	magnetic susceptibility per gram
X _M	magnetic susceptibility per mole
Xv	magnetic susceptibility per unit volume

INTRODUCTION

Alkali metals dissolve to form solutions in ammonia and in some amines and ethers. Research on metal ammonia solutions dates from 1863 (1) and is still very active. Five international conferences have been held on the subject, all with published proceedings (2-6). The dissertation research described here is founded on this old research field and a new field of alkali metal chemistry made possible by the synthesis of efficient alkali metal cation complexing agents.

This section is intended to provide a background to the doctoral research. The background begins with an introduction to metal ammonia solutions (MAS) by considering briefly the nature of MAS, particularly species in solution such as the solvated electron. Species in ammonia solutions then serve as a comparison for models and species in amine and ether metal solutions. Evidence for one of these species, the alkali metal anion (M⁻), will be summarized. The essential role that the synthetic alkali metal cation complexing agents played in opening a new field of chemistry in these metal solutions is described. These agents permitted synthesis of a new class of compounds - salts of the alkali metal anions -

and the properties of the first member of this class are discussed. This leads to a description of doctoral research objectives.

I.A. Metal-Ammonia Solutions

Alkali metals dissolve in ammonia to form blue solutions when dilute, and metallic bronze solutions when concentrated. These solutions can be very concentrated; the saturation concentration (7) is 20 mole per cent metal (MPM) for Li and 16 MPM for Na, K, and Rb. The saturation concentrations show little temperature dependence. However, cesium is miscible with ammonia in all proportions at the melting point of cesium (28.7°C).

The behavior of these solutions can be divided into three categories based on concentration. The dilute solutions ($\frac{1}{2}$ MPM $\frac{1}{2}$.5 M) show electrolytic behavior. The solutions with a concentration greater than about 8 MPM exhibit metallic characteristics. The third concentration range, from about 2 MPM to 8 MPM, is the metal-to-nonmetal transition range. Properties which change during this transition do so smoothly, so the concentrations given above for the three regions are somewhat arbitrary.

In MAS which are $< 2 \cdot 10^{-4}$ MPM ($< 10^{-3}$ M), the major species are the solvated cation and the solvated electron (e_{solv}^{-}) which form as

$$M_{(s)} \rightarrow M^{+} + e_{solv}^{-}$$
 (1)

The solvated electron is thermodynamically unstable and can react with the solvent:

$$e_{solv}^{-} + NH_3 + 1/2H_2 + NH_2^{-}$$
 (2)

However, if the solvent is pure and free of catalysts such as iron, then the solutions are kinetically stable. Very dilute solutions absorb in the near infrared with a peak at 6900 cm⁻¹ (1450 nm). The absorption is asymmetric with a high energy tail extending into the red portion of the spectral region. This tailing portion is responsible for the blue color of the solutions.

The most widely accepted model for the solvated electron is the cavity model as first proposed by Ogg (8) and elaborated quantitatively by Jortner (9). The electron is trapped in a cavity from which one or more ammonia molecules have been excluded. The cavity radius in the simple Jortner model is 3.2-3.4 A. The electron is stablized by orientation of the molecules in the first solvation shell and by long range polarization effects from molecules outside the first solvation shell. Jortner used hydrogenic 1s and 2p variational wavefunctions to account for the optical spectrum as a 1s to 2p transition. Several other experimental values were correctly derived. However, the potential function used was oversimplified and others have tried more complex computations (10).

The properties of these very dilute MAS are independent of the cation. As the concentration increases, the variation with concentration of such properties as optical spectrum, magnetic susceptibility, conductivity, activity coefficient, and density is nearly independent of cation. This suggests that any new species formed retain the essential characteristics of the solvated cation and probably the solvated electron. This hypothesis forms the basis of the ionic aggregation model (11,12). A nonconducting ion-pair formed between M⁺ and e leads to a weak magnetic interaction of the electron with the metal nucleus. This interaction is observed in the paramagnetic shifts in alkali metal NMR spectra (13-14). As the concentration is increased, the model predicts that ion triples such as $e^- \cdot M^+ \cdot e^$ form with electron-electron interactions strong enough to give a singlet ground state. Static susceptibilities (15-16) and ESR spin susceptibilities (17-19) show that the electron spins pair and form diamagnetic states. Presumably, higher aggregates with stoichiometries such as M_2 and M_2 could also form.

As the metal concentration is increased from 3 MPM to 8 MPM, the electrical behavior of the solution changes from electrolytic or nonmetallic to metallic. This metal-to-nonmetal transition is of great interest to physicists. Six theories and hybrids between them to explain the transition have been reviewed by Thompson (80), who commented that "the dominant mechanism [of

the metal-to-nonmetal transition] is not universally acknowledged." For a qualitative picture of the transition, Thompson suggests the following gedanken experiment. An electron is placed in a MAS whose concentration is at the low end of the transition. The electron may spin pair with another electron in a preexisting cavity to form e_2^{-2} , if the dielectron is stable. If not, then the electron must form its own cavity. However, many solvent molecules are already involved in solvating other electrons and cations and may not be readily available for participation in further cavity formation. The added electron may then be forced to enter the conduction band. This last option is dominant at high concentrations in the metal-to-nonmetal transition range.

Metal-ammonia solutions at concentrations higher than 8 MPM exhibit metallic characteristics, qualitatively behaving like liquid metals. For example, the conductivity of the most concentrated MAS is greater than that of liquid mercury. Optical studies of concentrated MAS have been almost exclusively reflectance spectra which show (81) the solvated electron band disappearing between 5.3 and 6.2 MPM, while an absorption edge (plasma edge) due to conduction electrons builds in with increasing concentration. This plasma edge is at about 10,000 cm⁻¹ (1000 nm) when first formed but shifts to the blue at higher concentrations. Other properties of concentrated MAS have been reviewed by Thompson (80).

Gold-colored compounds form upon freezing concentrated MAS of the six metals Li, Ca, Sr, Ba, Eu, and Yb. The compounds have the stoichiometry $M(NH_3)_6$ except Li, which is $Li(NH_3)_4$. The compounds are metallic with the metal's valence electrons contributing to formation of a conduction band. As an example, the conductivity of $Li(NH_3)_4$ is about equal to that of platinum.

Lithium tetrammine is the most studied of these solids. Single crystals have not been obtained and the stoichiometry is slightly variable. The structure seems to be face centered cubic between 82 K and 88 K and hexagonal below 82 K (80). The distance between Li(NH₃)⁺ ions in the face centered cubic form is 7 A. By comparison, the lithium-lithium distance in lithium metal is 3.5 A. The large effective ionic radius makes these compounds low-density metals or, as they are often called, expanded metals. Expanded metals are on the edge of the metal-nonmetal transition and provide experimental tests for metal-nonmetal transition theories.

Except for the very dilute solutions, the nature of the species present in metal-ammonia solutions up to concentrations beginning the nonmetal-to-metal transition is still controversial. In contrast, metal solutions in amines and ethers give specific evidence for three reducing species: the solvated electron (e_{solv}^-) , a species of stoichiometry M, and the alkali metal anion (M^-) .

I.B. Metal Solutions in Amines and Ethers

The alkali metals dissolve in certain amines and ethers to form blue solutions. These solutions differ from MAS in two respects. The amine and ether metal solutions have saturation concentrations much lower than MAS, except for lithium in methylamine. For example, the solubility of sodium in EDA at 25° is only 2.4 · 10^{-3} M (34). Sodium and lithium will not produce blue solutions in the ethers, indicating that their solubility is lower than 10^{-6} M. The second distinguishing characteristic is that amine and ether metal solutions may display both the e_{solv}^- optical absorption band and a second band at higher energies than the e_{solv} band. The position of this higher-energy band depends on the specific dissolved metal (20) as shown in Figure 1 for alkali metals dissolved in ethylenediamine (EDA). The spectrum produced by dissolving Li is that of e_{solv}. The asymmetry and high energy tail mentioned early for e_{solv}^{-} can be clearly seen. This e_{solv}^{-} band appears as a shoulder on the spectra from EDA solutions of K, Rb, and Cs. The sodium solution spectrum clearly does not contain appreciable amounts of esolv. The single peak in the visible region for sodium solutions has been called a V-band, as have the main peaks in the K, Rb, and Cs spectra shown. The esolv band in the near-infrared is sometimes referred to as the R-band. The V-bands have been assigned to spherically symmetric alkali metal

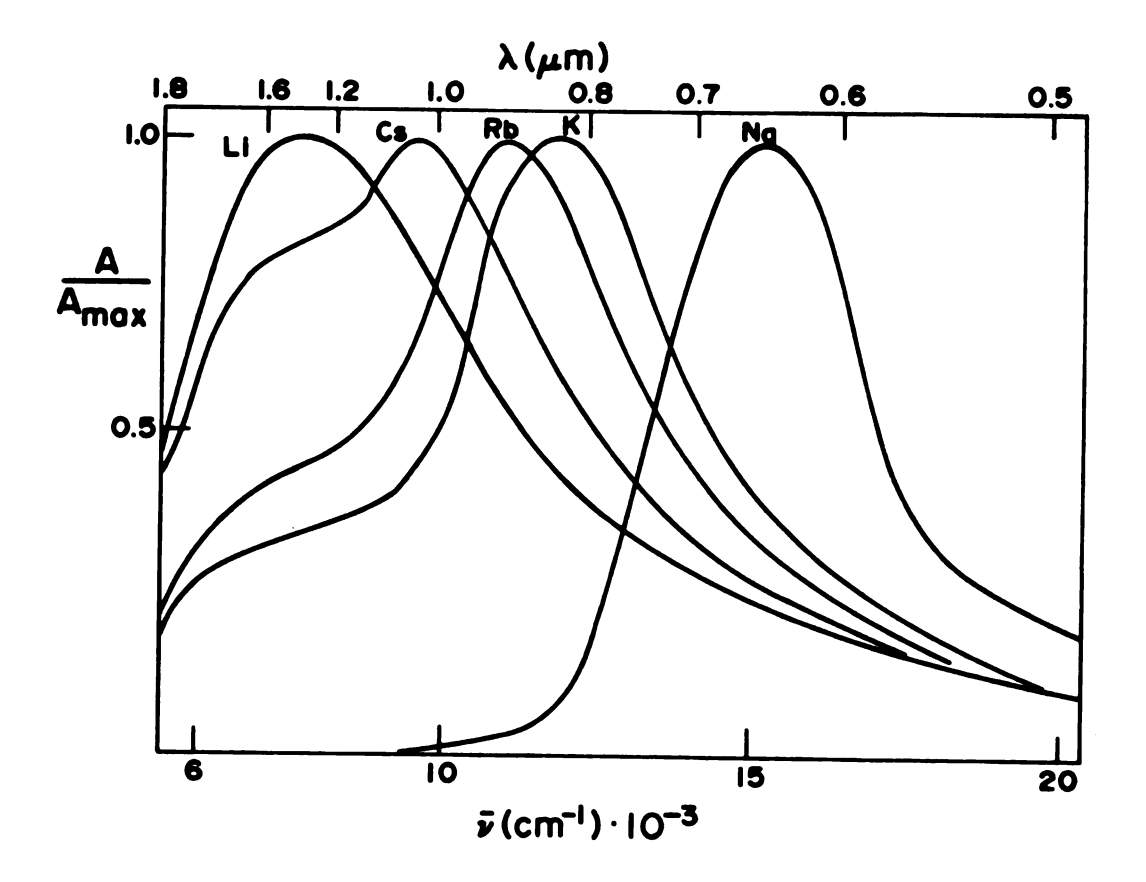


Figure 1. Optical spectra of alkali metal-EDA solutions.

anions, M. Peak positions for metal-EDA solutions are given in Table 1.

Table 1. Peak positions in metal-EDA solutions

Species	Peak Posit	ion (20)
Na -	15,400 cm ⁻¹	650 nm
K ⁻	12,000	833
Rb -	11,200	893
Cs	9,800	1020
e _{solv}	7,810	1280

The ratio of the absorbances of the e_{solv}^- and M bands depends on the solvent and the metal. The ratio decreases, together with metal solubility, along the solvent series: NH₃, HMPA, MeNH₂, EDA, EtNH₂, PrNH₂, ethers where HMPA is hexamethylphosphoryltriamide, $[(CH_3)_2N]_3PO$. For a given solvent, the ratio and solubility decrease from Cs to Na.

The identification of the V-bands as M was accelerated by two papers appearing in 1968 and 1969. In the first paper, Hurley, Tuttle, and Golden (21) clarified the confusion about the number and types of optical bands in metal amine and ether solutions. For K, Rb, and Cs solutions, some workers had reported an R-band, a metal-dependent V-band, and a metal-independent V-band

(also seen with lithium solutions), while other workers observed only the first two of the three bands. Hurley et al. realized that the metal-independent V-band arose from contamination of the solution with sodium by exchange of Li⁺, K⁺, Rb⁺, or Cs⁺ with Na⁺ from the sodium borosilicate glass of the apparatus. Thus, a given metal in solution gives rise to no more than two absorption bands.

In 1969, Matalon, Golden and Ottolenghi (22) suggested that the metal-dependent V-bands were due to the anions Na, K, Rb, and Cs. This suggestion was based on their comparison of the solvent, temperature, and metal dependence of the V-bands with predictions of charge transfer to solvent (CTTS) theory. Several relationships characteristic of a CTTS transition were observed. The absorption maximum shows a marked solvent dependence. The maximum shifts to lower energies with an increase in temperature. A correlation exists between the peak position in a solvent and the temperature coefficient of the peak. The absorption maximum correlates with the size of the anion with a shift to lower energies for larger anions. As predicted by CTTS theory (22), the transition energy minus the atomic electron affinity is a function of the inverse of the anion radius. This agreement of experiment with predictions of CTTS theory does not show that the species has stoichiometry M^- (the spectrum of e_{solv}^- shows most of the above behavior). However, this assignment of the

V-bands to a singlet ground state species M⁻ is consistent with earlier ESR studies (23-25) on solutions showing only V-bands. The ESR studies indicated a diamagnetic species in solution.

Further studies strengthened the hypothesis of a species having stoichiometry M^- . DeBacker and Dye (26) determined the extinction coefficient of the V-band in EDA-sodium solutions. Assuming one sodium in each absorbing unit, they calculated an oscillator strength of 1.9 \pm 0.2. This result required that two equivalent electrons be involved in the species undergoing transition; this is satisfied by the stoichiometry Na $^-$.

The reaction of Na^+ with electrons produced by pulse radiolysis in EDA was studied (27). The reaction followed was

$$Na^+ + 2e_{solv}^- \rightarrow Na^-$$
.

The reaction was second order in e_{solv}^- and dependent on sodium only when $[Na^+] < 0.01 \, \underline{\text{M}}$. The decay of e_{solv}^- and growth of Na $^-$ occurred at the same rate. Other studies indicating M $^-$ as the correct assignment were M $^-$ photolysis (28-33), conductivity (34-35), and the Faraday effect (36).

After the stoichiometry had been established, the structure of M was still unknown. Four possibilities existed: an ion triple between two solvated electrons and the cation, an ion pair between the cation and the dielectron e_2^{-2} (two spin-paired electrons residing in

one cavity), an expanded orbital species in which the two electrons were located on the primary solvation shell molecules for the cation, and a genuine anion, M, where the two electrons were located in a cation s orbital. The first three of these models are shown in Figure 2. Conclusive experimental discrimination between these models depended on use of alkali metal NMR along with the synthetic cation-complexers and will be described shortly.

The solvated cation, anion, and electron are the three major species in metal amine and ether solutions. A fourth species whose relative concentration is low is called the monomer and has stoichiometry M. The monomer is never present at high enough concentrations in static solutions to be observed optically. The observation of ESR hyperfine splitting (37-39) in metal-amine solutions was the first clear indication that species of stoichiometry M exist. When the monomer lifetime is long and electron exchange is slow, the ESR signal shows 2I + 1 hyperfine lines where I is the alkali metal nuclear spin. The hyperfine splitting as measured by the separations in the multiplet is proportional to the average contact density of the electron at the nucleus. The percent atomic character of M is obtained by comparing the splitting to that of the free gaseous atom. percent atomic character can reach nearly 30% for Cs in i-PrNH, (40). The hyperfine splitting is greatly influenced by solvent and temperature.

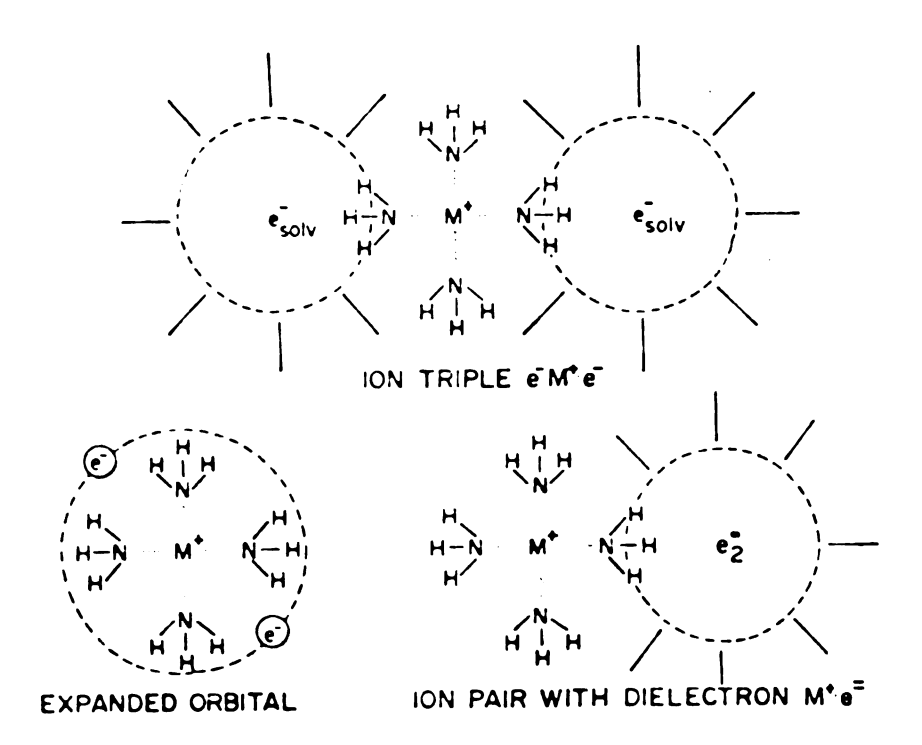


Figure 2. Models for species of stoichiometry M^{-} . A fourth structure is the spherically symmetric alkali metal anion M^{-} with an s^2 configuration.

Optical spectra of the monomer as a transient have been obtained by photolysis of M^- (28,29,31) and by pulsed radiolysis of M^+ (41,42). The monomer band occurs between that of M^- and e^-_{solv} . The shift of the M band from the e^-_{solv} band is solvent dependent and can be as large as 3600 cm⁻¹, as shown in Table 2 for the potassium monomer (42).

Table 2. Solvent dependence of the optical band shift of the K monomer from e_{solv}

Solvent	$\overline{v}_{K} - \overline{v}_{e_{solv}} - (cm^{-1})$
NH ₃	0 to -600
MeNH ₂	0
EtNH ₂	1600
THF	3600

Two models have been proposed for the monomer. In the static or continuum model, there is a single species whose structure depends on temperature. In the dynamic or multistate model, there is a temperature-dependent equilibrium between two (or more) species whose structure is relatively independent of temperature. Pulsed radiolysis techniques have been used to show that the optical spectrum arises from the same monomer species as observed by ESR (82). The optical shift between the

monomer and e_{solv}^- was correlated with the hyperfine splitting observed (83). Pulsed radiolysis (83) also showed two optical bands for the monomer species in THF, dimethoxyethane, diglyme, and triglyme where the latter three are glymes with the general formula $CH_3O(CH_2CH_2O)_nCH_3$ with n = 1, 2, and 3, respectively. The two bands were assigned to two monomer species: one a contact ion pair between M^+ and e_{solv}^- and the other a solvent-shared ion pair. This observation supports the dynamic model with an equilibrium between two species. In better solvents such as the amines, only one optical band is observed and the monomer structure must lie between the extremes of contact and solvent shared ion pair. Here the static model is appropriate; both models are needed for all observed behavior.

Dye has proposed (43) the following equilibrium scheme for metal solutions:

$$2M_{(s)} \stackrel{?}{\neq} M^{+} + M^{-}$$
 (3)

$$M \stackrel{?}{=} M + e_{solv}$$
 (4)

$$M \stackrel{?}{\leftarrow} M^{+} + e_{solv}^{-}$$
 (5)

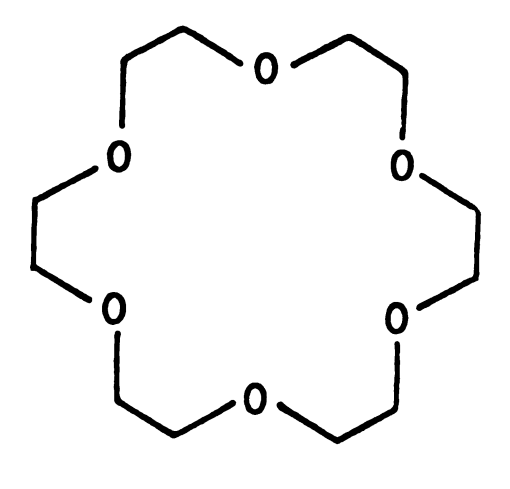
In MeNH₂, EDA, and HMPA, the three species M, M, and e_{solv} may be detected, depending on the metal. In EtNH₂, THF, and the glymes, M predominates and very little M or e^- can be detected. An additional equilibrium will be added when an alkali-metal cation complexer is also in solution.

I.C. Alkali-Metal Cation Complexing Agents

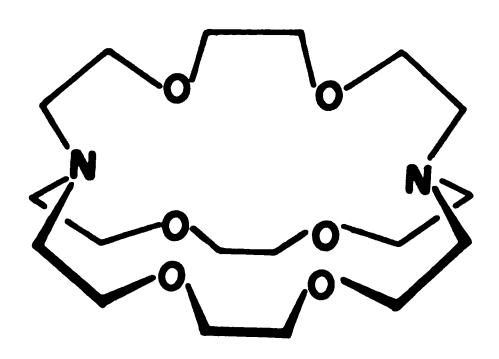
A few complexing agents for the alkali metal cations were known prior to 1967 (45), but it was at that time that Pedersen (44,45) serendipitously synthesized the first of fifty complexers which he called crowns. The compound, 18-Crown-6, or 18C6 (Figure 3), with 18 atoms in the ring and six ether oxygens, was used in this work. (The IUPAC names of these compounds are cumbersome and the trivial nomenclature of Pedersen (45) is now widely used.) In addition to synthesis of these compounds, Pedersen demonstrated (45) selectivity among cations in complex formation for a given crown and the solubilization of salts in solvents in which they would otherwise be insoluble. The crown 18C6 surrounds the cation and usually takes on a planar arrangement. This can be considered two dimensional complexation.

Lehn and co-workers synthesized (46) a series of cation complexing agents which enclose the cation inside a molecular cavity - effecting a three dimensional complexation. These are the well-known complexers, the cryptands. The cryptand(2,2,2), or C222, appears in Figure 3. The IUPAC names for cryptands are even more cumbersome than for crowns. The numbers in the trivial name refer to the number of oxygens in each strand.

The cryptands exhibit very high complexation constants for the alkali metal cations - 10^8 or higher in some cases. Additionally, there is a selectivity among cations by a given cryptand. The selectivity depends



18-Crown-6



Cryptand(2,2,2)

Figure 3. Molecular structure of 18-Crown-6 and cryptand(2,2,2).

largely on the cation size compared to the cryptand cavity size and also on the cation charge. Complexation constants and cation selectivity are shown in Figure 4 for C222, C221, and C211 with alkali metal cations in 95% methanol (88).

The complexation properties of the cryptands constitute a macrobicyclic cryptate effect characterized by high stability, high selectivity, and shielding of the complexed cation from the environment. Kauffmann, Lehn, and Sauvage (47) have found that the cryptate effect is due to enthalpic effects and not entropy effects.

The general impact of macrocyclic ligands and the cryptate effect is too great to be reviewed in detail here. Broad areas of application will be summarized and references can be found in reviews (48-52,97). The cryptate effect has been used 1) to solubilize salts,

2) to break up ion pairs, increasing the anion reactivity or elucidating the cation's role in reaction mechanism,

3) to study cation transport in membranes, 4) to cause anionic polymerization or phase transfer catalysis,

5) to effect separations of isotopes and racemic mixtures, and 6) for possible medical and toxicological

I.D. Use of Complexing Agents in Metal Solutions

applications.

Use of the cryptate effect in metal solution research began when Dye et al. reported in 1970 (53) and 1971 (54)

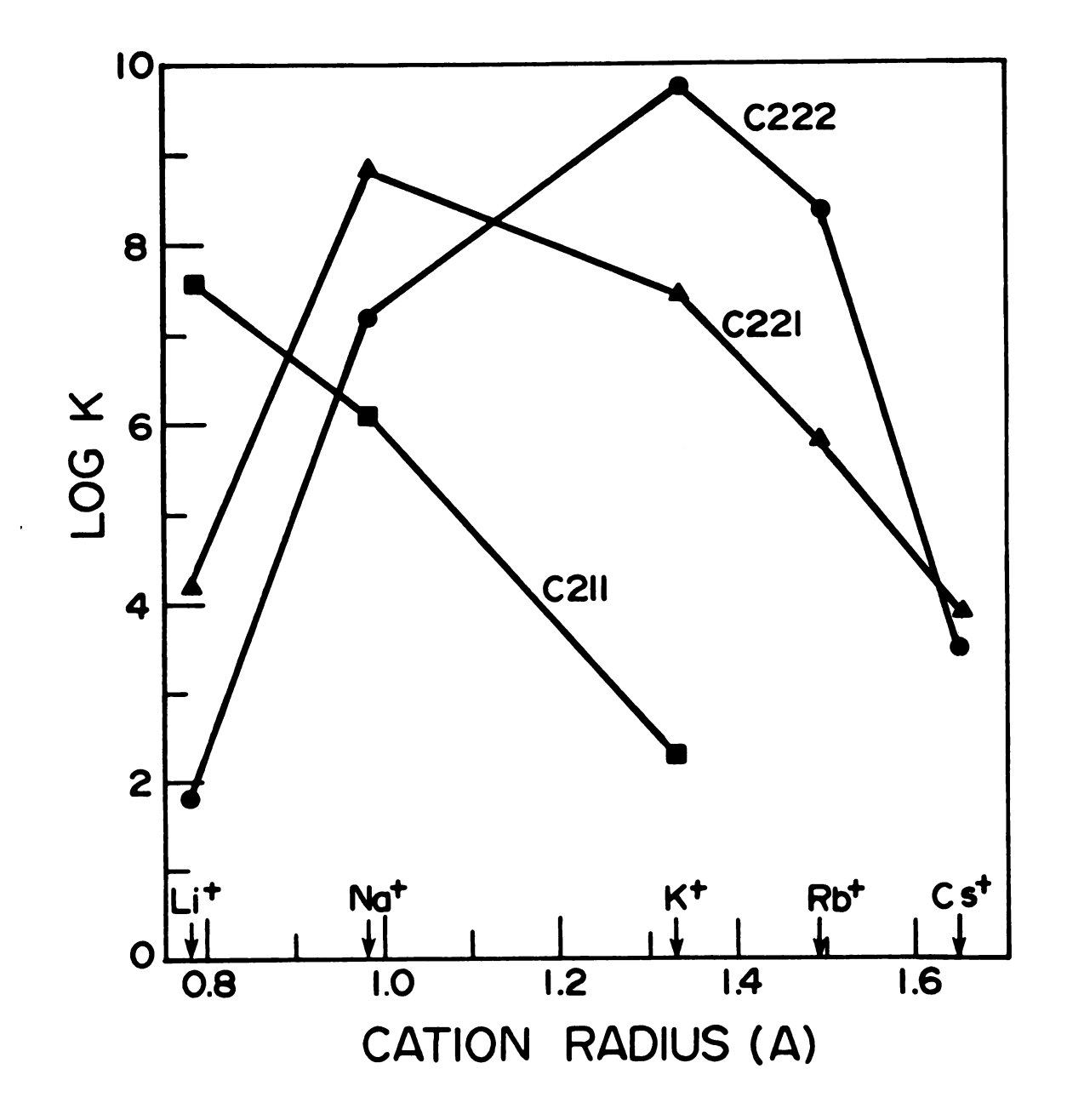


Figure 4. Selectivity and stability of cryptand(2,2,2) complexes with alkali metal cations in 95% methanol.

the use of complexing agents to solubilize alkali metals in solvents which do not otherwise dissolve metal. For example, potassium was dissolved in several ethers using dicyclohexano-18-Crown-6 (44) and C222.

Metal solutions in amines and ethers which also contain a complexer, C, can be described by the equilibria in equations (3-5) and the equilibrium

$$M^{+} + C \not\equiv M^{+}C \tag{6}$$

where C is a complexing agent. Addition of complexing agent shifts equilibria (3) and (5) to the right by dissolving more metal and converting monomer M to M⁺ and e_{solv}. However, if the amount of metal is limited with respect to complexer, then it is possible in good solvents such as MeNH₂ to prepare solutions consisting mainly of M⁺C and e_{solv}. In the poorer solvents such as the ethers, solutions containing only M⁺C and M⁻ can be prepared (55) by limiting the complexer relative to metal. Thus, as a result of the cryptate effect, metal solutions which were impossible to prepare may be prepared and some control over solution species is possible. The cryptands' resistance to reduction is, of course, another important property.

Cryptands made possible experimental differentiation between models (see Figure 2) for the solution structure of M in amines and ethers. This differentiation was accomplished by Dye, Ceraso, and Andrews (56,57) using alkali metal NMR. In order to measure the alkali metal

NMR spectrum, the solutions had to be concentrated. Furthermore, presence of significant amounts of e_{solv}^- could broaden the M⁻ peak by exchange to the point that the signal would disappear. Use of cryptand solved both of these problems through solubilization to give concentrated solutions and through stoichiometry control to give primarily M⁺C222 and M⁻.

Sodium exchange was slow enough to observe a ²³Na NMR signal from both Na⁺C222 and Na⁻. Dye et al. found that the 2p electrons in Na are well shielded from interaction with the solvent and that Na is highly symmetric as indicated by the narrowness of its NMR signal. The former observation follows since the chemical shift for sodium depends on solvent interaction with the sodium 2p electrons. Popov et al. (58-61) had shown that sodium chemical shifts correlate well with solvent donicity as measured by the Guttman solvent donor number. The Na chemical shift shows no solvent dependence among the solvents methylamine, ethylamine, and THF and is equal to that calculated for Na(g). These observations eliminate three models for M, leaving only the spherically symmetric anion with two electrons in an s orbital. Resonances were also observed by Dye et al. for ⁸⁷Rb⁻ and ¹³³Cs⁻ with the counterion being the corresponding cryptated cation.

Solids have been obtained from concentrated amine and ether metal solutions containing complexers. This has been done in two ways. One is to slowly cool the

solution and wait for crystal formation. The second technique is solvent evaporation to dryness.

Crystals of (Na⁺C222)Na⁻ were grown (62) from an ethylamine solution and are the most fully characterized (63-64) of the solids. The shiny gold-colored crystals which grow as thin hexagonal plates were prepared as described in detail in the Experimental section (65).

The crystals are stable for long periods under vacuum at -30°C. The crystals are air, water, and temperature sensitive but they may be handled in an inert atmosphere box at room temperature for a quarter of an hour. This compound is the most stable of the solids studied to date, especially with respect to temperature sensitivity. (For further details on stability, see Chapter V.)

An x-ray structure determination of (Na⁺C222)Na⁻ was made by Tehan, Barnett, and Dye in 1974 (64). As shown in Figure 5, the sodium anions form parallel planes which are separated by cryptated sodium cations. The cryptand has three-fold symmetry and an antiprismatic oxygen atom arrangement about Na⁺. The structure is similar to that of (Na⁺C222)I⁻ but Na⁻ seems to be slightly larger than I⁻. The closest distance between sodium anions in the same plane is 8.83 A, while the closest distance between anions in different planes is 11.0 A.

The second kind of solid has been produced by solvent evaporation, chiefly from solutions containing

CRYPTAND

Figure 5. Structure of (Na⁺C222)Na⁻ based on x-ray study.

M⁺C and e_{solv}. These blue solids were characterized as having "paramagnetic character" (66) or as "strongly paramagnetic solids" (64,67). They may be solids of a new class of compounds in which the counterion for M⁺C is an electron. These blue solids are called electrides (98). Many solvent, complexer, and metal combinations were tried and blue or gold solid films were observed by solvent evaporation (68). Some optical and magnetic properties of this type of solid are the subject of this dissertation.

EXPERIMENTAL

II.A. Reagents

II.A.1. Solvents

Solvents listed below were stored in vacuum storage bottles (as in Figure 6 but without a sidearm) and were degassed by freeze-pump-thaw cycles before use.

 $\underline{\text{Ammonia}}$ (NH₃). Ammonia (anhydrous, 99.99%, Matheson) was treated twice with NaK₃ (see Metals) before transfer to a vacuum storage bottle.

Ethylamine (EA). Ethylamine (anhydrous, Eastman Kodak) was stirred over calcium hydride for 48-60 hours. It was then treated repeatedly with NaK₃ until the characteristic dark blue color remained 72 hours at ambient temperature. The solvent was then vacuum transferred immediately to a vacuum storage bottle.

Methylamine (MA). Methylamine (98%, J. T. Baker) was treated in the same way as ethylamine.

Tetrahydrofuran (THF). Tetrahydrofuran (Burdick and Jackson) was first dried over barium oxide with stirring and freeze-pump-thaw degassing. It was then transferred for storage to a vacuum storage bottle containing an excess of NaK₃ over benzophenone. The blue

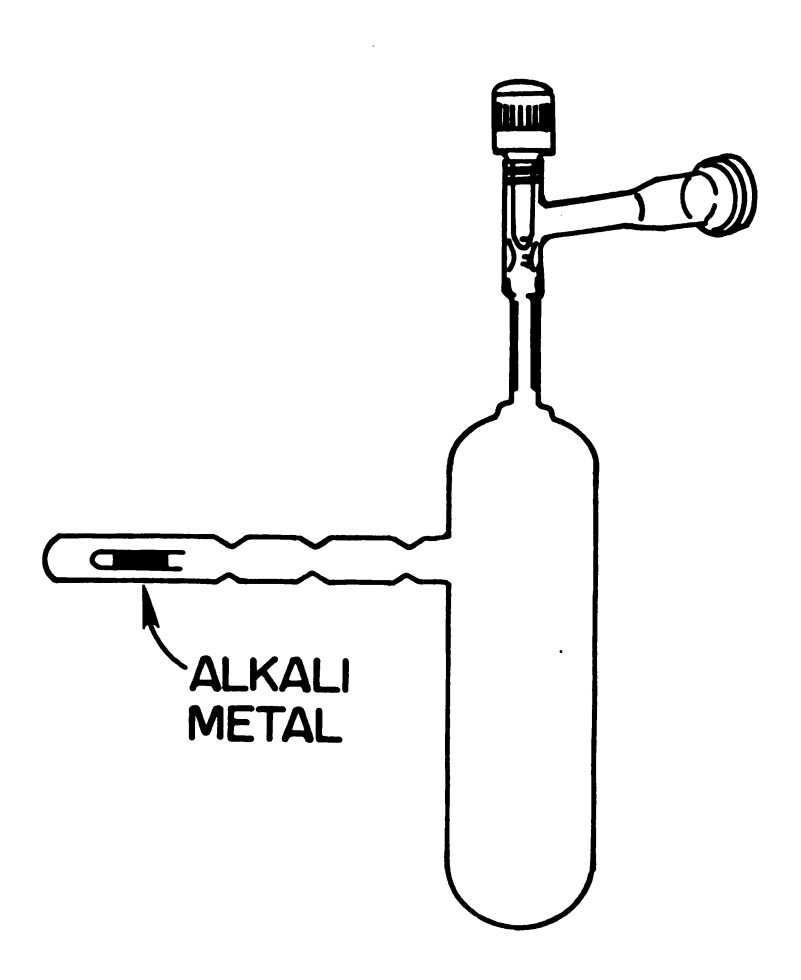


Figure 6. Vacuum bottle with sidearm for alkali metal distillation.

benzophenone ketyl served as a drying agent and dryness indicator (69).

<u>Diethyl ether</u> (DEE). Ether (Fisher) was refluxed over calcium hydride and then stored with benzophenone ketyl as in the case of THF.

II.A.2. Metals

Lithium. Lithium of 99.9% metallic purity (Alfa-Ventron) was received as ribbon under argon. Pieces of lithium were loaded into a tube in an argon-filled dry box as follows. A thin-walled glass tube of 3-5 mm O.D., sealed at one end, was pre-weighed and provided with a glass cap to which polyolefin heat-shrinkable tubing (from an electronics supply house) had been attached with heat. In the glove box, appropriately sized lithium pieces were inserted into the glass tubing. The cap was put on and heated to form a gas tight seal. After removal from the box, the glass tubing containing the lithium foil was cooled with liquid nitrogen and flame sealed. After cutting the heat-shrinkable tubing away with a razor blade, the glass tube and sealed-off piece were weighed to determine the mass of metal. The metal was introduced into the experimental apparatus as described under "General Preparative Technique", except that the lithium was not distilled (it reacts with hot glass).

Sodium, potassium, and rubidium. These metals
(Alfa-Ventron) were supplied under argon in sealed glass

ampules with breakseals. Total purities were 99.95, 99.95, and 99.93%, respectively, according to the supplier. The metals were stored under vacuum in measured small diameter glass tubes (2-8 mm O.D.) with sealed ends. Vacuum transfer of the metal from the five gram ampule to these tubes was accomplished as follows. ampule with breakseal was attached to the distribution apparatus shown in Figure 7. After evacuating the apparatus and breaking the breakseal, the metal was heated and ran downhill to fill each of the reservoirs in turn. Vacuum seal-offs were made at the constrictions. The metal was heated and allowed to run down into each of the straight portions of the tubes with known internal diameter. Appropriate seal-offs yielded partially filled straight tubes for later use in obtaining known amounts of metal.

Potassium, rubidium, and cesium were always heated with a torch flame free of added tank oxygen to avoid exchange of sodium from the glass at higher temperatures (26).

<u>Cesium</u>. This element (donated by Dow Chemical Co.) was distributed from an ampule to straight tubes as described above.

Barium. This metal (99.5% metallic purity, Alfa-Ventron) was supplied as a rod under argon. Shavings from the rod were loaded into a tube and sealed while in an argon-filled dry box as described above for lithium.

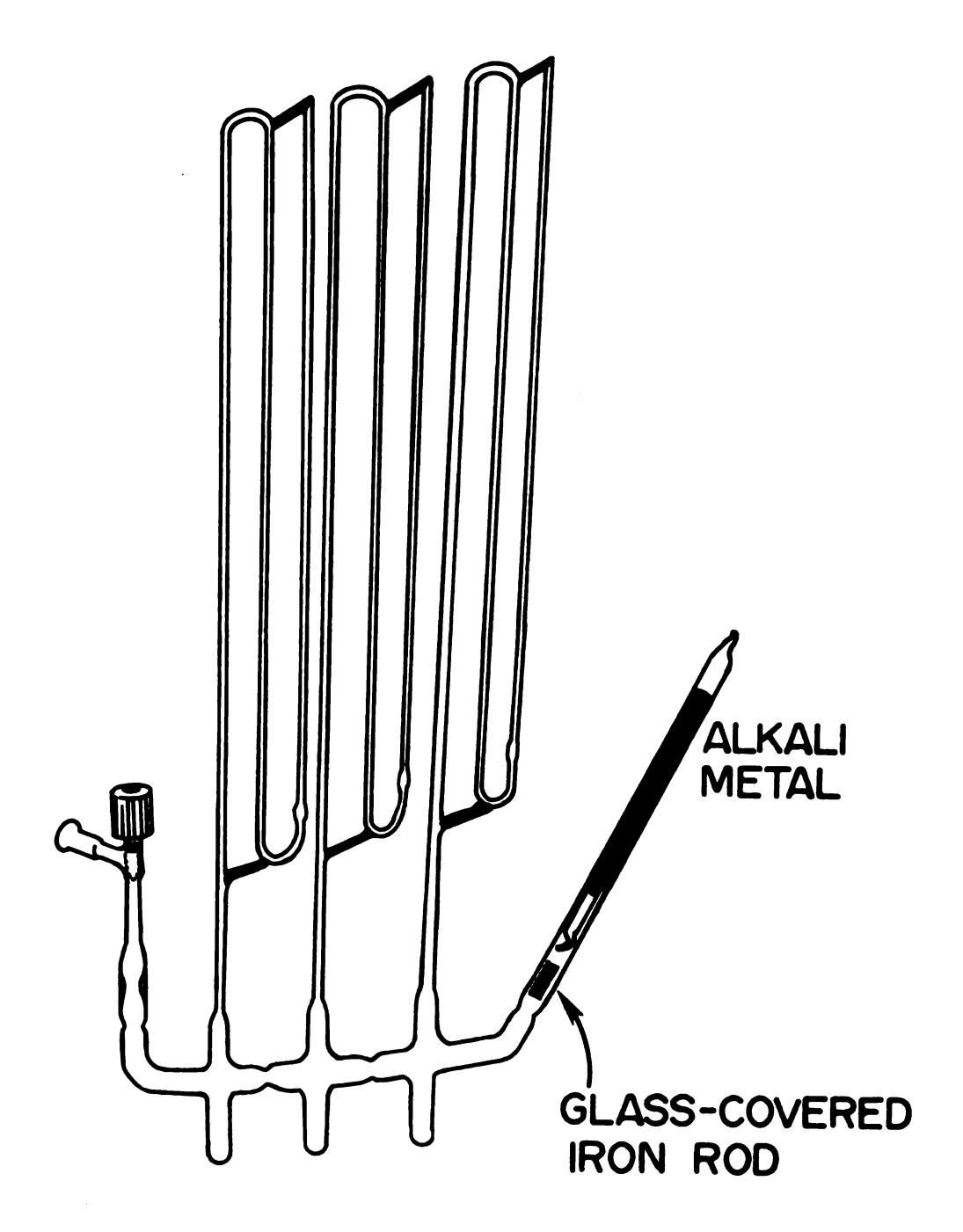


Figure 7. Apparatus for distribution of alkali metal under vacuum.

The barium surface darkened from nitride formation due to small amounts of nitrogen in the argon atmosphere.

Sodium-potassium alloy. Sodium and potassium

(J. T. Baker) metal in open-ended glass tubing was prepared by Tehan's method (67). These tubes were stored under mechanical pump vacuum to retard oxidation and subsequent deliquescent action by the oxides. To prepare the alloy in situ for drying of solvents, appropriate lengths of tubing containing sodium and potassium were co-distilled under vacuum in the solvent bottle sidearm and finally into the bottle (Figure 6).

II.A.3. Complexing Agents

2,2,2-Cryptand (C222 or IUPAC: 4,7,13,16,21,24-hexaoxa-1,10-diazabicyclo-(8,8,8)-hexacosane). 2,2,2-Cryptand (purchased from PCR, Inc., manufactured by E. Merck) was further purified by two procedures. One was high vacuum sublimation of the light sensitive substance, preferably in semidarkness. The second was sublimation after recrystallization from hexanes. After either procedure, the sublimed product was stored in darkness under mechanical pump vacuum. The melting point was 68°-69° (lit.(70): 68-9°).

18-Crown-6 (18C6 or IUPAC: 1,4,7,10,13,16-hexa-oxacyclo octadecane). 18-Crown-6 (PCR, Inc.) was recrystallized from warm acetonitrile to give a crown acetonitrile complex (71). Crown obtained from vacuum decomposition of the acetonitrile complex was

high-vacuum sublimed. The snow-white product gave a m.p. of 39° (lit.(72): 39-40°).

II.A.4. Miscellaneous Reagents

1,4-diazabicyclo[2.2.2]octane (DABCO). This bicyclic compound (Aldrich, 97%) was recrystallized twice from warm acetone to give white crystals which were sublimed. The hygroscopic crystals were handled in an inert atmosphere before and after sublimation.

 $\underline{\text{HF/HNO}_3/\text{detergent solution}}$. The HF glass cleaner is 33% $\underline{\text{HNO}_3}(16\ \underline{\text{M}})$, 5% $\underline{\text{HF}(28\ \underline{\text{M}})}$, 2% acid soluble detergent, and 60% distilled water, by volume (74). All acids were reagent grade.

Conductivity water. House distilled water was deionized (Crystalab Deeminizer) and distilled in glass with a high reflux ratio through a 70 cm column packed with seven-cm lengths of glass tubing. Final storage was in a sealed polypropylene container.

II.B. Glass Apparatus Cleaning

Apparatus which contacted solutions containing dissolved metal were first cleaned with the following ritual. The apparatus was first rinsed with HF/HNO₃/detergent solution (see Reagents), followed by six rinses by distilled water. The apparatus was then partially filled with freshly-prepared aqua regia (3:1 HCl to HNO₃). This was either allowed to stand overnight or was heated to effervescence and allowed to stand at least four hours. The vessel was then emptied, rinsed

six times with distilled water and six times with conductivity water, and oven-dried overnight at 120-135°. For experiments involving particularly unstable solutions, an extra step was added. Conductivity water was heated to boiling in the partially filled apparatus, prior to oven drying.

II.C. Greaseless High Vacuum System

A greaseless, all glass vacuum manifold was evacuated through a liquid nitrogen trap by an oil diffusion pump (Veeco pump model EP2A-1, Dow-Corning 704 oil) backed by a two-stage mechanical pump (Cenco HV-7). Greaseless vacuum stopcocks (Kontes no. K-826610) were used routinely to 5·10⁻⁶ torr (7·10⁻⁴ Pa) on the manifold and on individual apparatus. Greaseless connections from the manifold to the apparatus were made with five-or nine-millimeter Solv-Seal glass joints with Teflon seals (both joints and seals from Lab-Crest Division, Fischer and Porter Co., no. 571-190). The manifold was continuously heated to about 70° with heating tape. For vacuum measurement, an ionization gauge (Veeco RG75-P) located directly on the manifold provided the signal for an electronic readout (Veeco RGLL-6).

II.D. <u>Inert Atmosphere Manipulations</u>

A dry box gas recirculation and purification system was constructed similar to that described by Ashby and Schwartz (75). This system purified the argon atmosphere by removal of O_2 , H_2O , and certain hydrocarbons.

A major source of contamination of the box atmosphere is diffusion of air and water through the gloves while the box is not in use, even if special elastomers are used for the gloves (76). An unusual feature in our system was the reduction of this daily diffusion. Since the box was evacuable, the gloves could be pushed into the box and the glove ports sealed. The gloves could then be flushed either with box atmosphere or tank gas, thus greatly reducing air diffusion into the box.

II.E. Sample Preparation and Instrumental Technique

II.E.1. General Preparative Techniques

The synthesis of crystals of (Na⁺C222)Na⁻ involves many techniques used in preparing other samples and so will be described in detail (65). The apparatus in Figure 8, having been rigorously cleaned as described earlier, was ready for reagent loading. Sodium in the mg range, measured by volume and density, was introduced as follows. The sodium stock, sealed under vacuum in tubes of known internal diameter (see Reagents), was heated until a length of metal occupied one end of the partially filled tube. A seal-off was then made, giving a measured amount of clean metal. This small tube of sodium was scored around the middle and put in the apparatus sidearm. A piece of shrink tubing (Flo-Tite tubing, Pope Scientific Co.) was heat-sealed on the end of the sidearm. This shrink tubing consists of two concentric tubes. The inner tube (Teflon FEP), softened

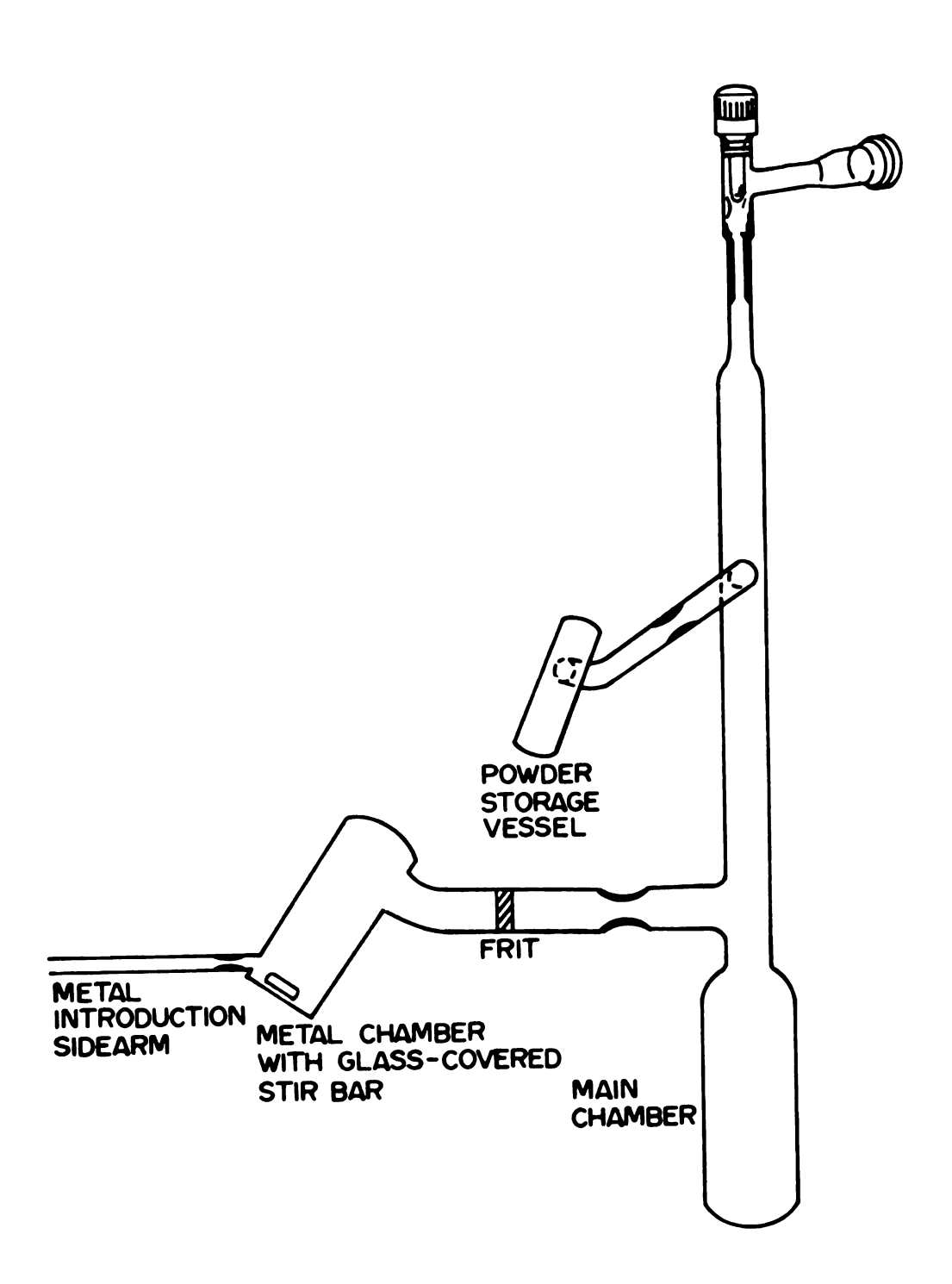


Figure 8. Apparatus for preparation of (Na C222) Na crystals.

by the heat, is pressed against the glass by the outer tube (Teflon TFE) as it shrinks from the heat. The other end of the shrink tubing was sealed onto a short piece of glass tubing sealed at one end.

The weighed cryptand was loaded through the valve, the valve stem inserted, and the apparatus pumped down to $\sim 10^{-5}$ torr ($\sim 10^{-3}$ Pa). With the valve shut and the apparatus off the vacuum line, the sodium ampule was then bent, breaking open the metal ampule as in Figure 10. The two ampule pieces were shaken down the sidearm until they were close to the constriction and the shrink tubing end of the sidearm was removed by a glass seal-off under dynamic vacuum of $\sim 10^{-5}$ torr $(\sim 10^{-3} \text{ Pa})$. The apparatus was then left overnight under a static vacuum. The apparatus and the solvent bottle were attached to a vacuum tee (Figure 9) connected to the vacuum manifold. With the apparatus and tee at high vacuum, the sodium was distilled into the metal chamber (Figure 8) and a seal-off was made at the constriction. Ethylamine was then condensed in from the main chamber from the solvent bottle through the tee by chilling the main chamber to -78°. Use of the vacuum tee for all solvent distillations prevented contamination of the high vacuum manifold. With the apparatus valve shut, the apparatus was moved to a large ice-water bath (20x25x14 cm deep). Using this size bath and a cheesecloth baster, the glass in contact with the reactive solution was kept cold and solution decomposition

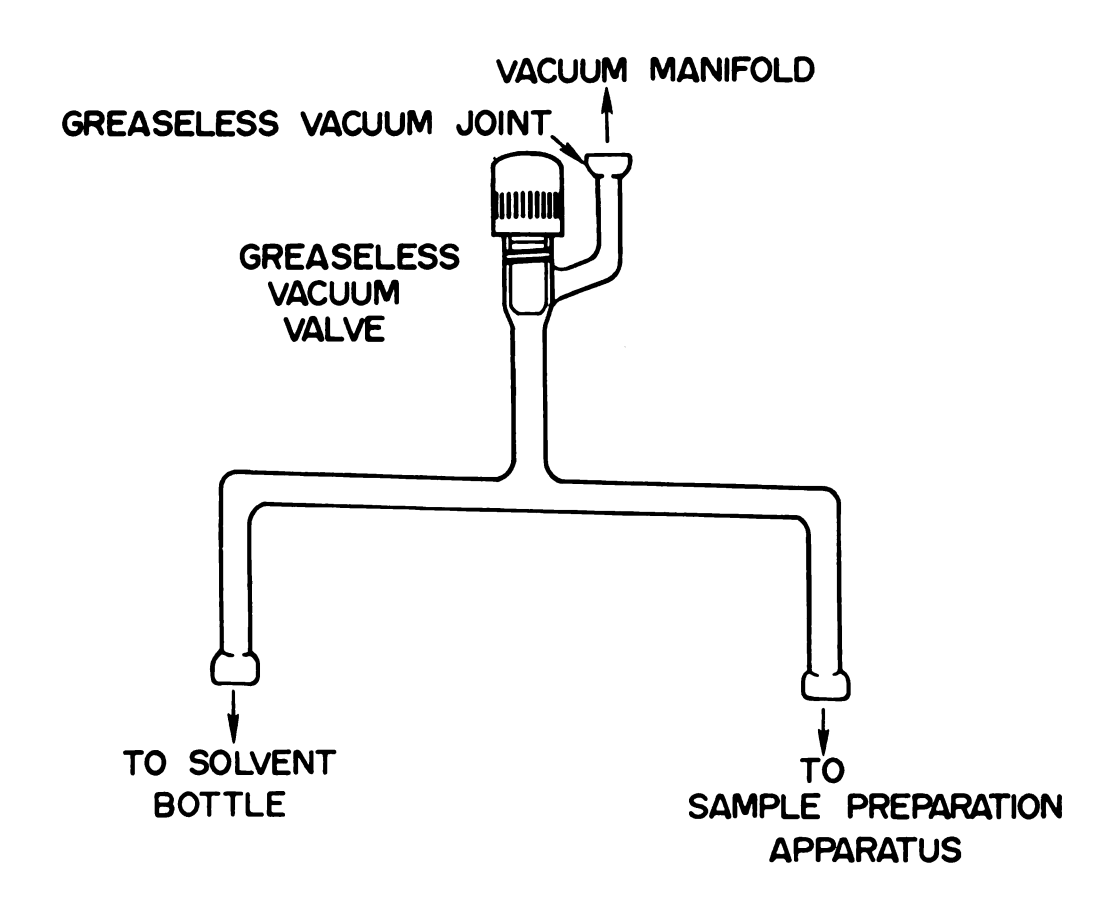


Figure 9. Vacuum tee use.

minimized. Agitation dissolved the cryptand in the ethylamine and the solution was poured onto the sodium mirror. A dark blue solution resulted immediately. In order to collect cryptand remaining on the walls in the main chamber, the blue solution was poured into that chamber and then back to the metal chamber.

The stoichiometric amount of sodium mirror was dissolved by magnetic stirring for several hours at 0°. The solution was then poured back to the main chamber for crystal growth at -78°. The intervening frit prevented sodium mirror flakes from entering the main chamber.

Crystal growth occurred as the solution stood at -78° overnight. The solution was decanted into the metal chamber and chilled to -78°. The constriction next to the frit was sealed off under dynamic vacuum with the crystals in the main chamber also at -78°. Diethyl ether was condensed onto the crystals and the slurry transferred to the upper chamber. The ether was then used to wash the crystals four or five times. The ether was frozen in the main chamber and the crystals pumped while they were held at 0°. A seal-off separated the crystal-containing upper chamber from the apparatus. The crystals were kept at -30° until they were distributed in the dry box into sample tubes or holders for use in other experiments.

II.E.2. Optical Spectra

Solutions were prepared in the apparatus shown in Figure 10. Spectra of films made from these solutions were obtained through the optical cell on the apparatus. With the exception of the graded seal and sodium borosilicate valve, the apparatus was constructed of fused silica. Fused silica was chosen to avoid the well-known sodium-exchange contamination of alkali metal solutions in contact with sodium borosilicate glass (21,26).

Appropriate amounts of metal, solid complexer, and solvent were loaded into the apparatus using techniques described in the last section. Ammonia or methylamine was used as the solvent for most samples. Solutions were generally made such that all of the complexer would dissolve before contact with metal.

In methylamine, ethylamine, and diethyl ether, the cryptand concentration was about 0.04~M. In ammonia, however, the cryptand solubility found in this work is only $\sim 0.02~M$ at -20° and $\sim 0.002~M$ at -55° . The alkali metals, highly soluble in NH₃ unassisted by complexers (7), enhance the cryptand solubility in ammonia. A similar enhancement of complexer solubility by cation was reported for crowns (45). The solutions were handled at -25° and below in a large dry ice cooled isopropanol bath.

Films were formed in the optical cell by first pouring most of the solution into the upper chamber.

Apparatus for preparation of films for optical spectroscopy. Figure 10.

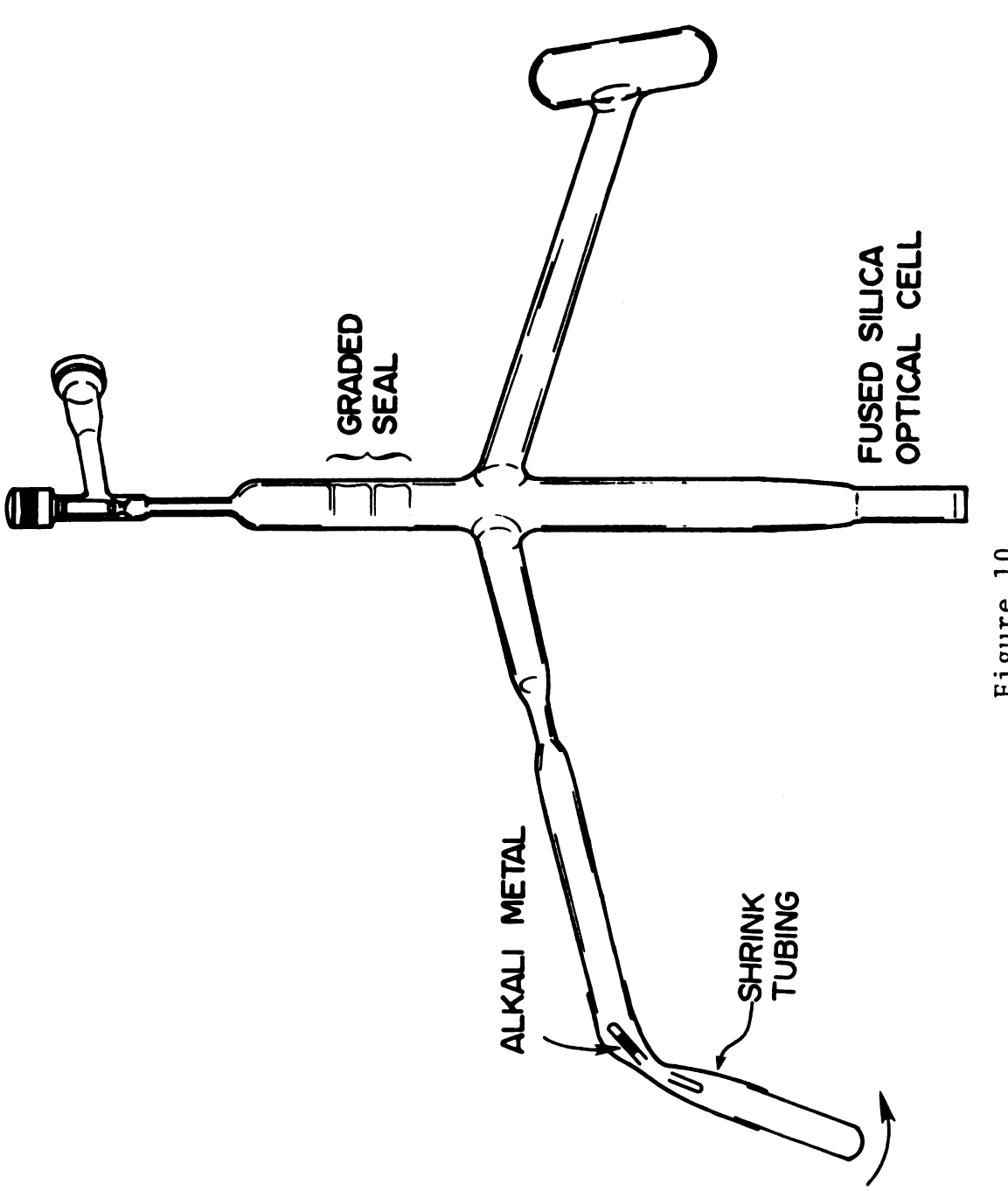


Figure 10.

While freezing the bulk of solution with liquid nitrogen, the cell was kept in the cold isopropanol bath and was shaken vigorously side to side, about the axis through the sidearm. The vigorous shaking threw the solution onto the optical cell window. Film formation resulted from flash evaporation of solvent from the solution on the cell window. If the absorbance of the resulting film was too high, then the bulk solution was thawed, poured back into the cell, and the process repeated to obtain a solvent-free or dry film of lower absorbance.

The quantity of solvent remaining in the films was Since ammonia has a considerably higher vapor pressure than methylamine, it is assumed that films from ammonia were at least as solvent-free as similar films prepared from methylamine solutions. To check the quantity of solvent remaining in the films from methylamine, an analysis was made on $\mathrm{D}_2\mathrm{O}$ solutions of powders prepared under conditions similar to those of film formation. One methylamine test solution for powder formation contained Na⁺C and Na⁻; a second solution contained $K^{\dagger}C$ and e_{solv}^{-} . The resulting powders were dissolved in $\mathrm{D}_2\mathrm{O}$ and the methylamine/cryptand mole ratio determined by PMR (Bruker model WH-180). The detection limit is a ratio of 0.001. A mole ratio of < 0.002 was found for the powder from a Na⁺C, Na⁻ solution and 0.08 for the powder from $K^{+}C$, e_{solv}^{-} solution. No impurities or decomposition products were seen. Therefore, the

films were essentially free of solvent and were stoichiometrically identical to the solute.

Some spectra were taken of films deliberately prepared to contain solvent, usually ammonia. The film was formed in the usual manner and the "dry film" spectrum recorded. A "wet film" was made by warming the bulk solution to ten or fifteen degrees below the film temperature and a new spectrum obtained.

Most spectra were obtained on a double beam recording spectrophotometer (Beckman DK-2A) capable of scanning from the ultraviolet to the infrared. The optical cell and film could be maintained at constant temperature ranging from 0° to -55° with an arrangement similar to that used by Douthit (77). A thermocouple placed near the cell provided the signal for temperature readout (Doric model DS-350). Spectra of films of (Na⁺C)Na⁻ were also obtained from -30 to 20°C with a Cary recording spectrophotometer.

The spectra were obtained with air in the reference beam and were baseline-corrected by subtracting either the spectrum of an empty quartz cell or a decomposed film. The same general spectral features resulted in either case. The observed baseline may shift due to light scattering, so the lowest absorbance in each spectrum was arbitrarily set to zero. Each spectrum was then normalized to the highest absorbance, and this appears as A/A_{max} in the figures showing spectra. Because of these problems, the spectral shapes are

qualitative: the true shapes may be slightly different. Thickness variations in the films could not be avoided and these variations can distort the spectral shape, particularly at high absorbances. Accordingly, film thicknesses were chosen to given absorbances below 1.0-1.5. The films should be thick enough to avoid quartz-film interface effects except for possible orientation effects.

II.E.3. ESR Sample Preparation and Instrumentation

The fused silica apparatus was similar to the apparatus in Figure 11, except that a 3 mm O.D. fused silica tube was substituted for the 5 mm O.D. ESR tube shown. The apparatus was loaded with metal, complexer, and solvent as described earlier. Part of the blue solution was poured into the sidearm to a height of several centimeters. The solvent was then evaporated slowly to avoid bumping. To accomplish this slow evaporation, the ESR tube was held at -55° for ammonia solutions and -45° for methylamine solutions, while the main chamber was kept at -78°. After evaporation was complete, the main solution was frozen in liquid nitrogen. Some samples were then dynamically pumped before seal-off. In all cases the sample was chilled to -196° during seal-off.

ESR spectra were obtained on an X-band spectrometer (Varian model E-4 with E-4534 sample cavity). The klystron power was calibrated with a power meter

(Hewlett-Packard model 432A). Variable sample temperatures above 77 K were obtained in the usual way by passing a regulated cold nitrogen stream around the sample. The variable temperature controller (Varian) scale was calibrated with a copper-constantan thermocouple with digital readout (Doric model DS-350). Temperatures between 3.6 and 77 K were provided by a liquid helium continuous flow cryostat system (Oxford Instrument Co., Ltd., model ESR 9). Digital temperature readout and control were based on an Au + 0.03% Fe/chromel thermocouple near the sample.

II.E.4. Magnetic Susceptibility: Faraday Technique

In the Faraday method of magnetic susceptibility determination, a small powdered sample is placed in a nonhomogeneous magnetic field. The vertical force, \mathbf{f}_{7} , on an isotropic sample is

$$f_z = m\chi_g H_x \frac{\partial H_x}{\partial z} \tag{7}$$

where m is the mass, χ_g is the magnetic susceptibility per gram, H is the magnetic field strength, and x is the axis connecting the magnet pole pieces. The force, f_z , on the sample is obtained by subtracting the force on the sample container from the force on the container loaded with sample. The susceptibility is usually not determined directly from equation (7) since the measurement of the field gradient is difficult. The sample is compared to a compound of known susceptibility in the

following way. The force, f_z^i , on the standard compound of known susceptibility, χ_g^i , is measured. Assuming that $H_X(\partial H_X/\partial z)$ is the same over both sample and standard, then the sample susceptibility is

$$\chi_{g} = \frac{f_{z}}{f_{z}^{\dagger}} \frac{m^{\dagger}}{m} \chi_{g}^{\dagger}$$
 (8)

where primes denote quantities involving the standard. This is the working equation for the Faraday method. Further general experimental details of the Faraday method appear in the literature (78).

Faraday balance measurements were made on the departmental balance (Alpha Scientific Laboratories), except for measurements on (Na⁺C222)Na⁻. (These were made on the balance at Institut de Chimie, Université Louis Pasteur, Strasbourg, France.) The departmental balance has a sensitivity of 0.01 mg. The variable-temperature cryostat Dewar and controller, calibrated with a copper-constantan thermocouple, provide temperatures from 77 K to above room temperature. The vertical temperature gradient in the cryostat was found to be only a few tenths of a degree per cm in the region of the sample.

The sample container was suspended in the field with a sapphire filament as described by Zatko and Davis (79). This material hangs straight and is better than wire suspensions, which sometimes retain curvature and contact the Dewar walls. The sapphire filament is more flexible and not as easily broken as a quartz fiber

which is sometimes used. A Teflon sample container was used for powders such as $(Na^{+}C222)Na^{-}$ and pure complexing agents. This nonreactive, diamagnetic container was easily loaded in a glove box and cleaned with aqua regia between uses.

In order to measure the susceptibility of reactive electrides which would decompose under glove box handling conditions such as room temperature, a new sample holding technique was developed. The electride solid was prepared by solution evaporation in a vertical glass sidearm of the fused silica apparatus shown in Figure 11.

The solutions were prepared as described earlier. All of the solution was poured into the vertical sidearm. nearly filling it. The solvent was evaporated slowly to avoid bumping. To accomplish this slow evaporation, the ESR tube sidearm was held at -48° for methylamine solutions or -72° for ammonia solutions, while the main chamber was kept at -78°. The solutions left a residue on the walls after evaporation. When sample preparation was complete, this residue had to be in the bottom of the tube and less than about one centimeter in height in order for all the sample to be in the region of constant force. When the solution had evaporated to about onethird of its original height, leaving residue along the other two-thirds, the sidearm was placed in the -78° bath while the solvent in the main chamber was warmed above -78°. The solvent condensed on the cold residuecovered walls, washing the residue down. This washing

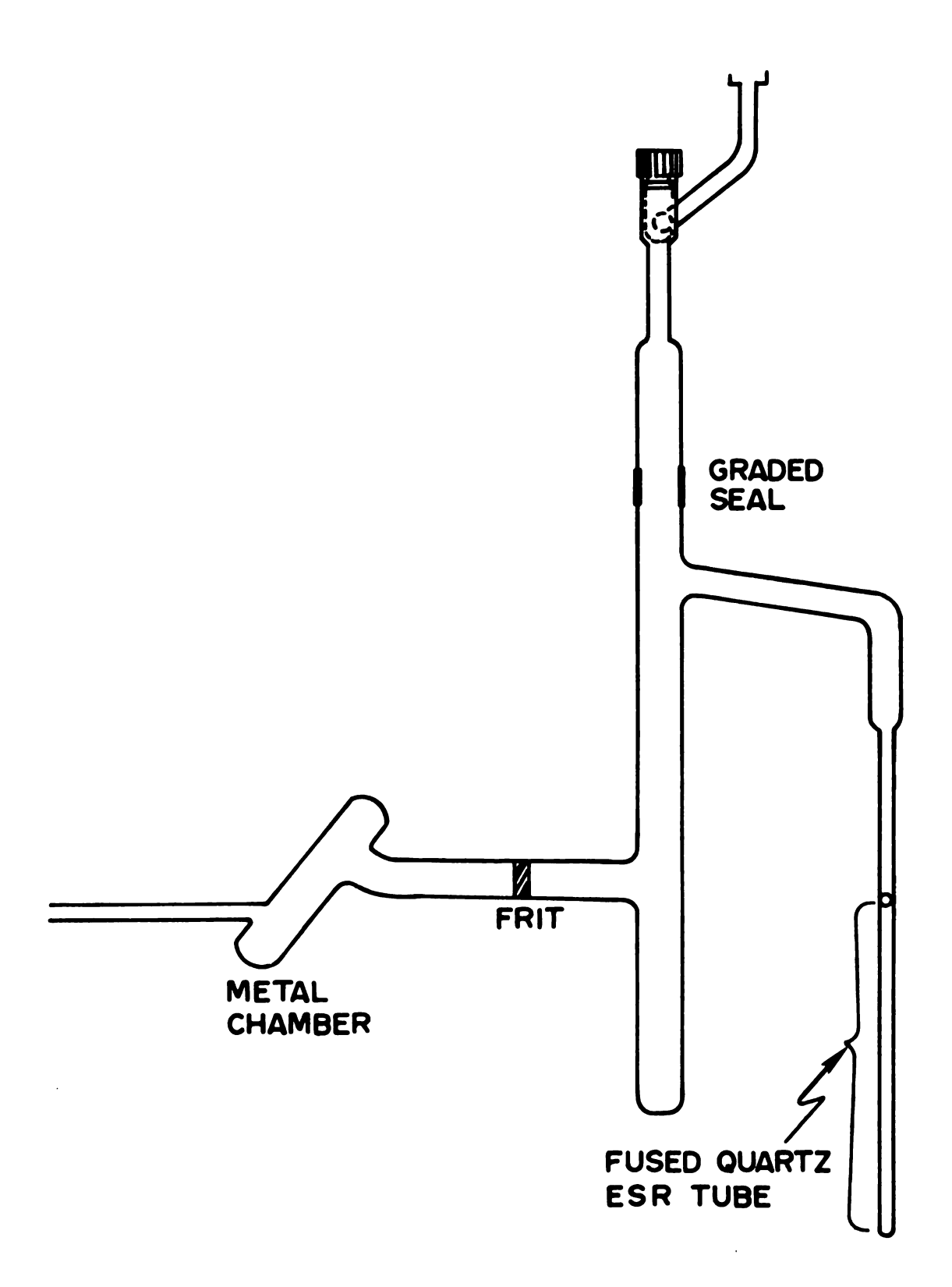


Figure 11. Apparatus for preparation of magnetic susceptibility samples.

action was continued until the walls were clean. The tube was then usually about two-thirds full compared to the original solution height. Evaporation from the ESR tube was started again. Three to four of these evaporation-wash cycles were generally sufficient to give a dry residue about one centimeter in height in the tube bottom. The sample was dynamically pumped before seal-off. The sample temperature during seal-off was -196°. A small fused silica loop and stem were attached to the sample tube.

A 5 mm O.D. fused silica ESR tube was chosen for the sidearm for several reasons. The use of fused silica avoids the well-known sodium exchange contamination (21) by sodium borosilicate glass. The outside diameter of the tube permitted easy passage into the narrow Dewar cryostat. The thin wall minimized solution bumping during evaporation by maximizing the tube's inside cross The thin wall also minimized the amount of section. fused silica in the magnetic field. The tubes are manufactured to close tolerances and this is important, as seen below. If tubes are longer than a critical length and the lower end is reproducibly placed in the field, then the force on the tube is independent of the tube length. This critical length was found empirically and depends, of course, on the magnetic field strength, pole gap, and balance sensitivity. Once conditions are met such that the force is independent of tube length, then

different tubes may be used for sample, standard, and container measurements in the susceptibility determination.

OPTICAL SPECTRA

Some of the optical studies described here were a cooperative effort with other researchers (98-100).

III.A. Films from Methylamine

III.A.1. Results

Figure 12 shows dry film spectra made from four methylamine solutions containing M⁺C222 (abbreviated as M⁺C) and M⁻ where M is Na, K, Rb, or Cs. These films were blue in color by transmission and gold-bronze by reflection. The (Na⁺C222)Na⁻ film spectrum, the dotted line, has three main features: the main absorption at 15,400 cm⁻¹ (~650 nm), a shoulder at 18,900 cm⁻¹ (~530 nm), and a small distinct peak at 24,500 cm⁻¹ (~410 nm). The same spectrum was observed in films from MeNH₂ solutions prepared from (Na⁺C222)Na⁻ crystals. In contrast, the three spectra of (K⁺C)K⁻, (Rb⁺C)Rb⁻, and (Cs⁺C)Cs⁻ exhibit only one main band. These bands are tabulated and compared to M⁻ bands in EDA (20) in Table 3. The ethylenediamine M⁻ band positions are marked by arrowheads in Figure 12.

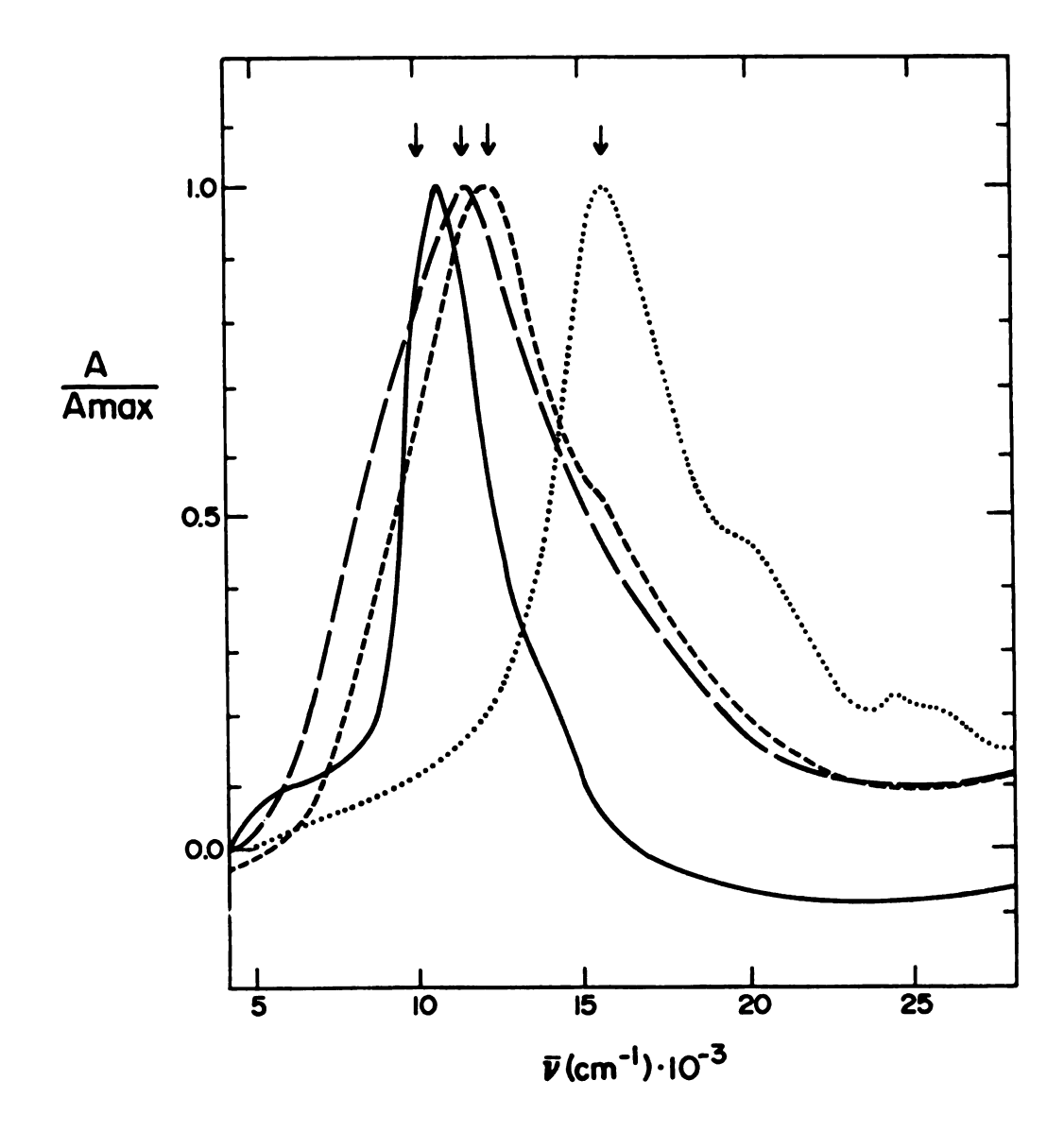


Figure 12. Spectra of films prepared by evaporation of methylamine solutions which contain M^+C and M^- : from left to right (peak positions) M = Cs, Rb, K, Na, respectively. The arrows indicate the position of the absorption maxima for the corresponding anions in ethylenediamine.

Table 3. Comparison of alkali metal anion peak positions in solid films from methylamine and in metal-EDA solutions

	Solid film	EDA solution (20)
Na -	15,400 cm ⁻¹ (650 nm)	15,400 cm ⁻¹ (650 nm)
K ⁻	$11,900 \text{ cm}^{-1}$ (840 nm)	12,000 cm ⁻¹ (833 nm)
Rb -	11,600 cm ⁻¹ (860 nm)	11,200 cm ⁻¹ (893 nm)
Cs	10,500 cm ⁻¹ (950 nm)	9,800 cm ⁻¹ (1,020 nm)

It was of interest to determine whether the shoulder and high energy peak (18,900 cm⁻¹ and 24,500 cm⁻¹) were characteristic not only of Na but also of the counterion, Na⁺C. For the following reasons, it was expected that a solution of K⁺C and Na could be prepared by contacting a C222 solution with Na and K metals. The addition of Na⁺ to a solution of K causes Na and K formation; i.e., Na is thermodynamically and kinetically favored over K (21,26). Also, C222 binds K more strongly than Na⁺ (88). Additionally, a C222 solution contacted with Na and K shows a Na signal and no Na C signal in the 23 Na NMR spectrum. The film absorption spectra of (K⁺C)Na and (Na⁺C)Na are shown in Figure 13. For (K⁺C)Na, the Na peak is red-shifted by $^{\sim}$ 300 cm⁻¹ and the shoulder and high energy peak are absent. The Na

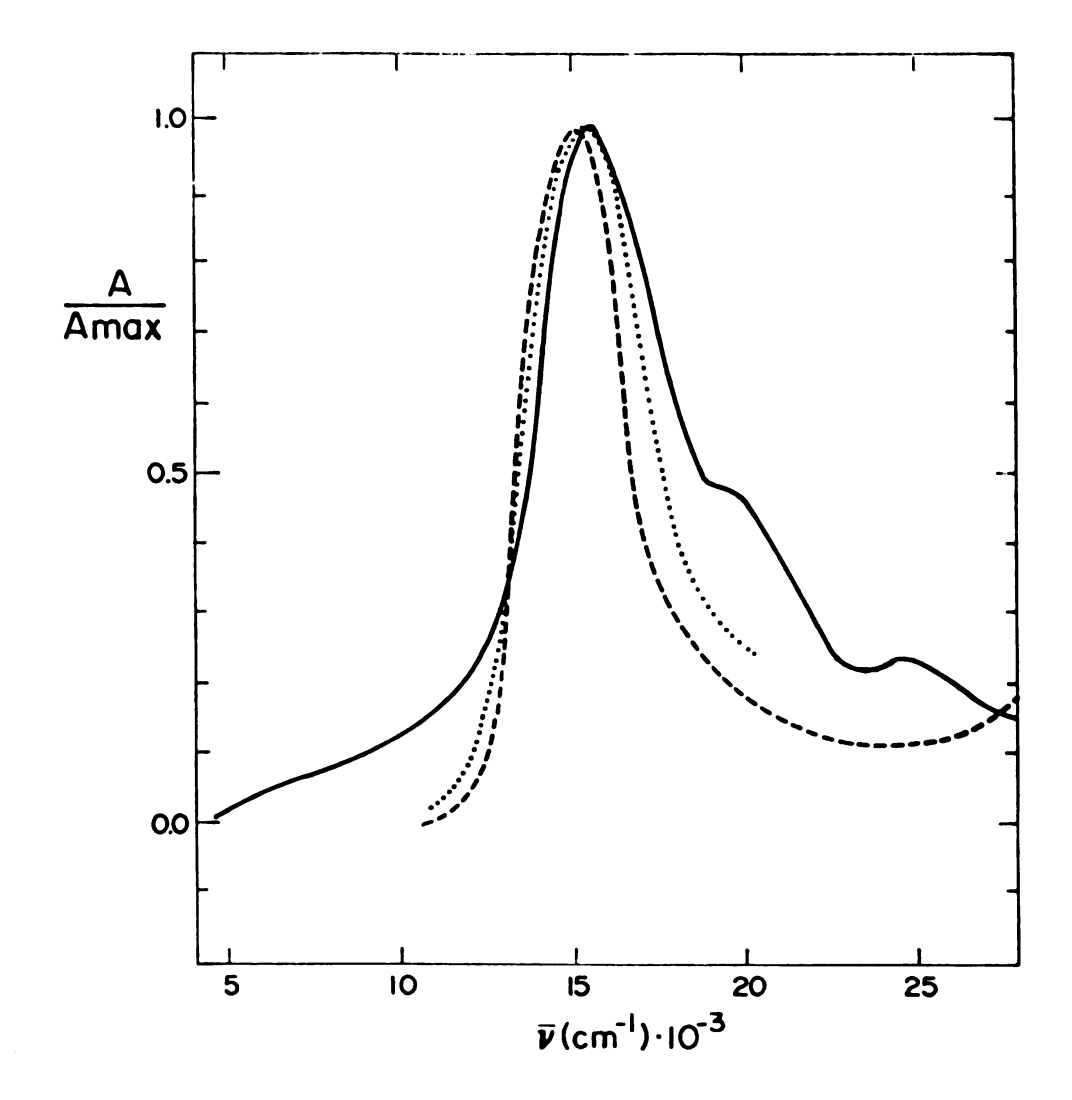


Figure 13. Baseline-corrected normalized spectra of the sodium anion under various conditions: solid line, (Na⁺C)Na⁻ film from methylamine; dashed line, (K⁺C)Na⁻ film from methylamine; dotted line, Na⁻ in ethylenediamine.

spectrum from sodium dissolved in ethylenediamine is also shown (87).

The position of the Na maximum and the peak width at half-height were slightly temperature dependent. The position of the maximum shifted to the red with increasing temperature with $d\overline{\nu}/dT \approx -1.6$ cm⁻¹ deg⁻¹. The width at half-height increased by ~ 1.1 cm⁻¹ deg⁻¹.

Equimolar potassium metal and C222 in methylamine yield solutions of stoichiometry K^+C and e_{solv}^- . Solvent evaporation leaves a dark-blue solvent-free residue (see later sections for ESR spectra and magnetic susceptibilities of this material). The absorption spectrum of a film made from such a solution is spectrum A in Figure 14. The maximum absorbance occurs at 7,400 cm⁻¹ (\sim 1350 nm) and the assignment is the trapped electron. When the potassium to C222 mole ratio in solution is between one and two, two peaks which are the absorptions of trapped electrons and K^- are observed as shown in spectrum B of Figure 14. At K/C222 mole ratios of two or greater, spectrum C of Figure 14 is seen, in which only the K^- band appears at 11,900 cm⁻¹ (840 nm).

A similar spectral dependence on metal to C222 ratio was observed for the rubidium system, as shown by the solid and dashed line spectra in Figure 15. The dotted line spectrum was made of a film from a rubidium solution prepared in a sodium borosilicate glass apparatus. The main peak is due to Rb and the shoulder presumably to Na which results from the reaction (21,26):

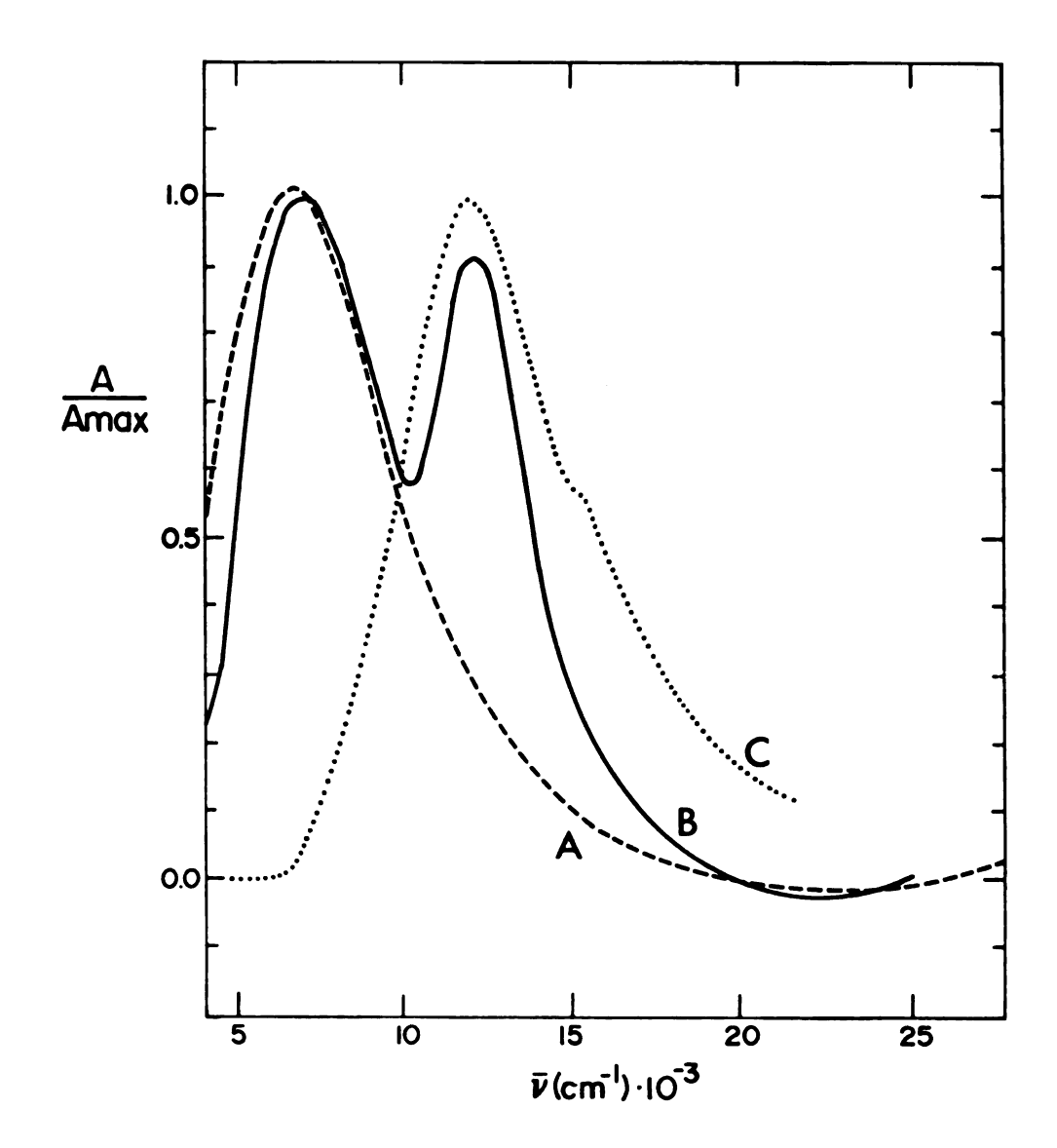


Figure 14. Spectra of films produced by evaporation of methylamine from solutions containing cryptand(2,2,2) and various relative amounts of potassium: spectra of films produced from solutions containing progressively lower concentrations of solvated electrons and higher concentrations of K⁻ are in the order A, B, C.

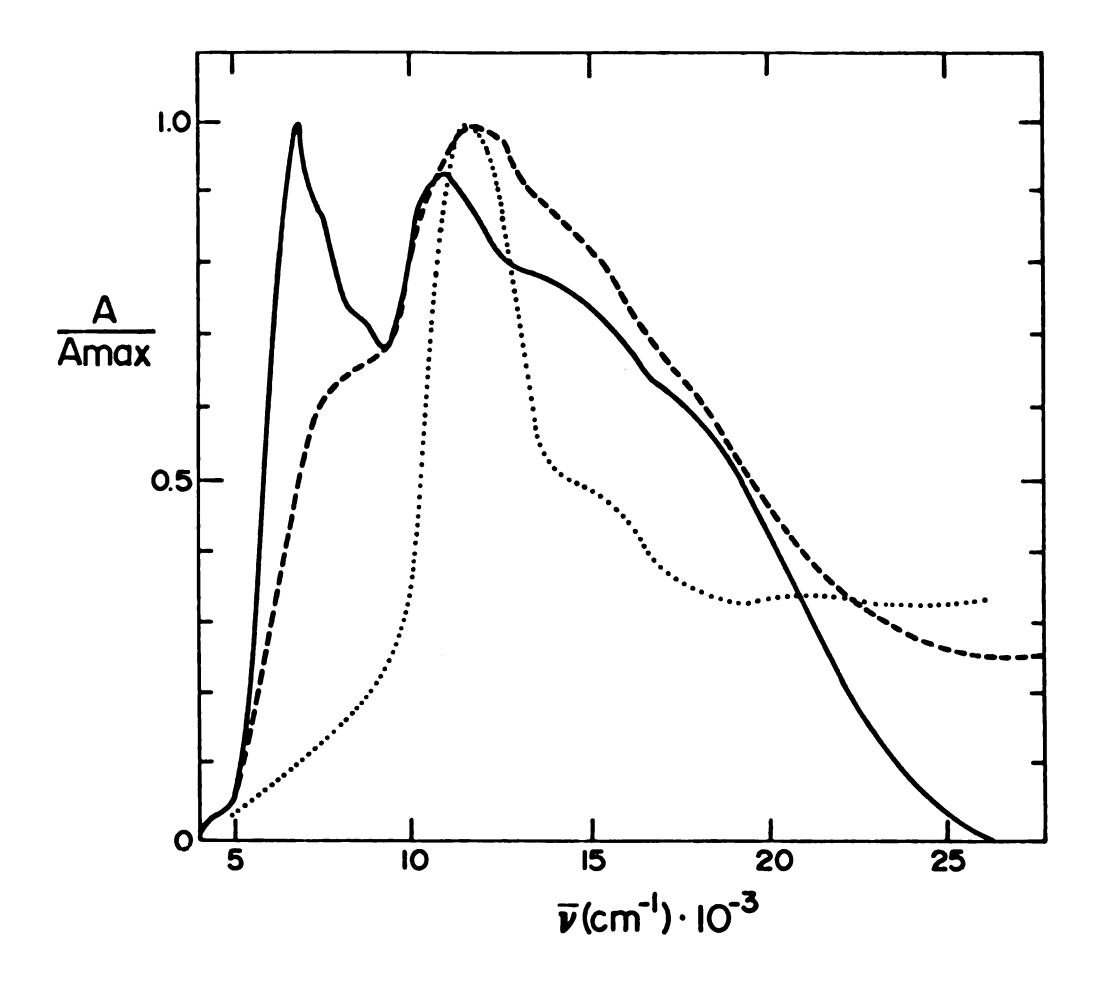


Figure 15. Spectra of films produced by evaporation of methylamine solutions containing cryptand(2,2,2) and various relative amounts of rubidium anions and solvated electrons (solid and dashed lines). The dotted line spectrum is from a film prepared from a sodium borosilicate glass apparatus; the solution presumably contained some Na.

$$Rb^{-}_{(sol)} + Na^{+}_{(wall)} \rightarrow Rb^{+}_{(wall)} + Na^{-}_{(sol)}$$
 (9)

In contrast to the potassium and rubidium cases, spectra of films from sodium or cesium-cryptand methylamine solutions do not show the near-IR absorption of the trapped electron regardless of the metal to C222 ratio.

By far the most stable films were those obtained from solutions of Na $^+$ C and Na $^-$. One such film showed only a 20% decline in the absorption maximum after two days at room temperature. The stability series seems to be Na $^-$ > Cs $^-$ > Rb $^-$ > K $^-$. Films of K $^-$ are the least stable and the half-life of a (K $^+$ C)K $^-$ film at room temperature was about four minutes. Stability also varied from one solution preparation to another of the same composition. The spectra of films from fresh and decomposing solutions displayed the same qualitative features. If the solutions and films were handled at cold temperatures (-30° and below for anything but Na solutions), decomposition slowed considerably and was negligible below -50°.

Films and blue solid residues were also formed from methylamine solutions of cesium and 18C6. Figure 16 shows the absorption spectrum of a film made from a cesium-crown solution with a metal to complexer mole ratio, R, of 0.5. The single absorption at 6500 cm⁻¹ (1540 nm) is assigned to the trapped electron. The small band at 15,400 cm⁻¹ is probably caused by Na⁻ as an impurity. Films formed from solutions with R=2, 1

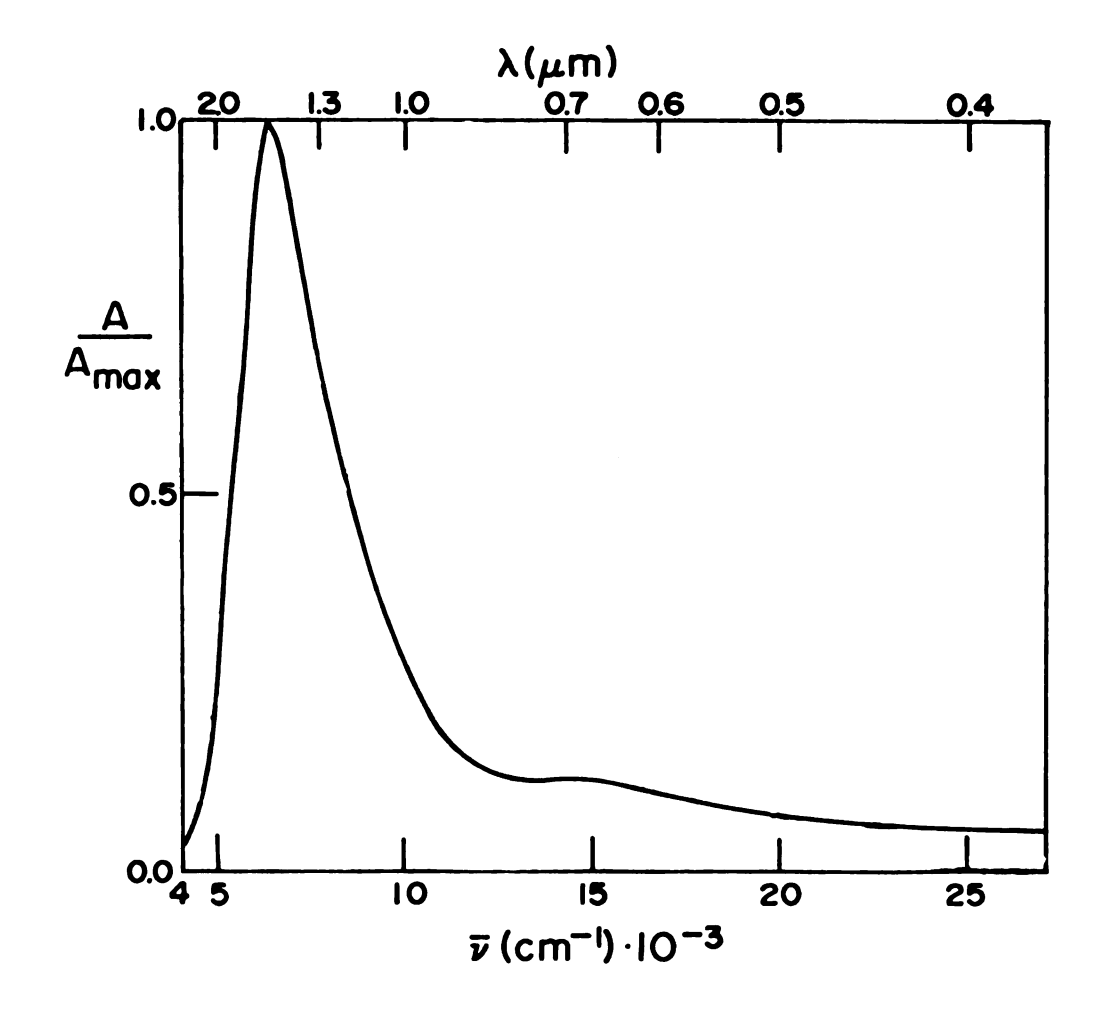


Figure 16. Film spectrum from a methylamine R=0.5 solution of Cs and 18C6.

and 0.1 also show a single band in the region 6400-6700 cm⁻¹ (1560-1500 nm). The Cs-18C6 film spectra show only the et band, while the Cs-C222 film spectra show only the Cs band for R=2 (Figure 12) and R=1. Stability of the Cs-18C6 blue films and residues is excellent, but not as good as $(Na^{\dagger}C222)Na^{\dagger}$ stability. ESR spectra and magnetic susceptibility of the Cs-18C6 R=0.5 residue are presented in a later section.

III.A.2. Discussion

The ctts band of I has been observed in thirty-eight solvents and mixtures as well as in crystalline RbI and CsI (89). The I ctts band persists from solution to the crystalline solid. The I ctts band in crystals lies at lower energies than in hydroxylic solvents and at higher energies than in amine and ether solvents. The solution spectra of Na, K, Rb, and Cs have been called ctts bands (22) and the film spectra indicate that the bands persist in the solid. The bands are at nearly the same position as the M bands in EDA (Figure 12) and the widths are comparable (Figure 13).

In the (Na⁺C222)Na⁻ spectrum, the origin of the shoulder at 18,000 cm⁻¹ and the high energy peak at 24,500 cm⁻¹ is uncertain. These features need not be present to observe the Na⁻ band, as shown by the spectrum of (K⁺C222)Na⁻. The simplest explanation of these features is the presence of sodium metal, since thin films of alkali metals show complex spectra (90).

However, optical spectra of films consisting of DABCO (see Reagents) and sodium metal showed no absorption bands. The bicyclic diamine DABCO was chosen as a noncomplexing diluent which is similar in size and shape to C222. A second explanation is that one or both bands result from a charge transfer from Na to Na C222 (91). This is partially supported by the absence of the two bands in the (K⁺C222)Na⁻ spectrum. However, the absence of the two bands in the latter spectrum could also be due to an expected change in crystal structure from $(Na^{\dagger}C222)Na^{\dagger}$ to $(K^{\dagger}C222)Na^{\dagger}$. In $(M^{\dagger}C222)I^{\dagger}$, the cryptand strands twist from antiprismatic to a prismatic arrangement when Na is replaced by K (92). There is another possible explanation for the shoulder. The band gap for $(Na^{+}C)Na^{-}$ is 2.3 ev (84) or 18,600 cm⁻¹. The shoulder could be a transition from the valence band to the conduction band in the semiconductor.

The band of Na in the film is very similar to that in solution. The band of Na in solution has been attributed to a bound-bound transition (3s → 3p) with some contribution from a bound-continuum band (85). The bound excited state may autoionize into the continuum. Alkali metal anions in the gas phase exhibit photodetachment through autoionization (86). The solution transition for Na and the other alkali metal anions in solid films is modified by crystal field effects.

A longstanding question has concerned the origin of the metallic appearance of alkali metal anion salt

crystals. The spectra show absorption bands with high intensity in the near-infrared and a sharp cutoff in the visible, behavior similar to the plasma absorption of metals. This can lead to a strikingly metallic appearance even for nonconducting crystals (93).

The band assigned to trapped electrons in films from K-C222 R=1 solutions is very similar to optical bands of trapped electrons in both crystalline and glassy solids. Shida et al. (94) reported the optical spectra of the trapped electron in more than forty organic and aqueous glasses. These bands are in the near-infrared and visible and exhibit a high energy tail similar to the solvated electron band.

A highly studied trapped electron in crystalline solids is the color center or F-center (German, farbzentrum) in alkali halides (95). The F-center is an electron localized in an anion vacancy defect in the solid. If the dark blue solid which forms from a solution of K⁺C222 and e_{solv} is (K⁺C222)e⁻, then it can be thought of as an F-center solid in which all anion vacancies are filled by electrons.

For F-centers in alkali halides, the energy of maximum absorption, E_{max} , is closely related to the size of the anion vacancy. This is expressed in the semi-empirical equation of Ivey and Mollwo (95):

$$E_{\text{max}} = 17.4 \text{ a}^{-1.83}$$
 (10)

where a is the interionic (cation-anion) distance in units of 10^{-8} cm and $E_{\rm max}$ is in electron volts. The Ivey-Mollwo equation holds for alkali halides with the NaCl structure, which is face-centered cubic. (This excludes the chloride, bromide, and iodide of cesium, which have simple cubic structures.) The simplest structural model for the electride $(K^+C)e^-$ is a closest-packed structure of cryptated potassium cations with trapped electrons in the octahedral interstices. The radius of K^+C222 is about 5.5 A, which would give an interionic distance of 7.77 A. The Ivey-Mollwo equation predicts an absorption maximum in the infrared at 3300 cm⁻¹ (3000 nm).

This is the correct spectral region, but the equation obviously fails quantitatively. This is not too surprising, since the two systems present very different environments for the trapped electron. In the F-center case, the electron is surrounded by cations which are small compared to the anions. For example, the radius ratio r_+/r_- for NaCl is 0.53 where r_+ and r_- are the cation and anion radii, respectively. The radius ratio for CsF is 1.24. In contrast to the alkali halides, the radius ratio for $(K^+C)e^-$ in the proposed model is 2.4. The environment for the trapped electron in this solid is then exactly opposite that in the alkali halides. The trapped electron is surrounded by cations effectively large in size and presumably small anions (other trapped electrons). If the Ivey-Mollwo equation is recast using

the anion radius instead of the interionic distance, the predicted absorption energy is in the visible portion of the spectrum.

Another model is the particle in a spherical container with an infinite potential outside and zero potential inside the container. Assuming a sphere radius of 2.28 A (as before) for the trapped electron in both the ground and excited states, the model predicts an s to p transition at 3190 cm⁻¹ (3100 nm). Thus, the prediction by the Ivey-Mollwo equation and the spherical container calculation of absorption in the infrared are in qualitative agreement with experiment. The physical situation is, however, much more complex than these simple models and awaits a better model.

Shoulders on the et and M peaks may represent different environments or sites for these species. The trapped electron in glasses, for example, is sensitive to its local environment as found in mixed solvent glasses (96). Mixtures of similar solvents cause shifts in the absorption maximum. Mixtures of two dissimilar solvents can result in two separate trapped electron absorptions. Different environments for et and M could result from heterogeneous film formation, occurrence of more than one crystalline phase, or grain boundary effects.

III.B. Films from Ammonia

Spectra were observed of films made from ammonia solutions of metal with and without complexing agents. The spectra were taken of dry films and of solvent-containing films. To produce solvent-containing films, the bulk solution in the sidearm trap was warmed until spectral changes appeared. These films with minimal solvent content are called damp films. At the other extreme are wet films, which run off the cell walls if the solvent content is increased further. Films with intermediate solvent content were also produced by controlling the temperature difference between the cell and the bulk solution. The presence of ammonia in the film was observed by absorptions in the near-ir at slightly less than 2.0 um.

In the dry films from ammonia solutions, spectra which were time-dependent over a period of minutes were sometimes observed. Only reproducible features are reported here, and this includes some time-dependent phenomena.

III.B.1. Sodium-Cryptand Films

Solutions containing sodium and C222 with R=2 give dry film spectra having the shape shown by spectrum A in Figure 17. In addition to a small near-infrared absorption at 7800 cm^{-1} (1300 nm), these films show three features similar to those obtained from methylamine: a strong absorption at 15,400 cm⁻¹ (650 nm), a pronounced

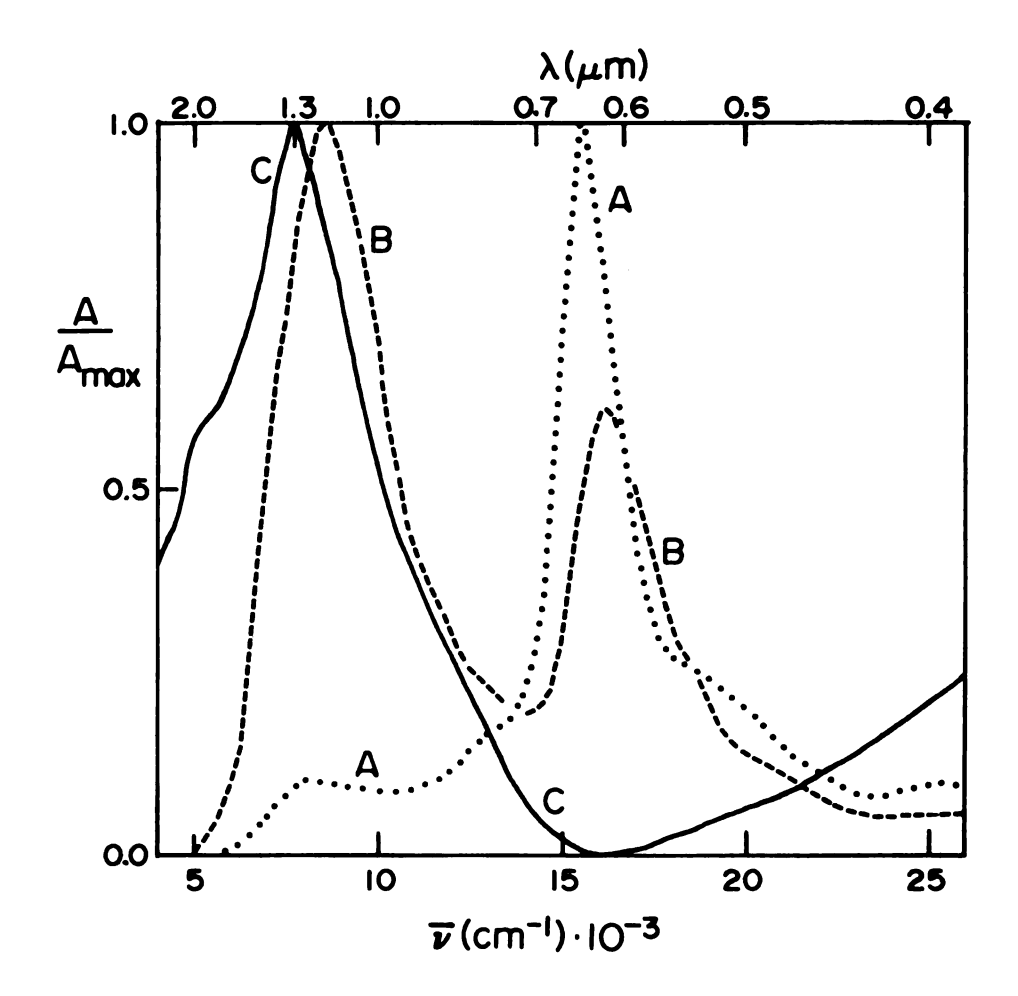


Figure 17. Spectra of sodium-C222 films from ammonia. A - dry film, R=2; B - dry film, R=1; C - wet film, R=2. The wet film spectrum with R=1 is essentially the same as C.

shoulder on the high energy side of this band, and a small distinct peak at 25,000 cm⁻¹ (400 nm). The UV spectrum is free of other bands to 41,700 cm⁻¹ (240 nm). The main absorption peak has a width at half-height of 1800 to 2100 cm⁻¹, which is considerably narrower than that obtained for Na⁻¹ in films from R=2 methylamine solutions (5200 cm⁻¹) and narrower than that of (K⁺C222)Na⁻¹ from methylamine (3400 cm⁻¹). The band at 15,400 cm⁻¹ is assigned to Na⁻¹. The small band at 7800 cm⁻¹ is assigned to trapped electrons.

When the dry film at -51°C was exposed to ammonia vapor at 45 torr or less for 20 minutes by holding the trap at dry-ice temperatures, no changes occurred in the spectrum. However, when the ammonia solution in the sidearm trap was warmed to -60°C with the film still at -51°C, pronounced spectral changes occurred in a few The peak of Na broadens, shifts to higher energies, and diminishes in intensity, while the peak of e_{t}^{-} grows in intensity. Re-freezing the ammonia in the trap with liquid nitrogen leads to a re-formed dry film showing partial recovery of the Na band and decrease of the e_{t}^{-} band, but the spectrum is not identical to that of a freshly deposited dry film. A wet film at -40°C with the ammonia solution at -51°C gave spectrum C in Figure 17, in which the Na band is absent and the peak of e_{solv}^{-} at 7700 cm⁻¹ (1300 nm) predominates.

To account for the existence of Na^- in damp and dry films, we presume that desolvated Na^+ is an efficient

electron trap. The first film to be deposited in dry film formation consists of $\mathrm{Na}^+\mathrm{C222}$, $\mathrm{Na}^+\mathrm{(NH_3)}_{\mathrm{X}}$, and $\mathrm{e}_{\mathrm{t}}^-$. As ammonia is removed from the solvated sodium cation, the electrons are trapped by Na^+ to form the more stable Na^- species. In the reverse of this process, Na^- is converted to $\mathrm{Na}^+\mathrm{(NH_3)}_{\mathrm{X}}$ and $\mathrm{e}_{\mathrm{t}}^-$ as ammonia is added. When enough ammonia is added, the film dissolves to produce a concentrated solution. The rather high absorption on the low energy side of the $\mathrm{e}_{\mathrm{solv}}^-$ band (C in Figure 17) may represent conduction electron absorption (also called a plasma edge absorption) in the concentrated solution.

There is little argument that a species having stoichiometry M exists in ammonia (5). However, there remains the question of whether this species in ammonia is the alkali metal anion M or another structure (see three possibilities shown in Figure 2). In amine and ether solvents, the alkali metal anion exists and has an optical absorption which depends on the metal: Na, K, Rb, or Cs. The M band position shows only a small solvent dependence. The M and e olvent solvent dependence of 7590 cm bands are widely separated with a difference of 7590 cm between Na and e olvent led of the solvent led of th

Metal-ammonia solutions show only one optical absorption band in the dilute concentration range. (As the concentration is increased, plasma edge absorption sets in.) The single band has a characteristic shape and location which does *not* depend on the metal dissolved (Li, Na, K, Rb, Cs, Ca, or Sr). The band location is

slightly concentration dependent, shifting from 6900 cm^{-1} at 10^{-4} MPM to 6530 cm^{-1} at 1 MPM (80). The band shape is only slightly concentration dependent. If M exists in ammonia, then its optical behavior must be very different than in all other solvents in which it is observed. In other words, the ${\tt M}^{\tt -}$ band in ${\tt NH}_3$ would have to metal-independent, absorb at much lower energies than in other solvents, and absorb within the solvated electron band. Dye (57) has summarized this situation by stating that "...there is no specific evidence for alkali anions in metal-ammonia solutions...." In the sodium-cryptand R=2 films, the shift of the Na to higher energies as ammonia is added and the complete disappearance of this band when the film becomes liquid provide evidence against the existence of the spherically symmetric anion, Na, in concentrated MAS.

Sodium solutions in ammonia with a sodium-to-cryptand mole ratio of 1.0 gave dry films whose spectrum at -45°C is shown in Figure 17 as curve B. This spectrum shows Na and e bands at 16,200 cm (615 nm) and 8600 cm (1160 nm), respectively. The spectrum does not change over a time period of 45 minutes. Spectra of wet films are virtually indistinguishable from those obtained with R=2 (spectrum C, Figure 17). However, the amount of absorbance at 4000 cm (2500 nm) in wet films with either R=1 or R=2 depends upon the amount of ammonia present and can vary from 10% of the peak absorbance to nearly 80% of the peak absorbance.

The peak of Na in a dry film with R=1 is broadened and blue-shifted by 800 cm⁻¹ compared to that obtained with R=2. When a re-formed dry film is made by evaporating ammonia from a wet film, considerably broader absorptions are observed for both Na and e_t , with the peak of the former at 15,800 cm⁻¹ (645 nm) and that of the latter at 7800 cm⁻¹ (1280 nm). Time-dependent spectra of R=1 dry films were observed in which an initial band at 5000 cm⁻¹ (2000 nm) decayed and the absorbances of both Na and e_t grew over a 16 minute period. This band at 5000 cm⁻¹ was observed a second time.

The presence of peaks for both Na and e_t when R=1 suggests that the complexation of Na by C222 in ammonia is not complete at a 1:1 mole ratio, so the initial film contains some uncomplexed Na and free cryptand. The Na acts as a trap for electrons and yields a quantity of Na equivalent to the initial amount of uncomplexed Na in the film. This explanation agrees with the behavior upon solution decomposition. Decomposition tends to destroy the cryptand, thus releasing complexed Na for reaction with e_t . As the solution aged, the ratio A_{Na} - A_{e_t} in dry film spectra increased from 0.61 to 2.0, as expected for films from a solution in which R increased.

III.B.2. Wet and Dry Metal Films in the Absence of Complexing Agent

In order to see whether precipitated metal might give rise to some of the observed absorption bands and

to determine the absorption spectra of concentrated metalammonia solutions (MAS), alkali metal films in the absence of crown ethers and cryptands were prepared by evaporating MAS to dryness on quartz cell walls. When solutions of either sodium or potassium in ammonia were evaporated, the blue color rapidly disappeared, leaving an inhomogeneous film which appeared to be gray-white flecks of Such dry "films" showed no absorption bands. experiment was carried out with the bicyclic diamine DABCO, N(CH₂CH₂)₃N (see Reagents) to provide a matrix for the metal similar to that provided by crowns and cryptands. An equimolar solution of sodium and DABCO was evaporated to form a dry film. No bands were observed in the dry film spectrum. All films when wet with ammonia had the general shape shown in Figure 18 for wet sodium (spectrum A) and wet potassium (spectrum B) films. They are similar in general shape to those calculated from reflectance spectra of 14 mole percent Na solutions in ammonia, but the latter do not show the continued rise in the infrared region below about 7000 cm⁻¹. Also, the rapid drop in absorbance (plasma edge) as calculated from reflectance spectra occurs about 2000 cm⁻¹ to the red compared with that observed here. A distribution of concentrations or film inhomogeneity could affect the spectra observed. Because of the general reproducibility of the spectra shown in Figure 18 for concentrated MAS, this shape will be considered representative of the plasma absorption of conduction

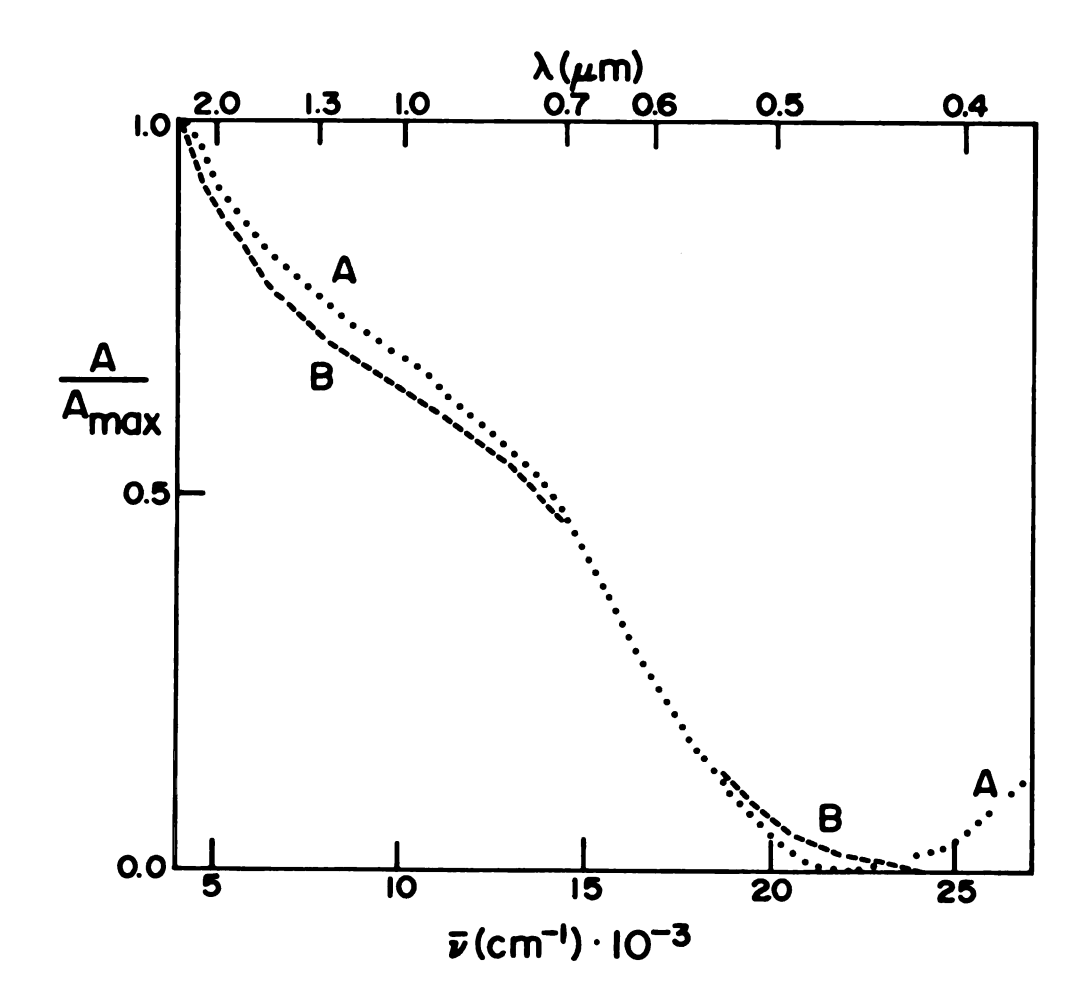


Figure 18. Wet film spectra of Na(A) and K(B) obtained by condensing ammonia onto dry metal films produced by evaporation of metal-ammonia solutions.

electrons. A particularly noteworthy feature is the high absorption in the infrared region below 5000 cm^{-1} . This contrasts with the behavior of the band attributed to trapped electrons in dry Na-C222 films with R=1 (spectrum B, Figure 17), which shows little absorption at 5000 cm^{-1} .

III.B.3. Potassium-Cryptand Films

Spectrum A in Figure 19 is from a film formed from a potassium R=2 ammonia solution. In addition to the peak of K^- at 11,200 cm⁻¹ (890 nm), there is an absorption at ~ 7700 cm⁻¹ (1300 nm) due to trapped electrons. The band of K^- is considerably broader than that observed from methylamine. This follows the general pattern of band-broadening when multiple bands are present. When the dry film was made progressively wetter with ammonia, the changes shown in B, C, and D of Figure 19 occurred. The peak of K^- diminished in intensity, while that of $e^+_{\rm t}$ grew and shifted to the red. At the same time, the infrared absorption at 4000 cm⁻¹ grew until a liquid film (spectrum D) formed, which appears to have considerable plasma absorption.

Dry films made from K-C222 with R=1 (nominal) yielded time-dependent spectra, as shown by A and B in Figure 20. A peak of K^- at 11,000 cm⁻¹ (900 nm) and a peak at 5600 cm⁻¹ (1800 nm) were present in fresh (or re-formed) dry films. Upon standing, the K^- peak decayed to a shoulder and the absorption of e_{τ}^- grew.

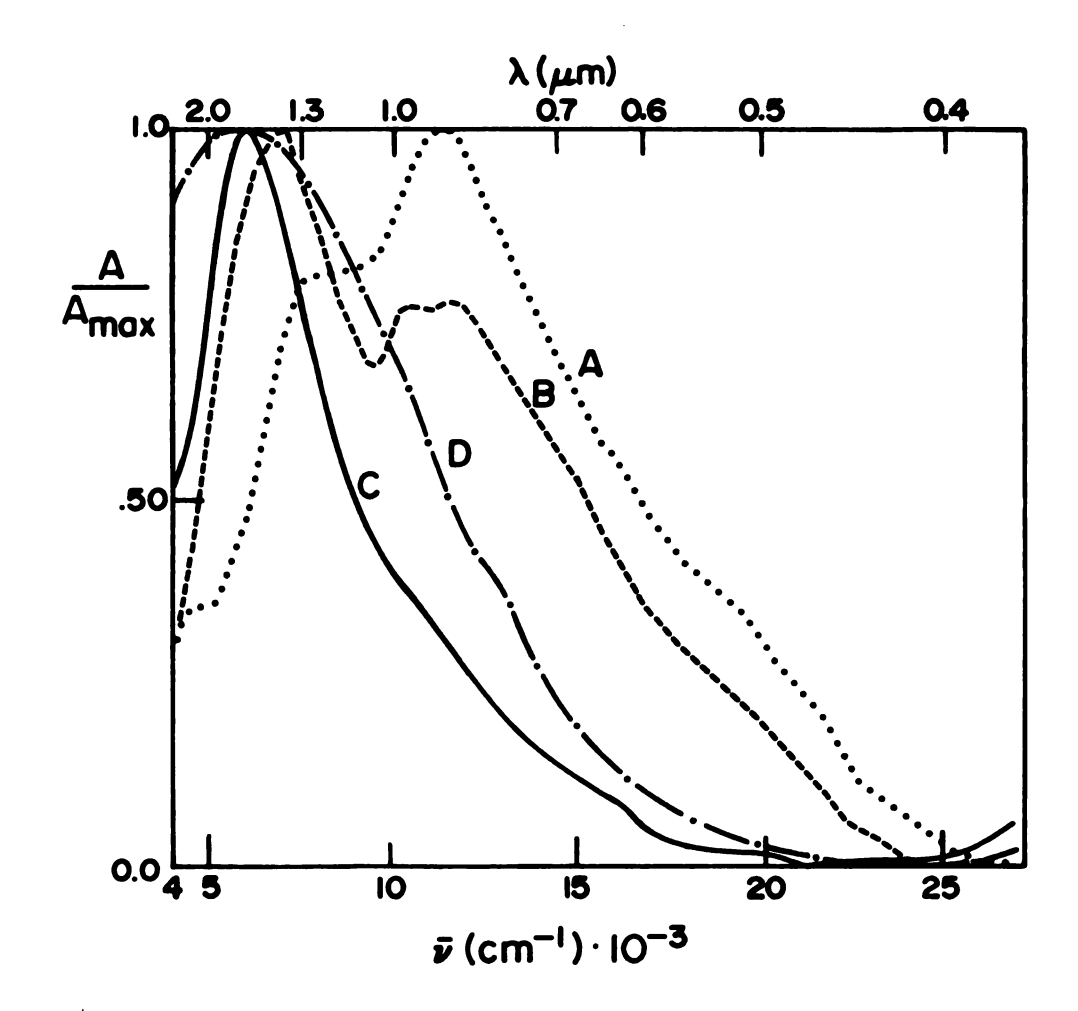


Figure 19. Spectra of K-C222 films from ammonia with R=2. A - dry film, B - damp film, D - wet film, C - intermediate film.

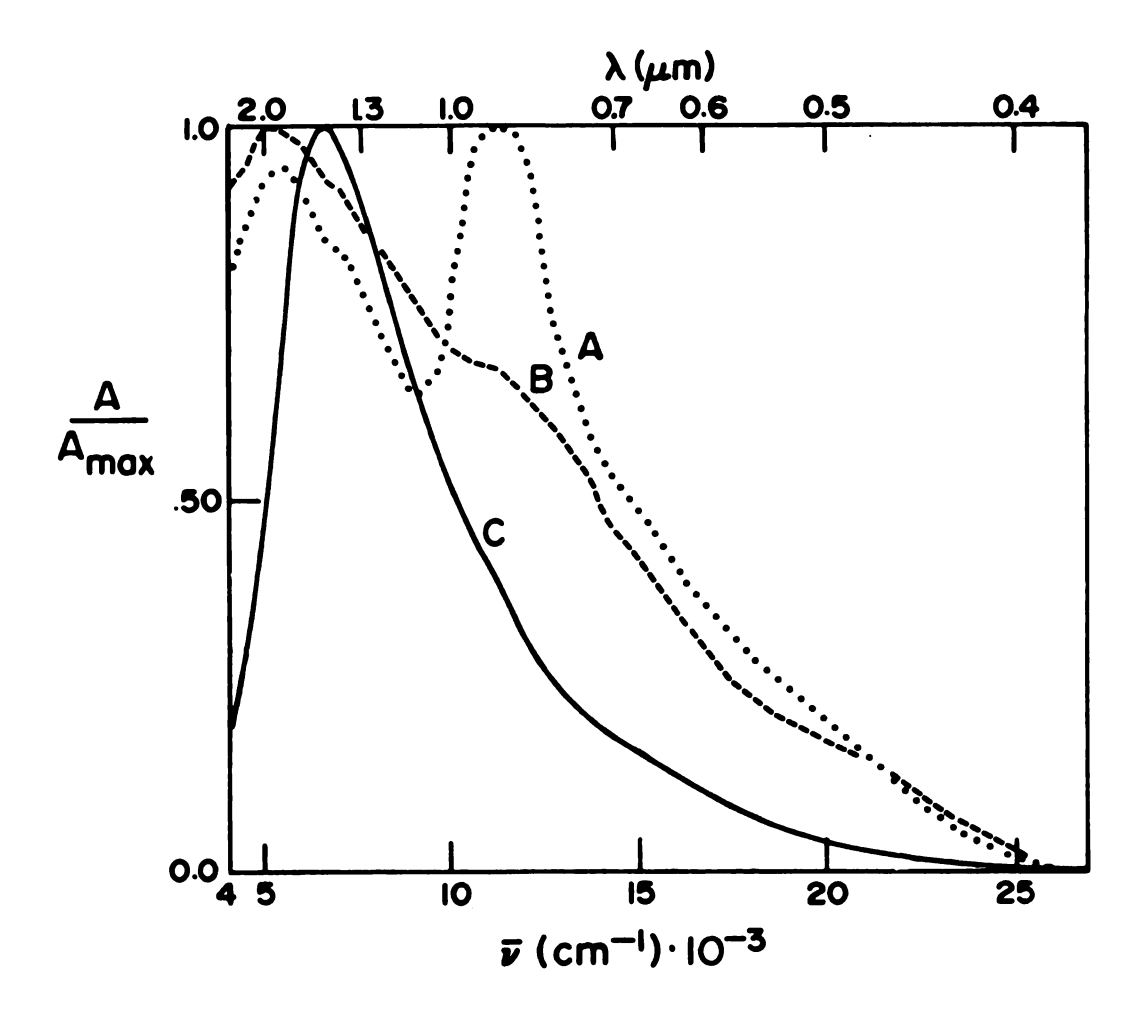


Figure 20. Spectra of K-C222 films from ammonia with R=1. A - initial dry film, B - dry "annealed" film, C - wet film.

The final spectrum (B in Figure 20) has a shape which is remarkably similar to the plasma absorption of conduction electrons in concentrated MAS and suggests delocalization of the trapped electron as in an expanded metal.

The spectra in Figure 20 are for films made from a potassium-rich (R=1.05) K-C222 solution. The film spectra from a cryptand-rich (R=0.95) K-C222 solution are also time dependent. The fresh unannealed film gave an absorption spectrum of trapped electron and little, if any, K⁻. The absorbance at 4000 cm⁻¹ (2500 nm) was zero. This film annealed at a higher temperature to give a spectrum similar to spectrum B of Figure 20. The same R=0.95 solution which was used to produce films for optical spectra was used to prepare a solid for an ESR study (see ESR results).

When the dry film (spectrum B of Figure 20) is wet with ammonia, the et peak shifts to higher energies, while the shoulder at 11,000 cm⁻¹ disappears to finally yield spectrum C of Figure 20. In contrast to the films with R=2, wet films with R=1 (more cryptand) show little absorption at 4000 cm⁻¹. It is possible that the presence of excess cryptand in potassium-ammonia solutions decreases the metallic character. However, this apparent plasma absorption may be due to shifting infrared bands.

III.B.4. Rubidium-Cryptand Films

The spectra of freshly-prepared dry Rb-C222 films with R=2 prepared from ammonia (spectrum A, Figure 21) are similar to those of potassium. The Rb peak occurs at 10,200 cm⁻¹ (980 nm), while the et shoulder is at 6700 cm⁻¹ (1500 nm). The spectra of all dry films are time-dependent, however. After about 45 minutes the peak of et has disappeared, while that of Rb has shifted to higher energies and occurs at 11,050 cm⁻¹ (905 nm). Spectrum B in Figure 21 shows a damp film with a peak of et at 6100 cm⁻¹ (1640 nm) and very little Rb absorption. Wet films appear to have a combination of the et absorption shifted to lower energies and a plasma absorption (spectrum C). Some damp films showed timedependent spectra with gradual decay of the et peak and growth of an Rb peak.

Spectrum A, Figure 22, is the initial spectrum of a dry Rb-C222 film with R=1. In contrast to the R=2 case, the major feature is an e_{t}^{-} peak at 6740 cm⁻¹ (1480 nm), while the Rb⁻ absorption is a shoulder. Over a period of 40 minutes, the spectral shape changed gradually to that shown by B in Figure 22. With the cell maintained at -50 \pm 2°C and the sidearm trap at liquid nitrogen temperatures, the magnitude of the e_{t}^{-} peak decreased by \sim 25% and the peak shifted to 5620 cm⁻¹ (1780 nm), a shift of 1100 cm⁻¹. The absorbance of the Rb⁻ peak remained nearly constant. Spectrum C, Figure 22, is that of a wet film which shows a high, broad

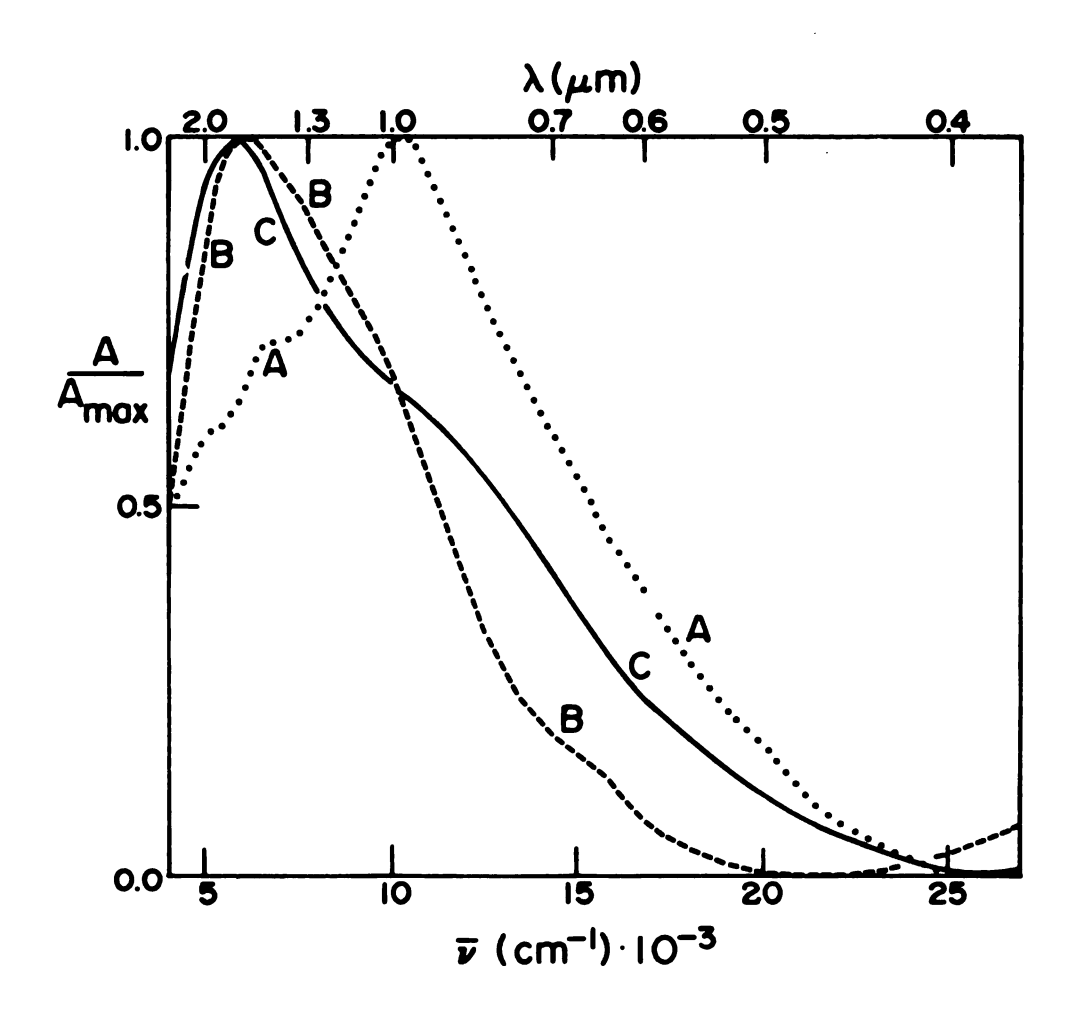


Figure 21. Spectra of Rb-C222 films from ammonia with R=2. A - dry film, B - damp film, C - wet film.

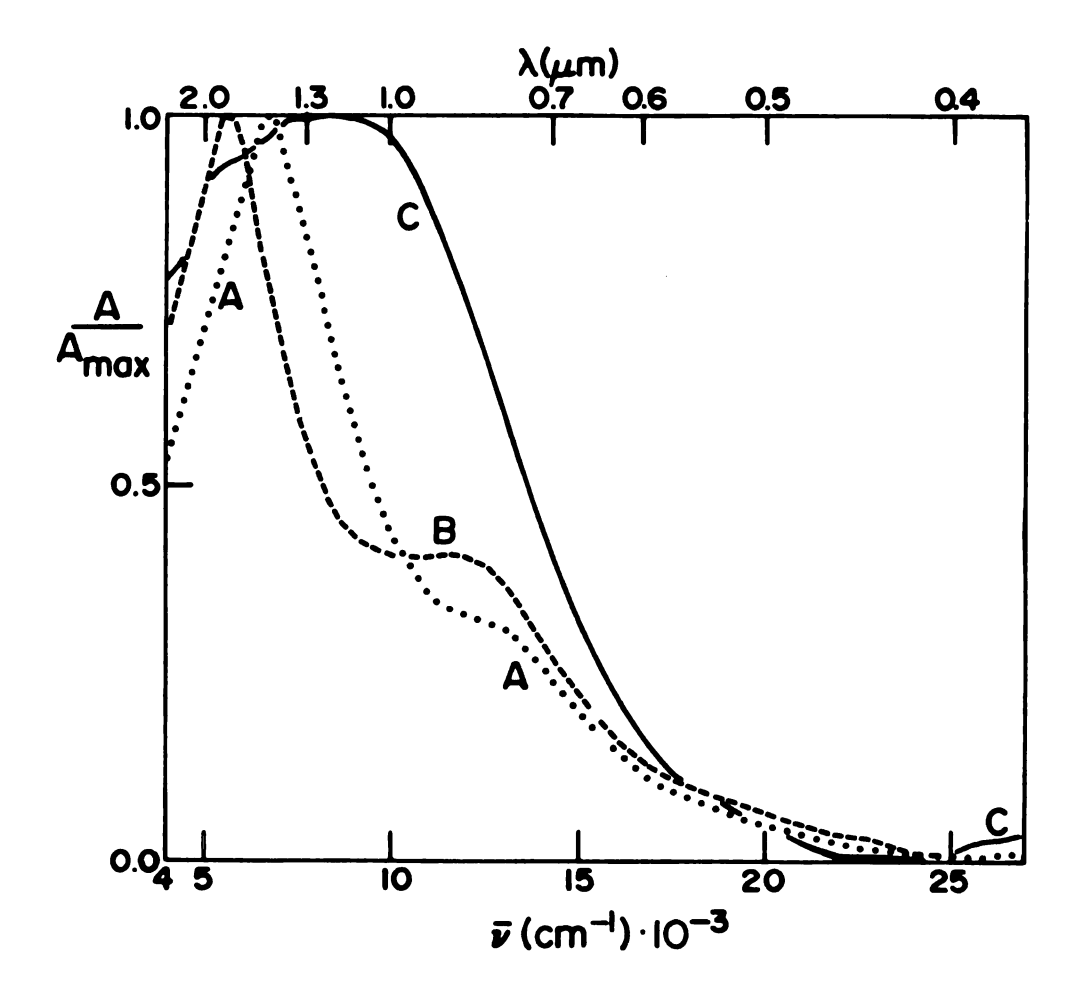


Figure 22. Spectra of Rb-C222 films from ammonia with R=1. A - initial dry film, B - film A after 40 minutes, C - wet film.

infrared absorption which appears to be a superposition of the solvated electron band with a plasma absorption.

III.B.5. Cesium-Cryptand Films

The spectrum of a dry film made from an ammonia solution containing two moles of cesium to each mole of cryptand (R=2) is shown as spectrum A in Figure 23. Main bands are at 6,400 cm⁻¹ (\sim 1560 nm), 9,600 cm⁻¹ (\sim 1040 nm), 11,600 cm⁻¹ (\sim 860 nm), and 13,700 cm⁻¹ (\sim 730 nm). The 6,400 cm⁻¹ band has a shoulder on the low energy side. In the dry films, the absorbance of the 6,400 cm⁻¹ band (e_{t}^{-}) is about equal to that of the 9,600 cm⁻¹ band.

Spectrum B in Figure 23 shows an intermediate wet film spectrum resulting from the bulk solution being melted and warmed to -60°. The triplet is diminished in intensity and the near-infrared band appears at $5,750~\text{cm}^{-1}$ ($\sim 1740~\text{nm}$), a red shift of 650 cm⁻¹. If the film is warmed to -34° and the bulk solution is warmed to -38°, the wet film spectrum A of Figure 24 is found, in which the only apparent band is the near-IR band at $5,750~\text{cm}^{-1}$.

The recovery behavior of such a wet film can be examined as shown in Figure 24. Spectrum B was taken from the film at -45° five minutes after the bulk solution was frozen with liquid nitrogen. The main band is at 9,100 cm⁻¹ (~ 1100 nm). The near-IR e⁻ peak appears as a shoulder on the main band. Spectrum C was observed 37 minutes later. The e⁻ shoulder had grown considerably

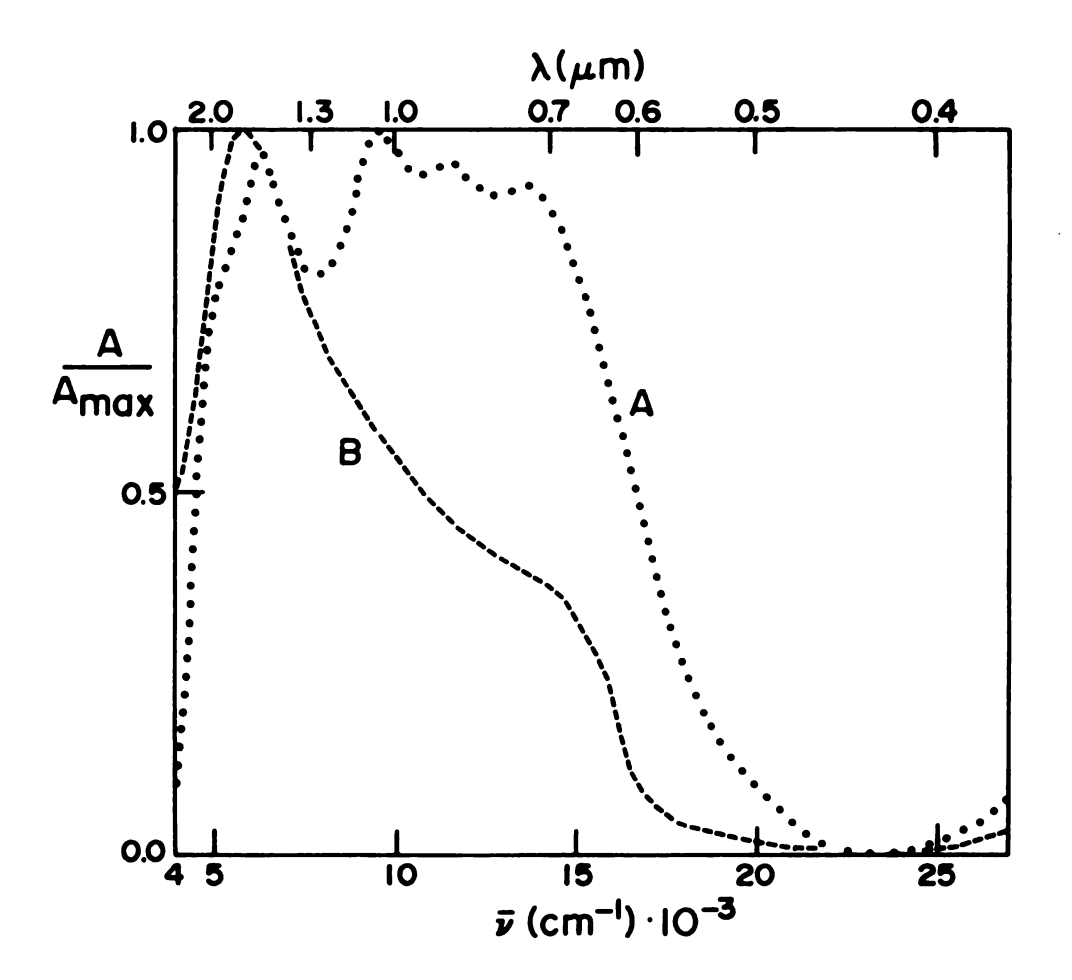


Figure 23. Spectra of Cs-C222 films from ammonia with R=2. A - dry film, B - damp film.

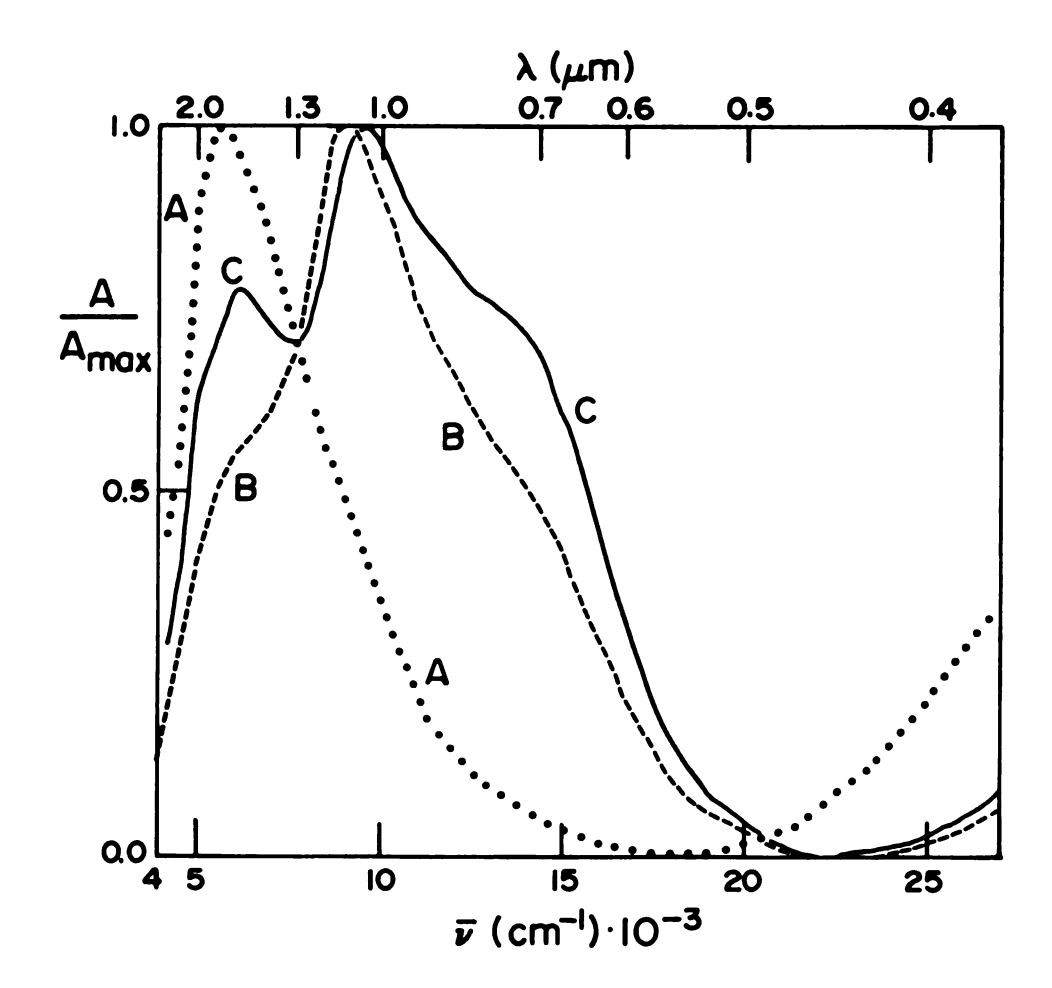


Figure 24. Spectra of Cs-C222 films from ammonia with R=2. A - wet film, B - same film 5 minutes after freezing bulk solution, C - 37 minutes after freezing bulk solution.

to a peak at 6,000 cm⁻¹ (~ 1670 nm). A rising absorbance on the high energy side of the shifted main band suggests the presence of the triplet observed in the dry film spectrum (Figure 23). Time-dependent changes of the film spectrum have also been observed for dry films.

A second type of wet film spectrum is shown in Figure 25. The spectrum resembles that of a plasma edge. The film was at -33° and the bulk solution was at -40° .

The dry-film spectra for cesium-cryptand R=2 from methylamine and ammonia are shown for comparison in Figure 26 as spectrum A and B, respectively. The film from methylamine (spectrum A) shows a single Cs band. The film from ammonia shows multiple peaks. It is known that C222 can form both inclusive and exclusive complexes with Cs in various solvents (87) and that the complexation constant is smaller than with K, Rb or Na (88). Therefore, in ammonia one might have free Cs and C222 as well as inclusive and exclusive complexes. As a result, films from ammonia probably contain a variety of sites for both e and Cs.

III.B.6. Cesium-Crown Films

The spectrum of a dry film made from an ammonia solution containing Cs and 18C6 with R=0.5 is shown as C in Figure 26. The main peak of $e_{\bar{t}}$ at 6800 cm⁻¹ (1470 nm) is similar to that in the corresponding film spectrum from methylamine (Figure 16). However, films

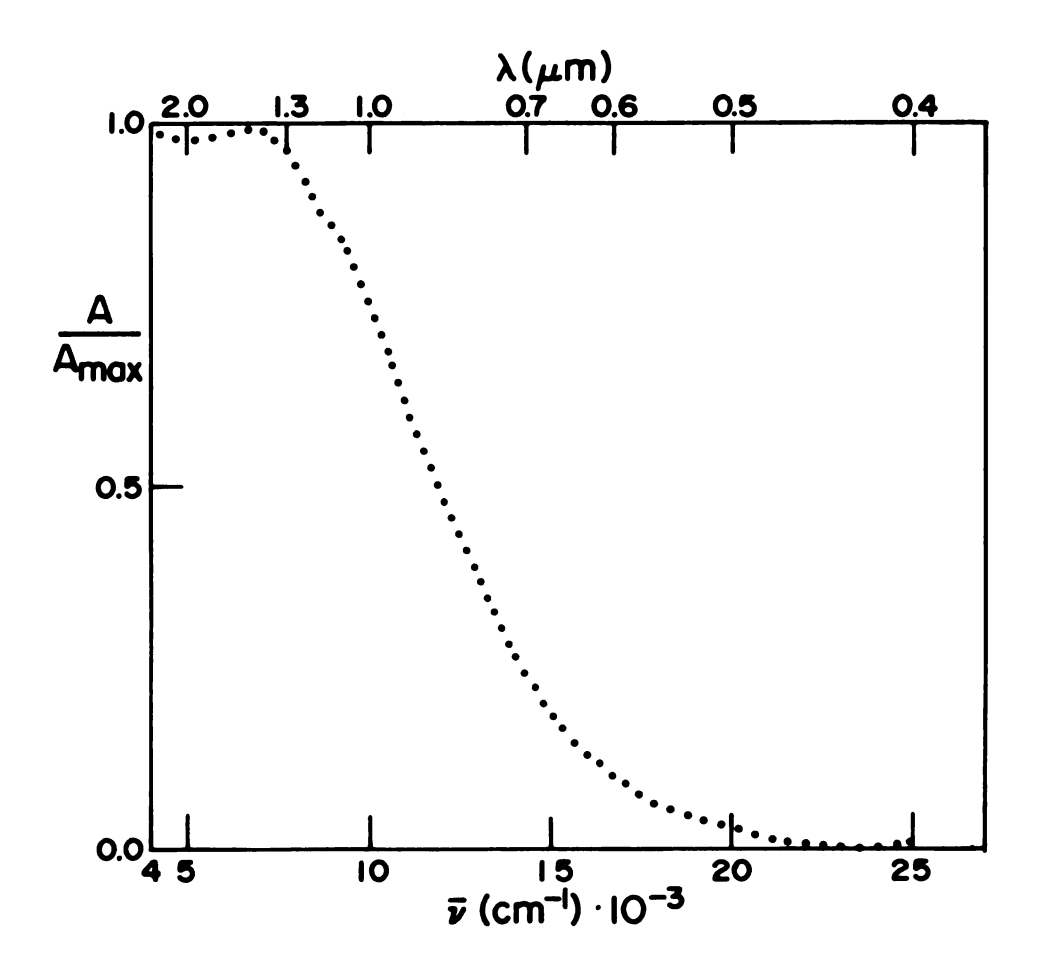


Figure 25. Spectrum of Cs-C222 wet film from ammonia with R=2.

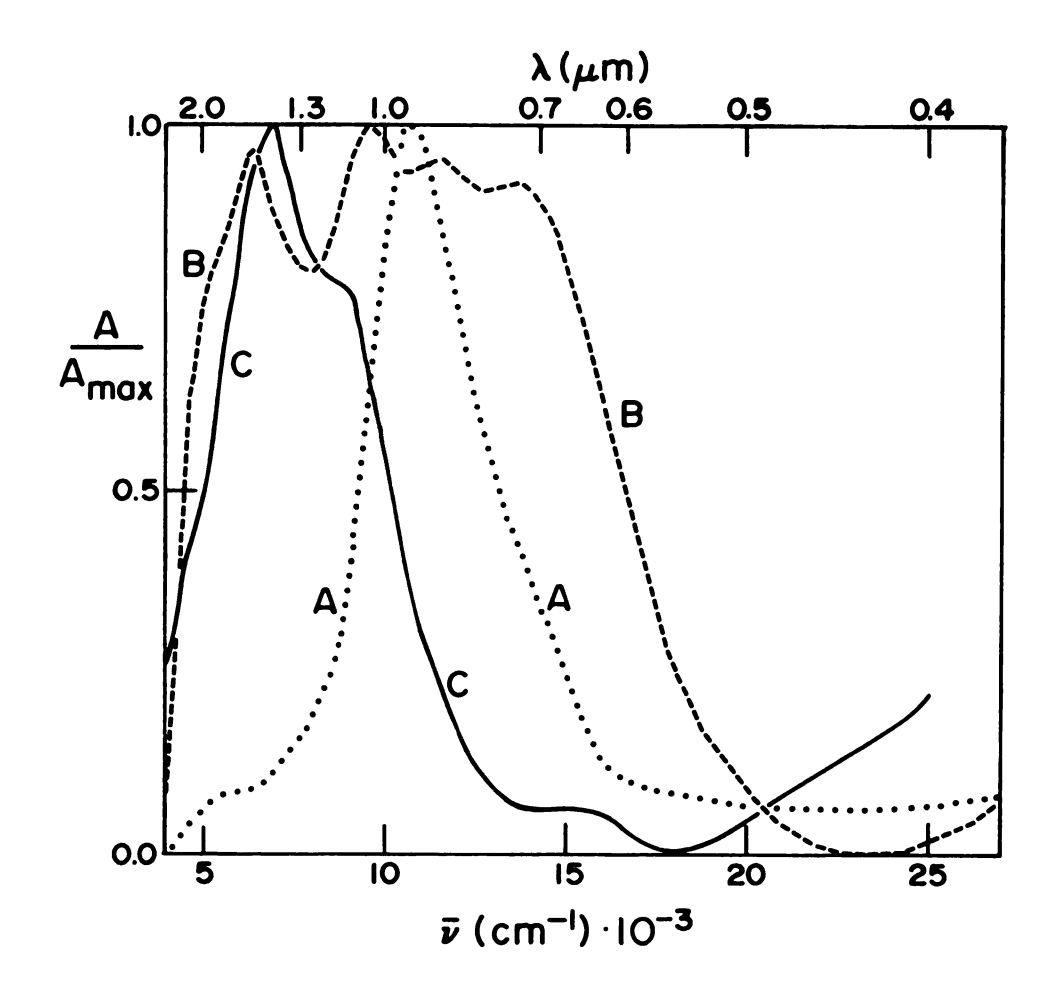


Figure 26. Spectra of Cs-C222 and Cs-18C6 dry films. A - Cs-C222 film, R=2, from methylamine; B - Cs-C222 film, R=2, from ammonia; C - Cs-18C6 film, R=0.5, from ammonia.

from ammonia show a shoulder at 8500 cm $^{-1}$ (1180 nm), probably due to interaction of e_t^- with Cs $^+$.

III.B.7. Lithium-Cryptand(2,1,1) Films

Cryptand C211 is optimal for complexation of Li⁺ (88), as shown in Figure 4. Films with R=2 from ammonia were formed. The dry film spectrum, spectrum A in Figure 27, shows no evidence for Li⁻ but does show a similarity to the plasma absorption of concentrated MAS (Figure 18). No additional bands were observed in the region 4000 to 45,450 cm⁻¹ (220-2500 nm). The plasma absorption suggests the formation of an expanded metal in which the electrons are delocalized. The formation of a damp film gives spectrum B of Figure 27, which also appears to be a plasma spectrum. When more ammonia is added, spectrum C is obtained. It shows an absorption at 8340 cm⁻¹ (1200 nm) with substantial absorption extending further into the infrared.

III.C. Summary of Optical Spectra

The peak positions in the films studied are summarized in Table 4. The optical spectrum in the systems observed depends on the metal, cation-complexing agent, and solvent used. Four types of solid films form:

- 1) solids which contain salts of alkali metal anions,
- 2) solids which contain trapped electrons, 3) solids which are mixtures of the latter two, and 4) solids which appear to be expanded metals.

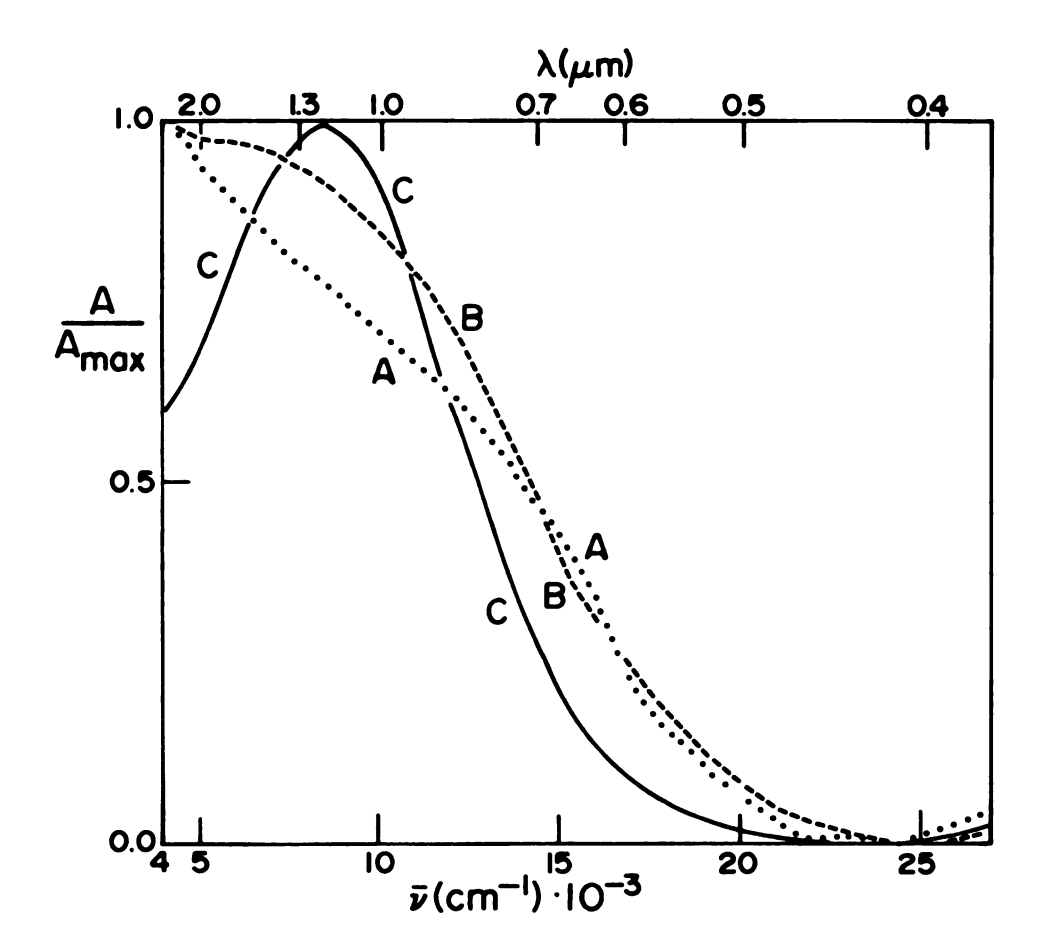


Figure 27. Spectra of lithium-C211 films from ammonia with R=2. A - dry film, B - damp film, C - wet film.

Summary of peak positions in optical spectra of films Table 4.

×	Solvent	Ligand	~	Film Con- ditiona	, W	eak Positi	Peak Positions ^b (cm ⁻¹)	Plasma Character? ^C
		0				ני		
Na	CH ₃ NH ₂	C222	2	dry	* 15,400(m)	:	18,900(s),24,500(sp)	No
	NH ₃	C222	7	dry	* 15,400(m)	7800(sp)	18,000(s),25,000(sp)	No
			7	wet		7700	;	Yes
			Н	dry	* 16,200	8600(m)	;	No
			1	wet	*	7700(m)	:	Yes
			1	dry(ref)	* 15,800	7800(m)	:	No
		none	ı	wet	1 1	:	plasma edge	Yes
×	CH ₃ NH ₂	C222	2	dry	11,900	!		No
			1	dry	1 1	7400	:	Yes
	NH ₃	C222	7	dry	11,200(m)	7700(s)	:	۰.
			7	damp	11,000	7000(m)	:	۰.
			7	wet	:	0009	•	Yes
			П	dry(fr)	11,000(m)	2600	!	Yes
							The second secon	

Table 4 (continued)

				1:1 TOD		eak Positi	Peak Positions ^b (cm ⁻¹)	Dlacma
X	Solvent Ligand	Ligand	24	ditiona	M-	e t	Others	Character?
×	NH ₃	C222	7	dry (ann)	11,000(s)	5000(m)		Yes
			-	wet	1	0099	!	N O
		none	ı	wet	!	:	plasma edge	Yes
Rb	Rb CH ₃ NH ₂	C222	2	dry	* 11,600	:	!	ON
			1	dry	* 11,000	7000(m)	15,000(s),18,000(s)	No
	NH ₃	C222	7	dry(fr)	* 10,200(m)	6700(s)	1 1	<i>د</i> ٠
			7	dry(ann)	* 11,050	;	!	<i>د</i> ٠
			7	damp	1 1 1	6100	!!!	Yes
			7	wet	1 1 1	0009	12,000(s)	Yes
			-	dry(fr)	* 12,000	6740(m)	;	Yes
			-	dry(ann)	ınn) * 12,000(s)	5620(m)	•	Yes

Table 4 (continued)

				ilm Con-			Peak Positions ^b (cm ⁻¹)	s ^b (cm ⁻¹)	
Σ	Solvent	Ligand	24	ditiona	'	-W	e.	Others	_ Character? ^C
Cs	Cs CH ₃ NH ₂	18C6	2,1, 0.5	dry		!!!	6400-6700	15,400(sp)	NO
		C222	2 or	dry	• •	10,500	!	;	NO
	NH ₃	18C6	0.5	dry	*	1 1	6800(m)	8500(s)	No
		C222	2	dry	*	0006 (m)	6400	11,600;13,700	No
			7	damp	*	!	6500	!	Yes
			2	wet	*	!	5750	:	<i>د</i> ٠
Li	NH ₃	C211	2	dry	*			:	Yes
			7	damb	*	!	1 1	!	Yes
			2	wet	*	!	!	8340	٠.

aref = re-formed, fr = fresh, ann = annealed.

bm = major peak, s = shoulder, sp = small peak.

As judged by absorbance at 4000 cm⁻¹.

Data by the author. Remainder in collaboration (98-100).

In films from methylamine, the species found are similar to those in solution. In ammonia, however, the significant number of uncomplexed cations caused by the low complexation constant plays a major role in the formation of dry film species. Thus, the solution bands in methylamine presumably persist from solution to solid, while solids from ammonia exhibit new bands not observed in ammonia solutions.

MAGNETIC STUDIES

The magnetic susceptibility of several solids was studied as a function of temperature. These solids include crystals of (Na⁺C222)Na⁻, the dark blue-black residue from R=1 solutions of K and C222, and the dark blue residue from R=0.5 solutions of Cs and 18C6. The ESR spectra of the latter two, in addition to the dark blue residue from a R=1 solution of Ba and C222, have been studied at temperatures down to liquid helium temperatures.

IV.A. Magnetic Susceptibility

IV.A.1. Background

When a substance is placed in a magnetic field of strength, \overline{H} , the magnetic induction, \overline{B} , in the substance is given by the equation:

$$\overline{B} = \overline{H} + 4\pi \overline{M} \tag{11}$$

where \overline{M} is the intensity of magnetization or the magnetic moment per unit volume of the substance. If the substance is isotropic, \overline{M} is a proportional to \overline{H} and the proportionality constant is the volume magnetic susceptibility

$$\chi_{v} = \frac{M}{H} \tag{12}$$

Two other bases are commonly used. The susceptibility per gram or specific susceptibility is defined as

$$\chi_{g} = \chi_{V}/\rho \tag{13}$$

where ρ is the density. If M is the molecular weight, the molar susceptibility χ_{M} is

$$\chi_{M} = M\chi_{g}. \tag{14}$$

If the net susceptibility is negative, the substance is diamagnetic. Substances with a positive net susceptibility are paramagnetic.

Various paramagnetic and diamagnetic terms which may contribute to the net susceptibility are shown in Figure 28 along with their behavior with temperature and their relative magnitudes. The diamagnetic susceptibility term arises from field-induced angular momentum and is present in all substances placed in a field.

Positive contributions to the net susceptibility may have several sources. The free spin paramagnetism in Figure 28 is the familiar paramagnetism due to unpaired electrons. The temperature dependence of this paramagnetism is often described by the Curie law:

$$\chi_{M} = \frac{Np^{2}\mu_{B}^{2}}{3kT} \tag{15}$$

where N is Avogadro's number, k is Boltzmann's constant, μ_B is the Bohr magneton (eh/4 mm), and p is the effective number of Bohr magnetons defined as

$$p = g[J(J + 1)]^{\frac{1}{2}}.$$
 (16)

Here g is the g-factor and J is the sum of orbital and spin angular momentum. For a single spin with no orbital angular momentum, g takes the free electron g value of 2.0023 and J=S. The Curie-Weiss law substitutes $(T-\theta)$ for T of the Curie law. The Weiss constant is θ . Often the Curie-Weiss law fits the behavior better than the Curie law. The free spin paramagnetism in simple paramagnets is much larger in magnitude than the diamagnetic contribution so the net susceptibility is positive.

Another example of paramagnetism occurs for conduction electrons in a metal. This is of interest here since some of the electrides appear to be expanded metals. The Pauli paramagnetism of conduction electrons is independent of temperature, as shown in Figure 28. To explain this result, Fermi-Dirac statistics are applied to a model for metals called the free electron or Fermi gas model. this model, the valence electrons of the atoms in the metal are assumed to move freely throughout the solid and forces between conduction electrons and ionic cores are neglected. The Fermi gas in one dimension is the particlein-a-box model. At absolute zero, all available energy levels up to a certain level, the Fermi energy (ϵ_F) , are filled. The Fermi energy depends only on conduction electron density. The Fermi energy defines the Fermi temperature:

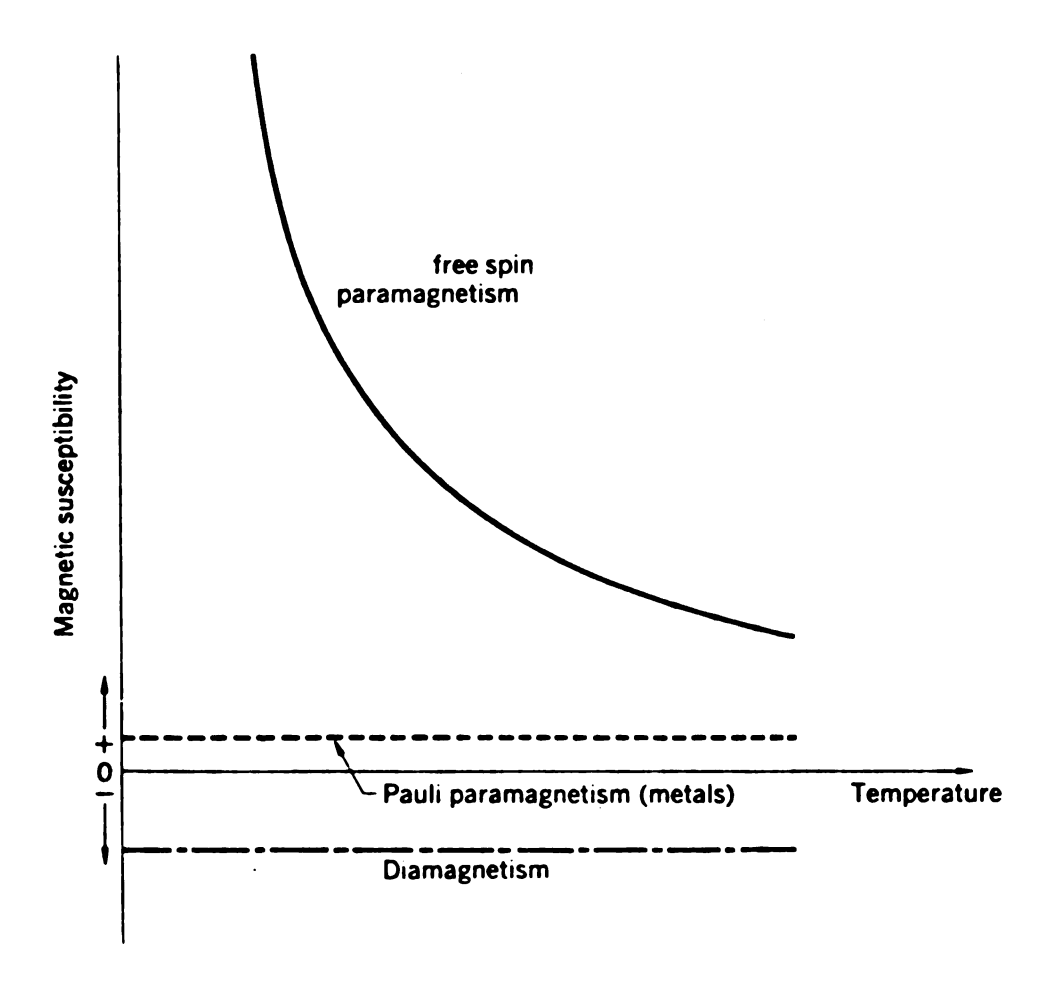


Figure 28. General temperature behavior of some diamagnetic and paramagnetic susceptibilities.

where m is the electron mass and $\frac{n}{V}$ is the number of electron in a given volume. As the temperature of the metal is increased, some energy levels which were vacant at absolute zero become filled as some previously filled orbitals become vacant. When the metal is placed in a magnetic field, only those electrons that are within about kT in energy of ε_F may change spin. So only the fraction T/T_F of electrons contributes to the conduction electron (Pauli) paramagnetism. The susceptibility of the free electron gas, then, is

$$\chi_{\mathbf{M}} = \frac{N\mu_{\mathbf{B}}}{\mathbf{k}T_{\mathbf{F}}}.$$
 (18)

The diamagnetism of the atom core electrons also contributes to the net susceptibility of the metal.

IV.A.2. Results and Discussion

IV.A.2.a. (Na⁺C222)Na⁻

Crystals of $(Na^+C222)Na^-$ are diamagnetic at 4.2, 100, and 300 K and show no evidence for magnetic ordering (such as in anti-ferromagnetism). The measured gram susceptibility is $-0.94 \cdot 10^{-5} \text{ cm}^3\text{g}^{-1}$. Using the density of 1.064 g cm⁻³ from the crystallographic study (67), the volume susceptibility is $-1.0 \cdot 10^{-5}$ and the molar susceptibility is $-4.2 \cdot 10^{-4} \text{ cm}^3\text{mole}^{-1}$.

The observed molar susceptibility can be compared to that calculated using Pascal's constants for diamagnetic

susceptibility. Pascal's method (78) assumes that the molar susceptibility can be calculated by summing the atomic susceptibilities (Pascal's constants) and adding a constitutive constant (for rings, double bonds, etc.). For example, the calculated $\chi_{\rm M}$ for C222 is -2.45 · 10⁻⁴ cm³mole⁻¹ with no constitutive constants (which are positive for rings) and the experimental value determined in this work is -1.8 · 10⁻⁴ cm³mole⁻¹. The calculated molar susceptibility for (Na⁺C222)Na⁻ is then

$$\chi_{(Na^+C)Na^-} = \chi_{C222} + \chi_{Na^+} + \chi_{Na^-}.$$
 (19)

The experimental value for χ_{C222} may be used with the Pascal constant for Na⁺, but there is no tabulated constant for Na⁻. However, the Langevin equation for diamagnetism states that the diamagnetic susceptibility is proportional to the mean square distance of the electrons from the nucleus. The radius of I⁻ is close to that of Na⁻, so χ_{I} is used for χ_{Na} in the calculation. The calculated value is then (from equation 19)

$$\chi_{(Na^+C)Na^-} = (-1.8 - 0.05 - 0.52) \cdot 10^{-4}$$

= -2.4 \cdot 10^{-4} \cdot cm^3 mole^{-1} (20)

which is comparable to the observed value of $-4.2 \cdot 10^{-4}$ cm 3 mole $^{-1}$.

IV.A.2.b. Solids from K-C222 R=1 Solutions

Four attempts to prepare a (K⁺C222)e⁻ solid from methylamine solutions for measurement in the Faraday balance resulted in one sample. It had some white solid at the top of the dark-blue solid. The other three samples decomposed during preparation. Measurements were made on the dark-blue sample at 77, 87, 126, 194, and 210 K. The dark-blue solid was allowed to decompose to a green solid and a yellow solid, and these were measured at 77, 126, and 210 K. The blue, green, and yellow states of the sample were all diamagnetic to nearly the same degree and showed no temperature dependence.

A sample was prepared in an apparatus similar to that used for Faraday balance samples. The dark-blue solid was measured at 4.2 K in a mutual inductance apparatus in Prof. J. Cowen's laboratory of the M.S.U. Physics Department. The susceptibility of the sample was below the instrument detection limit, indicating that the absolute value of $\chi_{\rm M}$ for the sample was less than $\sim 1 \cdot 10^{-3}~{\rm cm}^3{\rm mole}^{-1}$. If the undecomposed sample had consisted of locally trapped electrons and had obeyed Curie's law, the molar susceptibility would have been $5 \cdot 10^{-3}~{\rm cm}^3{\rm mole}^{-1}$, which is above the detection limit.

There are several possible explanations for the observed behavior of the samples measured. The first is that the samples were partially decomposed. The blue color could remain in a partially decomposed sample, since the trapped electron has a high extinction

coefficient ($\sim 2 \cdot 10^4 \ \text{M}^{-1} \ \text{cm}^{-1}$). This explanation seems likely for the sample which showed the same magnetic behavior when decomposed. It is more difficult to make these samples than to make ESR samples. The susceptibility sample requires much more mass in the final solid than for ESR. This in turn requires larger solvent volumes and longer evaporation times. During preparation, the sample is most likely to decompose while in the solution stage, particularly during long evaporation. As detailed in the Experimental section, several long evaporations are necessary for these samples for susceptibility. ESR samples require fewer and shorter evaporations.

A second possible explanation is that the spins have spin paired in traps in the solid. A third possible explanation is that the electrons are delocalized into a conduction band. The susceptibility can be calculated using equation 18 of the free gas model if a Fermi temperature is given. In the free electron gas model the Fermi temperature depends only on the conduction electron density, which can be estimated from the known (67) density of $(Na^+C222)Na^-$. The calculated Fermi temperature is 5.56 \cdot 10³ K and the calculated paramagnetic susceptibility is $0.67 \cdot 10^{-4} \text{ cm}^3 \text{mole}^{-1}$. The semi-empirical diamagnetism for (K^+C222) is -1.93 \cdot 10⁻⁴ cm³mole⁻¹, giving a net susceptibility for metallic $(K^+C222)e^-$ of -1.3 \cdot 10⁻⁴ cm³mole⁻¹. This is just at the detection limit of the mutual inductance instrument.

IV.A.2.c. Solid from Cs-18C6 R=0.5 Solutions

This blue solid exhibited paramagnetism over the range 77 to 210 K. The molar susceptibilities measured at seven temperatures are tabulated in Table 5. These molar susceptibilities were corrected for the diamagnetism of Cs⁺ and two moles of 18-crown-6 to give the corrected molar susceptibility, $\chi_{\rm M}^{\rm corr}$, in the Table. The diamagnetic correction is semi-empirical, since the value measured in this work for $\chi_{\rm M}(18C6)$ of -1.6 · 10⁻⁴ cm³mole⁻¹ was used with Pascal's constant for Cs⁺.

The Curie-Weiss law is

$$\chi_{\mathbf{M}} = \frac{Np^2 \mu_{\mathbf{B}}^2}{3k(T-\theta)} = \frac{C}{(T-\theta)}$$
 (21)

where C is the Curie constant. A weighted nonlinear least-squares fit (by KINFIT) of the data to this equation gave a Curie constant of 0.0811 \pm 0.0122 cm³ deg mol⁻¹ and a Weiss constant (θ) of -33 \pm 21.5 K. Equation (21) may be rearranged to

$$1/\chi_{M} = (1/C)T - (\theta/C)$$
 (22)

Figure 29 shows the χ_M^{corr} and T data graphed in this form.

On the basis of the total number of cesium valence electrons present, the fraction present as paramagnetic centers is $(21.6 \pm 3)\%$, calculated from the Curie constant. Thus, a significant fraction of the cesium valence electrons is present in what appear to be localized traps. This is consistent with the optical spectrum (Figure 16) which shows a single band at 6500 cm⁻¹ (1540 nm), assigned

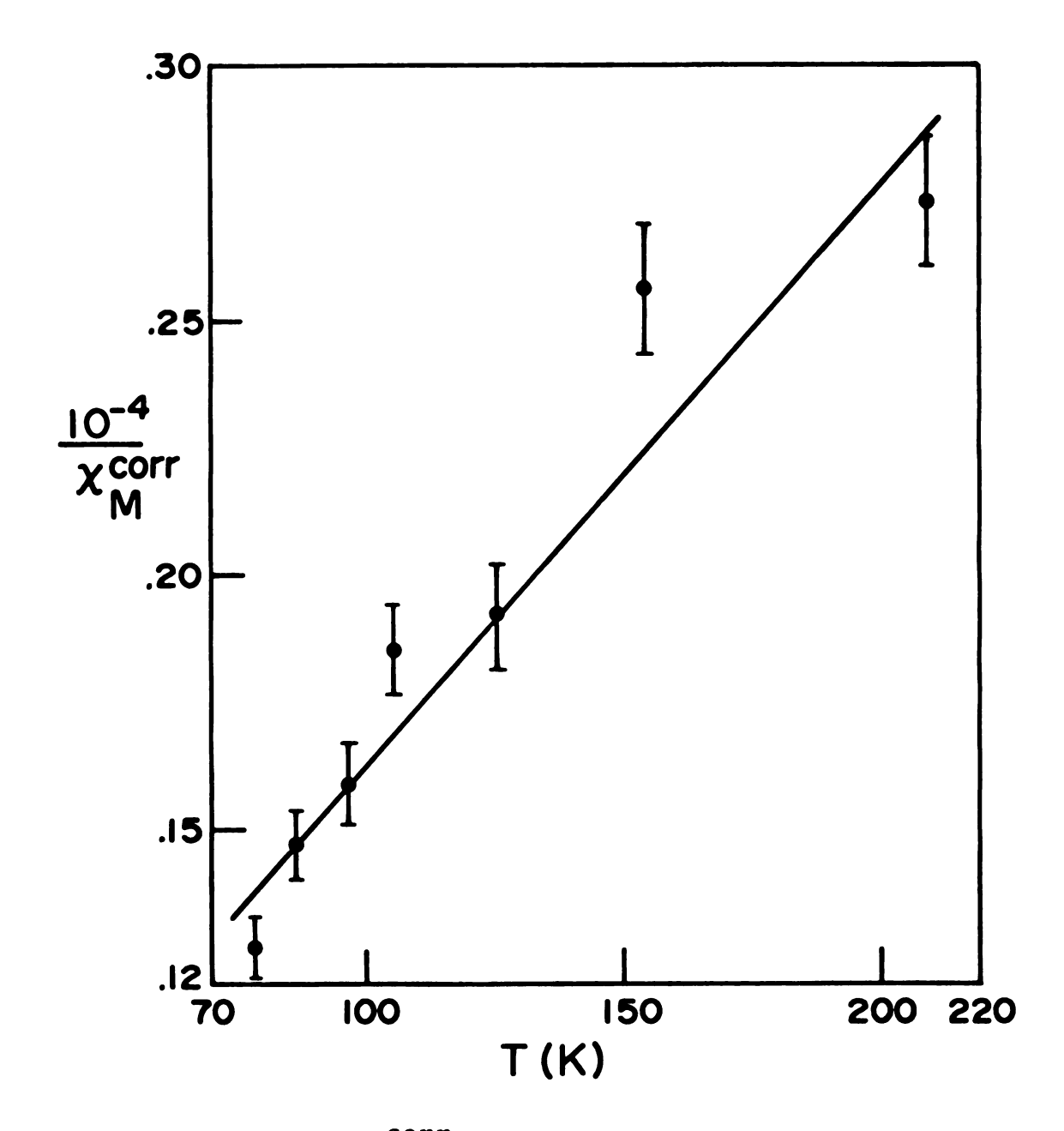


Figure 29. $1/\chi_M^{corr}$ vs. T for the residue from Cs-18C6 R=0.5 methylamine solutions.

Table 5. Temperature-dependent susceptibility of the residue from Cs-18C6 R=0.5 methylamine solutions

T(K)	χ _M · 10 ^{4(a)}	χ ^{corr} · 10 ^{4(b)}	10 ⁻⁴ /x _M corr
77.4	4.4	7.9	.127
86.5	3.3	6.8	.147
96.6	2.8	6.3	.159
106	1.9	5.4	.185
126	1.7	5.2	.192
155	0.4	3.9	.256
210	0.3	3.8	.263

Notes:

- (a) Calculated from raw χ_g data using equation (14), assuming M = 661 (the formula weight of Cs (18C6)₂).
- (b) χ_M^{corr} is χ_M corrected for diamagnetism of Cs⁺ and two moles of 18C6.

to the trapped electron. The spectrum shows no evidence of plasma absorption at 4000 cm^{-1} . The remaining electrons may be consumed by decomposition, spin paired, or present as precipitated metal.

IV.B. ESR

IV.B.1. Background

In the electron spin resonance (ESR) experiment, the degenerate spin energy levels are split into two levels by an applied magnetic field. Application of radiation to the sample in the field may cause transitions from the lower energy spin state to the higher energy state when the resonance condition, equation (23), is satisfied:

$$hv = g\mu_B H \tag{23}$$

where h is Planck's constant, ν is the radiation frequency, g is the g value (or factor), μ_B is the Bohr magneton, and H is the applied field strength.

Several points should be noted about the g value of equation (23). The g value has a characteristic value for different chemical systems, analogous to the chemical shift of NMR. It is a measure of the mixing of spin and orbital angular momentum for the electron giving the ESR signal. The free electron with spin angular momentum only has a g factor of 2.0023. The g value of equation (23) is a scalar for dilute solutions of low viscosity. In single crystals, the position of the absorption (and therefore the g value) often depends upon the relative

orientation of the crystal with respect to the field. The g factor is then a tensor. An anisotropic g factor is one in which not all g tensor diagonal elements are the same. Powders with anisotropic g values may exhibit a wide variety of ESR spectra depending on the degree of symmetry within the crystals, the extent of g anisotropy, and other factors. The general effect of g anisotropy for a powdered sample is the appearance of several spectral lines which may overlap.

The ESR experiment is almost always carried out at fixed frequency while the magnetic field is swept. A detection system is commonly used which generates a signal closely approximating the first derivative of the absorption spectrum. The positive and negative derivative spectra are both found in the literature. They are equivalent except in sign.

IV.B.2. Results and Discussion

IV.B.2.a. Solid from Cs-18C6 R=0.5 Solution

This solid from methylamine solutions containing two moles 18C6 for every mole of cesium gave a single line at $g = 2.0022 \pm 0.0001$. This signal is presumably not from cesium metal, which has a g value of 1.93 ± 0.02 (101). The linewidth at 214 K is 0.36 G and increases to 0.54 G for temperatures in the range from 106 to 181 K. After partial decomposition, the sample had a linewidth of 4.2 G at 112 K and 5.2 G at 4.4 K.

The g value of the free electron is 2.0023. The g value of the sample is within experimental error of this value, which indicates that there is little orbital angular momentum associated with the electron. Thus, the electron has little interaction with the cesium cation. The narrow linewidth is probably due to exchange among trapped electrons in the sample. This is consistent with the observed increase in linewidth when the solid had partially decomposed.

IV.B.2.b. Solids from K-C222 R=1 Solutions

The species formed when R=1 (nominal) solutions of K-C222 are evaporated are apparently sensitive to the metal to cryptand mole ratio, R. Two types of ESR behavior were observed from solids prepared from both methylamine and ammonia solutions which were prepared with R=1 (nominal). The first type of behavior was a single narrow ESR line at g = 2.0023, sometimes with a shoulder. The second type was a set of lines, usually three major lines, which appear only below 77 K. Samples deliberately made to be cryptand-rich (R=0.84) or metal-rich (R=1.37) exhibited the single line and multiple line behavior, respectively. Six samples were studied. Three showed the first type of behavior and the other three showed the second type of behavior.

Spectra varied slightly within these two types from sample to sample, as might be expected by different precipitation conditions. The first type of spectral behavior

will be described and discussed first. As an example of this behavior, the temperature-dependent spectra of a cryptand-rich (K⁺C222)e⁻ solid from ammonia is shown in Figures 30 and 31. In general, cryptand-rich samples above 200 K showed only a single line at the free electron g value. The linewidth varied from 0.4 to 0.6 G at liquid helium temperatures (4-5 K) and narrowed with increasing temperature to 0.1 to 0.4 G at 181 K.

It was of interest to see if the shoulder on the single line spectra was due to an anisotropic g value. Since single crystals of (K⁺C)e⁻ have not been isolated, this was tested by distilling potassium vapor onto a crystal of C222 at 77 K. The C222 crystal with deposited metal was warmed to 273 K to allow metal migration into the crystal. The blue crystal broke into three pieces of approximately equal size. The spectrum was taken at 4.2 K of the three crystals together. The signal of potassium metal was observed as well as that assigned to $(K^{\dagger}C)e^{-}$. The $(K^{\dagger}C)e^{-}$ signal exhibited a shoulder whose position changed substantially as the sample tube was rotated. Had the g value of (K⁺C)e⁻ been isotropic, this behavior would not have been observed. Thus, the g value is anisotropic in this system. This anisotropy may be present in (K⁺C)e⁻ solids prepared by evaporation and give rise to the observed shoulder.

Some cryptand-rich samples showed an asymmetric single line. The ratio of the low field lobe amplitude to the high field lobe amplitude is called the A/B ratio.

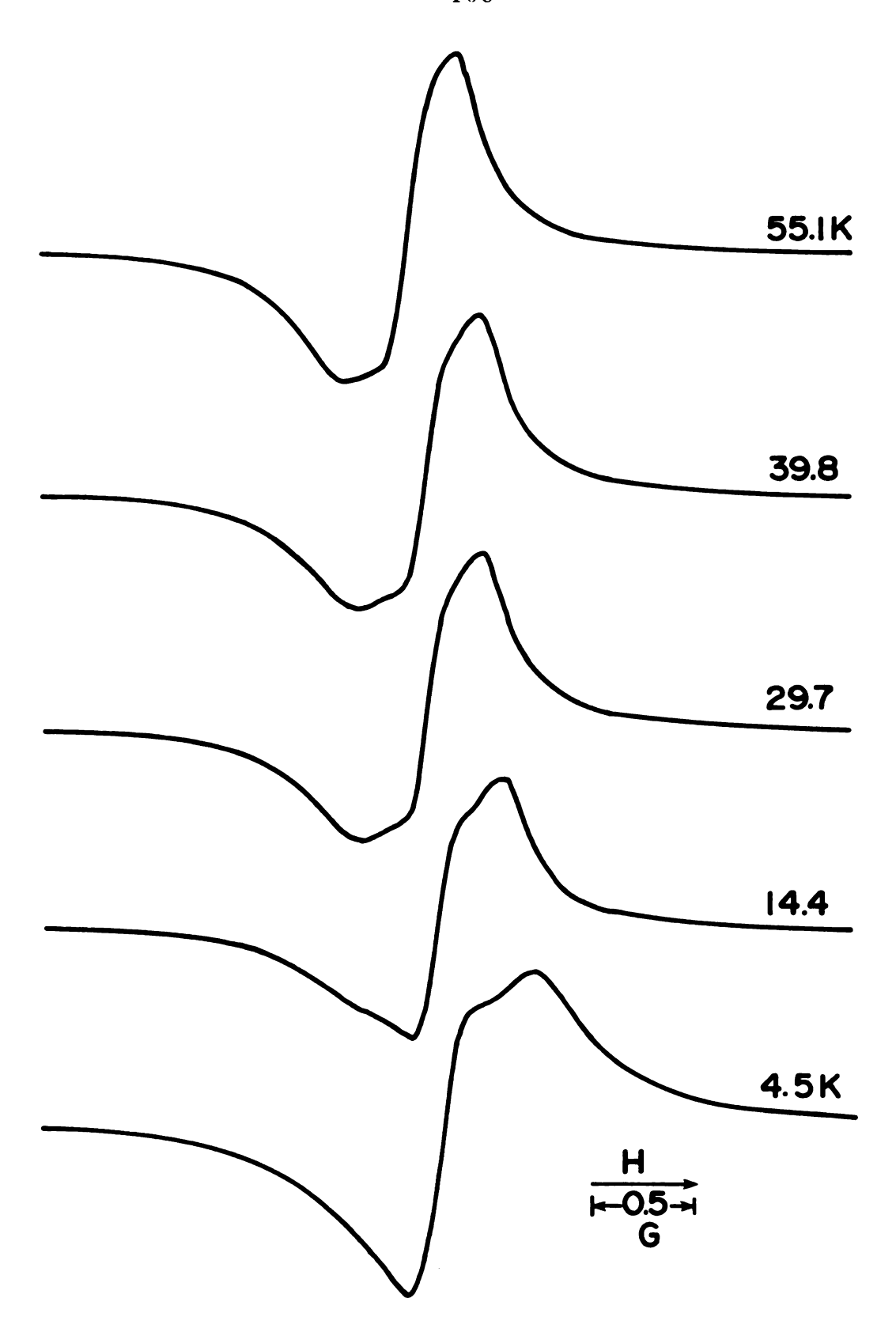


Figure 30. ESR spectra for cryptand-rich (K^+C222)e from 4.5 K to 55 K.

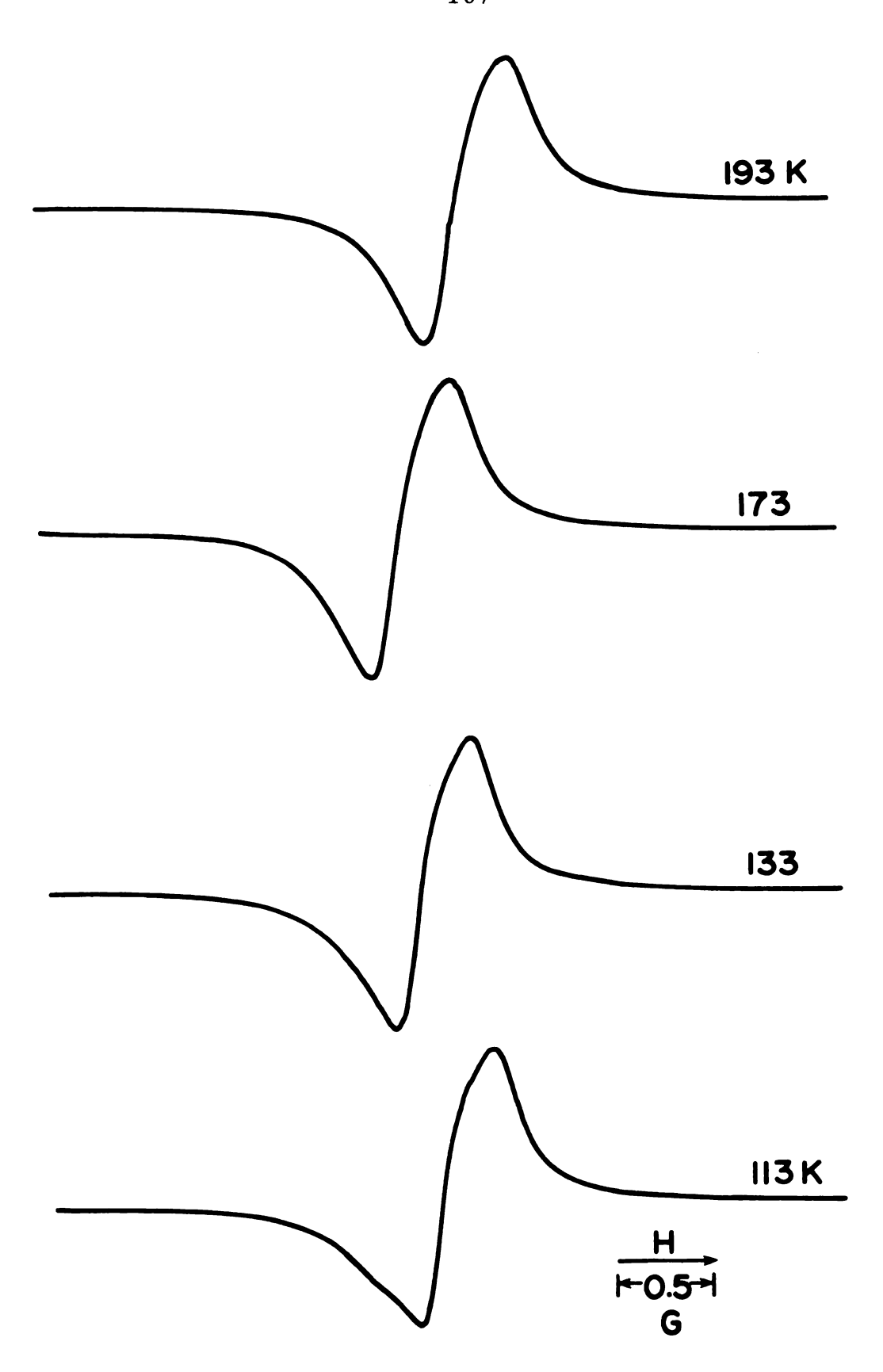


Figure 31. ESR spectra for cryptand-rich $(K^{+}C222)e^{-}$ from 113 to 193 K.

The highest A/B ratio observed was 1.4. This type of asymmetry is typical of the ESR of conduction electrons in metals. The theory of ESR line shapes for conduction electrons was worked out by Dyson (102) and confirmed experimentally by Feher and Kip (103). For Dysonian line shapes, the ESR line shape depends upon the particle size in the sample as compared to the depth to which the microwaves penetrate the sample. If the microwave radiation does not fully penetrate the sample, then the line shape may exhibit an A/B ratio from 1 to 20. Microwave conductivity (100) of a cryptand-rich (K⁺C)e⁻ sample indicates the solid is metallic, so the observed A/B ratio may be the result of ESR for conduction electrons. Another possible explanation is that the sample is metallic but with a particle size such that the particles are fully penetrated by microwaves. This case gives a line shape with A/B of 1. This line shape could be distorted by an anisotropic g value to give the observed asymmetric line.

An important ESR experiment was made on a cryptandrich (R=0.95) solid from an ammonia solution. The same solution was also used to form films for optical spectra. Before describing the ESR results, the optical results for this sample will be reviewed. The fresh film at -62° gave a spectrum of trapped electrons but with little K⁻ absorption or plasma absorption (at 4000 cm⁻¹). When the film annealed at -44°, it gave a spectrum similar to the plasma absorption of spectrum B of Figure 20. The ESR sample was probably annealed, since it had been at

temperatures higher than dry ice temperature (-78°). The ESR sample at 138, 157, 176, and 198 K showed the characteristic single line of other cryptand-rich samples. The ESR sample contained enough potassium to yield a maximum of 2.2 · 10¹⁸ spins if all spins were unpaired. The sample signal was compared to a numbered National Bureau of Standards ESR Intensity Standard (ruby) containing a certified number of spins. The sample signal at 157 K represented a quantity of unpaired electrons equal to only 2.4% of the potassium valence electrons present. If $(K^{\dagger}C)e^{-}$ is metallic, then only the fraction T/T_{F} of the valence electrons is unpaired and the measured fraction of 0.024 gives a Fermi temperature of 6.7 \cdot 10³ K. The Fermi temperature calculated earlier in this chapter from the estimated (K⁺C)e⁻ density (based on the known (Na⁺C)Na⁻ density of 1.064) and the free electron model is $5.6 \cdot 10^3$ K.

Another important result is that no signal from potassium metal was found. At the field used, the potassium metal signal should occur 37 G upfield from the free electron g value. The spectrum was scanned over a range which included 100 G on either side of the (K⁺C222)e⁻ signal, but a second signal was not found. Comparison of spectrometer conditions used for the ruby standard (while the sample was also in the cavity) and those used in searching for the potassium metal indicate that no more than 0.1% of the potassium present could have been present as potassium metal. The upper limit for potassium present

as nonmetallic potassium atom clusters is less than 0.1%, since presumably a fraction of electrons larger than T/T_F would contribute to the ESR signal of small clusters.

The second type of behavior, present in potassiumrich samples, is shown in Figures 32 and 33. The spectrum at 4.7 K consists of three lines and the narrow low field line is presumed to be most similar to (K⁺C)e⁻. In order to see whether the spectrum originates from three separate types of paramagnetic centers, this spectrum was fit to such a model by KINFIT. In all fits of the spectrum, three lines were assumed to be present. Line shapes used were Gaussian, Lorentzian, and a mixture of these two. The parameters of the fit were the width, amplitude, and location of each line. The Gaussian-Lorentzian line shape had a tenth parameter which was the percent Gaussian character. The Lorentzian and Gaussian fits were almost equally poor. The combination line shape fit was only slightly better. The observed and calculated (combination Gaussian-Lorentzian) line shapes are shown in Figure 34. The parameters for the 70% Gaussian fit are given in Table 6.

As the temperature is increased, the upfield lines gradually shift downfield and merge into one asymmetric line at 193 K. These spectra are reproducible in that they do not depend on past temperature cycling in the 4.7 to 193 K region studied. Thus, the observed spectra are not due to decomposition as the temperature is increased.

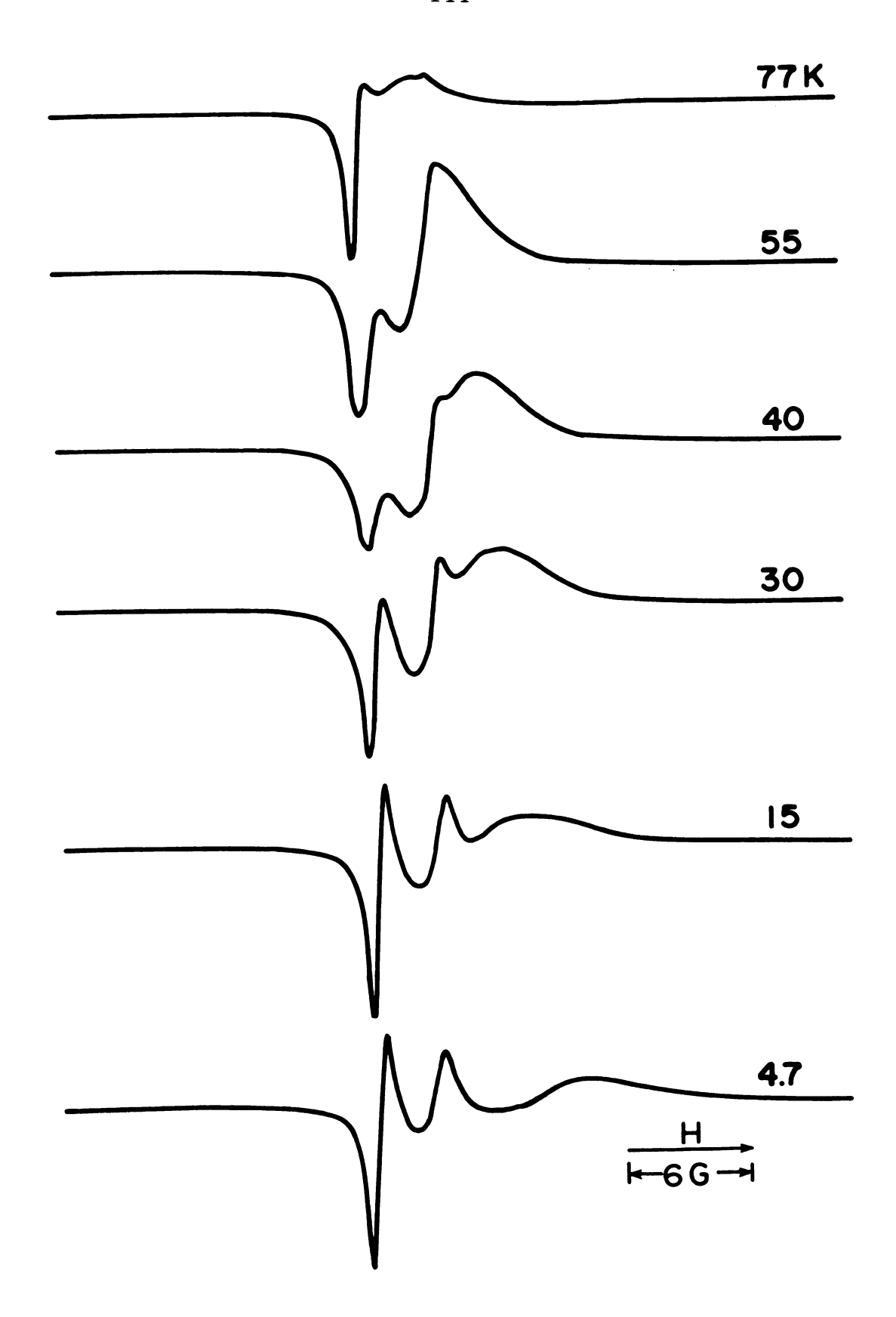


Figure 32. ESR spectra for potassium-rich $(K^{+}C222)e^{-}$ from 4.7 K to 77 K.

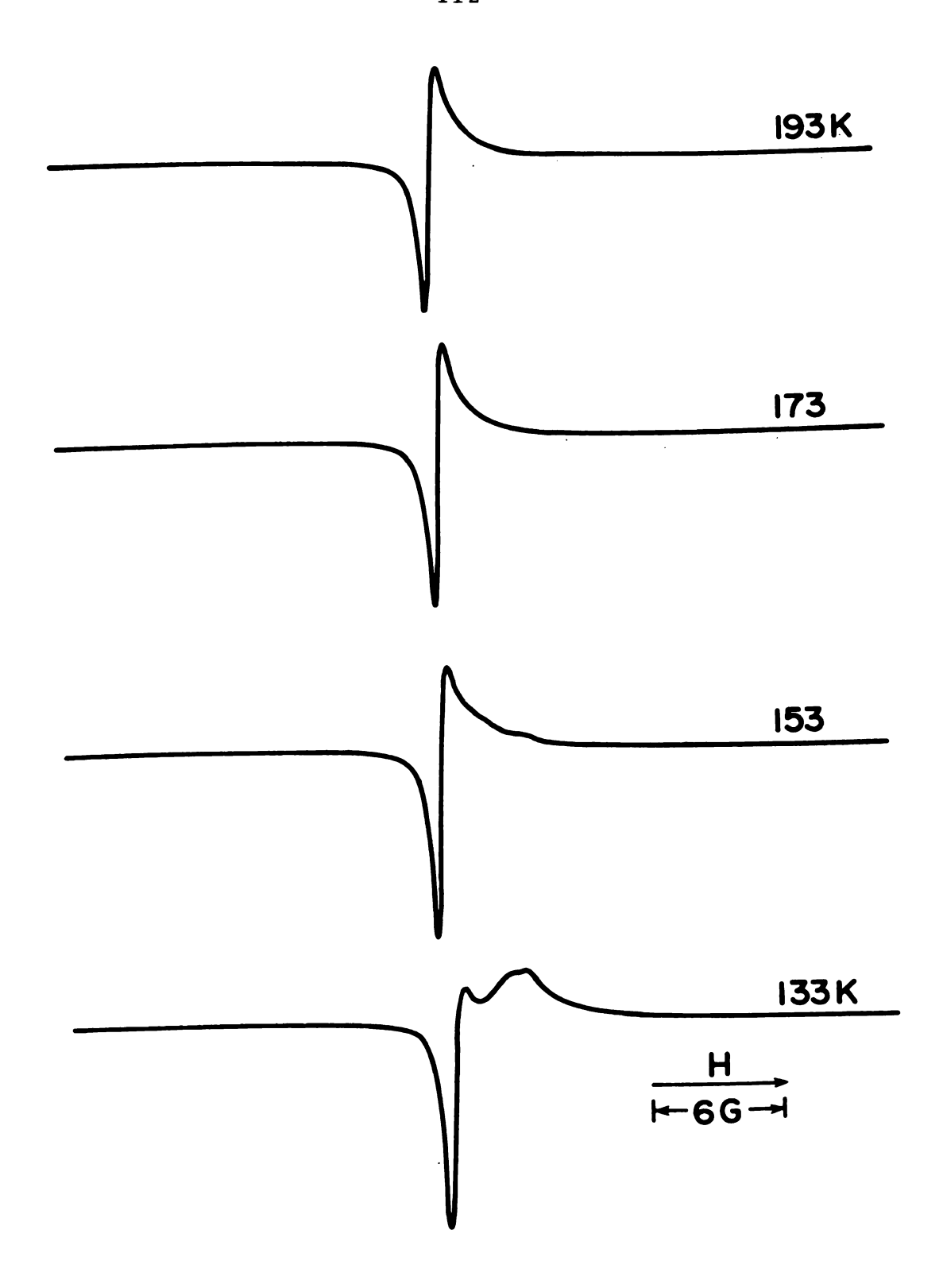


Figure 33. ESR spectra for potassium-rich (K⁺C222)e⁻ from 133 to 193 K.

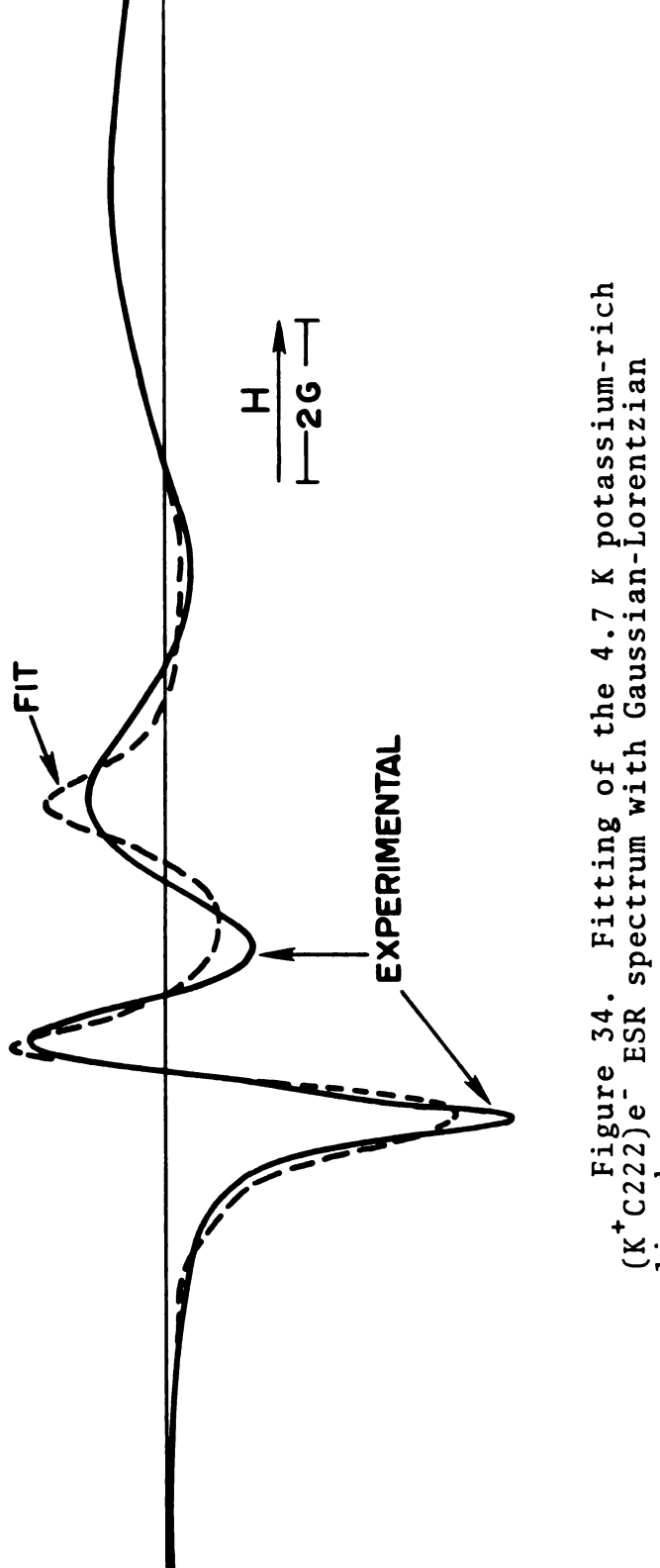


Figure 34. Fitting of the 4.7 K potassium-rich (K⁺C222)e⁻ ESR spectrum with Gaussian-Lorentzian lineshapes.

Table 6. Parameters in fitting of 4.7 K potassium-rich $(K^+C222)e^-$ ESR spectrum

	(Component		
	1	2	3	
amplitude ^a	3.07	1.43	0.60	
position ^b (G)	65.78	68.10	73.69	
width ^C (G)	1.02	2.43	6.17	

^aArbitrary units.

The above model was that of three species with isotropic g values. Another model is that there are two species present, one showing a powder pattern from an anisotropic g factor and the second having an isotropic g. However, each of the three samples which had this multiple line behavior exhibited a unique ESR pattern at liquid helium temperatures.

The optical spectra of these solids show shoulders on the main bands. These data along with the ESR spectra indicate that a number of species or sites for species exist. Such different kinds of sites could arise from heterogeneity in the solid resulting from differential precipitation during solid formation and from varying conditions for solid formation.

bMinus 3200 G.

 $^{^{}c}_{\Delta H_{pp}}$.

IV.B.2.c. Solid from Ba-C222 R=1 Solution

A dark-blue solid was obtained by evaporating an ammonia solution which presumably contained (Ba++C222) and 2 e_{solv}. A single ESR line with no fine structure at g = 2.0021 was observed at 4.2, 15, 40, 55, 77, and 128 K. The linewidths at the first five of these temperatures were 1.44, 1.4, 1.53, 1.66, and 2.1 G, respectively. The solid was probably partially decomposed, since the solution from which it was made was too unstable to obtain a film optical spectrum. (This instability probably arises from the impure barium (see Reagents) used to make the solution.) If the electrons are locally trapped and obey Curie's law, the area under the ESR absorption curve should be a linear function of 1/T. This linear dependence was found for the barium sample over the 4.2 to 77 K range, as shown in Figure 35. Thus, the $(Ba^{++}C222)(e^{-})_2$ could be metallic but, if it were partially decomposed, locally trapped electrons would be expected.

IV.C. Summary and Conclusions

At this point, it is appropriate to consider all evidence concerning the nature of the blue "electride" solids, particularly the Cs-18C6 R=0.5 and K-C222 R=1 solids. The cesium electride appears to consist of locally trapped electrons. The optical spectrum shows an absorption similar to other trapped electrons and no plasma absorption from delocalized electrons, the susceptibility indicates a substantial fraction of unpaired

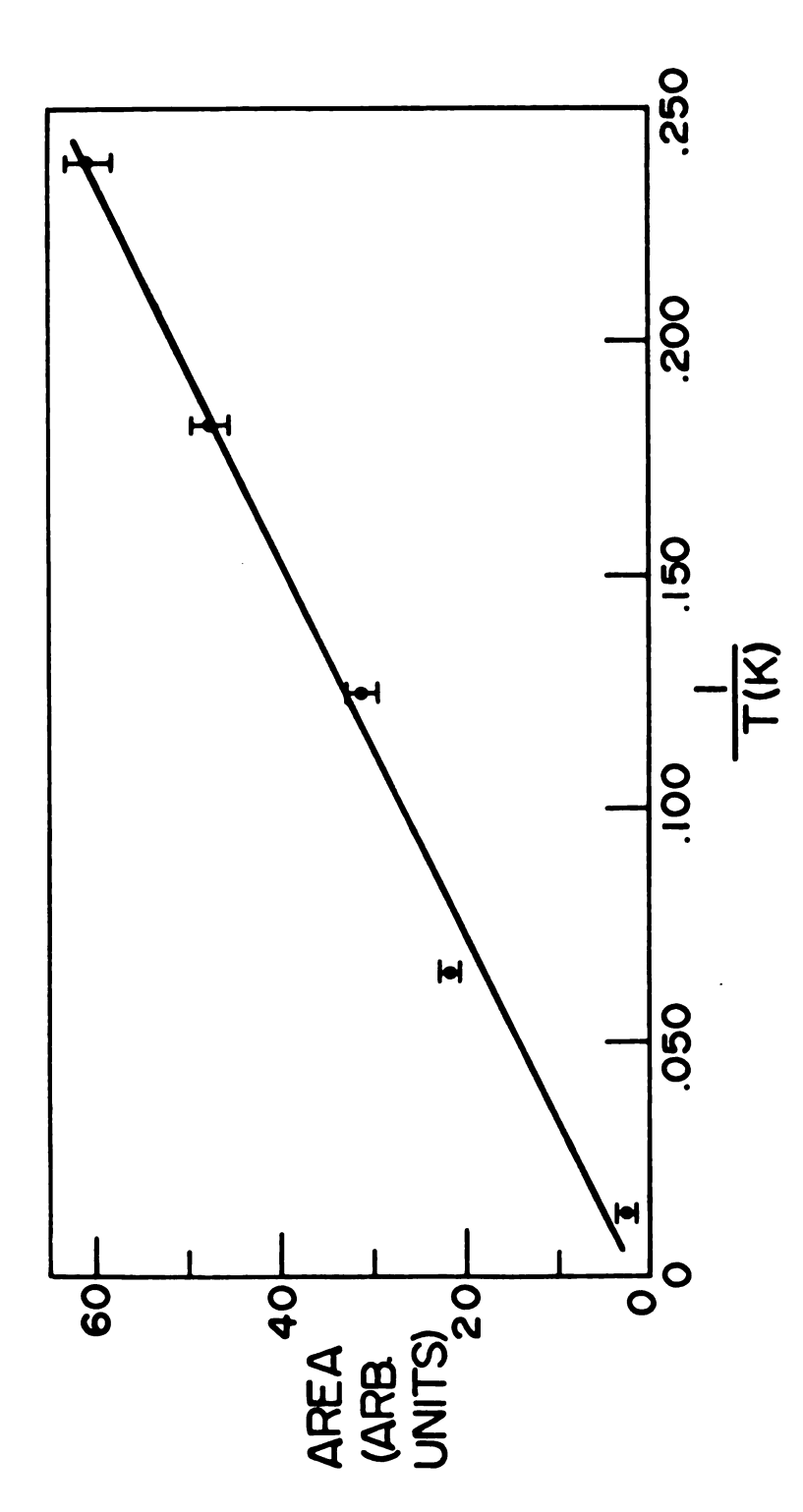


Figure 35. Area under the ESR absorption spectrum 1/T from 4.2 to 77 K for the solid from a Ba-C222 solution. vs. R=1

electrons, and the g value from ESR indicates little interaction of the electron with the cesium cation. The stability of this system is very good with respect to temperature and decomposition is not a major problem.

Several possibilities exist for the K-C222 system. The experimental evidence is strongest for the model of an electron balancing the charge on (K^+C222) . The data indicate further that this system may consist either of locally trapped electrons or delocalized electrons in an expanded metal and that the two systems may be interconverted. The evidence for locally trapped electrons in some $(K^+C222)e^-$ samples is the optical spectrum, which shows little or no absorption at 4000 cm⁻¹ (2500 nm).

The first evidence for metallic (K⁺C222)e⁻ was obtained in this work when the first ESR samples of (K⁺C222)e⁻ were placed in the spectrometer microwave cavity. It was impossible to tune the instrument when all the sample was in the cavity. Such behavior occurs when a sample with a high dielectric constant or a metallic character is placed in the cavity. Either type absorbs too much microwave power to allow cavity tuning. This problem was solved by placing only part of the sample in the cavity. In later experiments, smaller amounts of sample were used to overcome this problem. A second indication of metallic behavior was the absence of net paramagnetism expected for locally trapped electrons, although this could be interpreted as sample decomposition.

The optical spectra for K-C222 R=1 films exhibit a plasma edge very similar to the plasma edges which we observed for metallic metal-ammonia solutions. The microwave conductivity (100) also indicates metallic behavior, a result which could not have been found for a decomposed sample. Measurement of the number of spins found in the ESR experiment is also in agreement with assignment of metallic character to $(K^{\dagger}C222)e^{-}$.

One important question, especially in view of the microwave conductivity results, is the amount of potassium metal which might have been present in the (K⁺C222)e⁻ The ESR spectra of two separate samples showed no signal for potassium metal and, in one case, an upper limit of 0.1% potassium metal (potassium basis) could be established. An even smaller amount of potassium could have been detected if it were present as clusters. Another possibility which was considered is that potassium was present as dispersed atoms. However, sodium-ammonia or sodium-argon dispersions prepared at liquid helium temperatures do not exhibit metallic behavior until the concentration reaches 50 MPM (73). At higher concentrations, the valence electron wavefunction overlap is sufficient to give metallic behavior. The metallic behavior of (K⁺C222)e⁻ could not arise from potassium atom dispersions in cryptand because the potassium atoms would be too far apart for sufficient electron overlap. since cryptand is much larger than ammonia or argon.

The solid from Ba-C222 R=1 ammonia solution exhibited ESR behavior which indicates the presence of locally trapped electrons. However, it is likely that the one sample studied was partially decomposed.

THERMODYNAMIC STABILITY OF (Na + C222) Na - AT 273 K

A longstanding question has been whether (Na⁺C222)Na⁻ is thermodynamically or just kinetically stable. One experimental observation suggested that the compound is only kinetically stable. Crystals of the compound were stored in sealed tubes under vacuum at 243 K. After about one year of storage, the samples contained gray lumps which were presumably sodium metal. The samples with gray lumps could be dissolved to give stable blue solutions, which indicates that the lumps were probably not pieces of decomposed organic matter.

If the lumps were sodium metal, then the compound could have decomposed according to the reverse of reaction (24).

$$C222_{(s)} + 2Na_{(s)} \stackrel{?}{=} (Na^{+}C222)Na_{(s)}^{-}$$
 (24)

The compound is thermodynamically stable with respect to $C222_{(s)}$ and $Na_{(s)}$ if the free energy change for (24) is negative. The chemical potential of solid C222 must be greater than or equal to the chemical potential of the cryptand in solution (in the absence of supersaturation). Thus, the free energy change for equation (24) will be negative if the free energy change for equation (25) is negative.

$$C222_{(sol)} + 2Na_{(s)} \stackrel{?}{=} (Na^{+}C222)Na_{(s)}^{-}$$
 (25)

This equilibrium is the sum of the following two reactions:

$$C222_{(sol)} + 2Na_{(s)} \neq (Na^{+}C222)_{(sol)} + Na_{(sol)}^{-}$$
 (26)

$$(Na^{\dagger}C222)_{(sol)} + Na_{(sol)}^{-} \stackrel{?}{=} (Na^{\dagger}C222)Na_{(s)}^{-}$$
 (27)

Therefore, if a C222 solution over sodium metal isothermally gives crystals of $(Na^+C222)Na^-$, the compound is stable with respect to sodium metal and cryptand at that temperature. This spontaneous growth of $(Na^+C222)Na^-$ was observed in this work at 273 K.

Using the apparatus in Figure 8, an ethylamine solution of $0.04 \, \underline{\text{M}}$ C222 was stirred at 273 K over a sodium mirror which contained twice as many moles of sodium as there was C222 in solution. Before all the sodium had dissolved, many gold-colored (Na⁺C222)Na⁻ crystals formed in the blue solution.

This experiment proves that (Na⁺C222)Na⁻ is thermodynamically stable with respect to cryptand and sodium metal at 273 K. However, it is possible that the compound may slowly decompose, perhaps according to the following scheme:

$$(Na^{+}C222)(Na^{-})_{(s)} \rightarrow (Na^{+}C222)e_{(s)}^{-} + Na_{(s)}$$
Decomposition Products

(28)

This decomposition may be initiated by absorption of light. Several observations support the hypothesis that

the compound is photosensitive. A thin blue film of $(Na^{\dagger}C222)Na^{\dagger}$ was formed in a tube from a tetrahydrofuran solution of the crystals. The tube was stored at room temperature in a dark drawer and showed little decomposition over an eight week period. At the end of that period, the tube was exposed to ordinary fluorescent lighting of the room and the blue film bleached in 2 to 3 hours. During the photographing of some of the crystals at room temperature under light from a tungsten lamp, some of the gold-colored single crystals turned dark green irreversibly while others were unchanged.

CONCLUSIONS AND SUGGESTIONS FOR FUTURE WORK

VI.A. Conclusions

The species present in solids prepared by evaporating amine or ammonia solutions depend on the metal, cation-complexing agent, and solvent. Solids from methylamine contain species similar to those in solution. Solids from ammonia contain species which are not necessarily present in solution.

Several types of solids can be isolated. properties indicate the existence of three classes of compounds. The first class consists of salts of the alkali metal anions and is now well established. second class consists of electride salts, in which the balancing charge for the complexed cation is an electron which is locally trapped. While definitive proof of this assignment is not yet available, it is consistent with all measurements to date. The third class appears to consist of an expanded metal in which the cation is (K⁺C222). Mixtures of these three classes also appear to exist. The electride salt and expanded metal can occur together and, in some cases, appear interconvertible. Electrides and the corresponding expanded metals were first studied in detail in this work. If the assignments

are verified, these expanded metals represent new examples in that class of materials and electrides represent a new class of compounds.

The compound (Na⁺C222)Na⁻ is thermodynamically stable at 273 K with respect to sodium metal and solid cryptand.

VI.B. Suggestions for Future Work

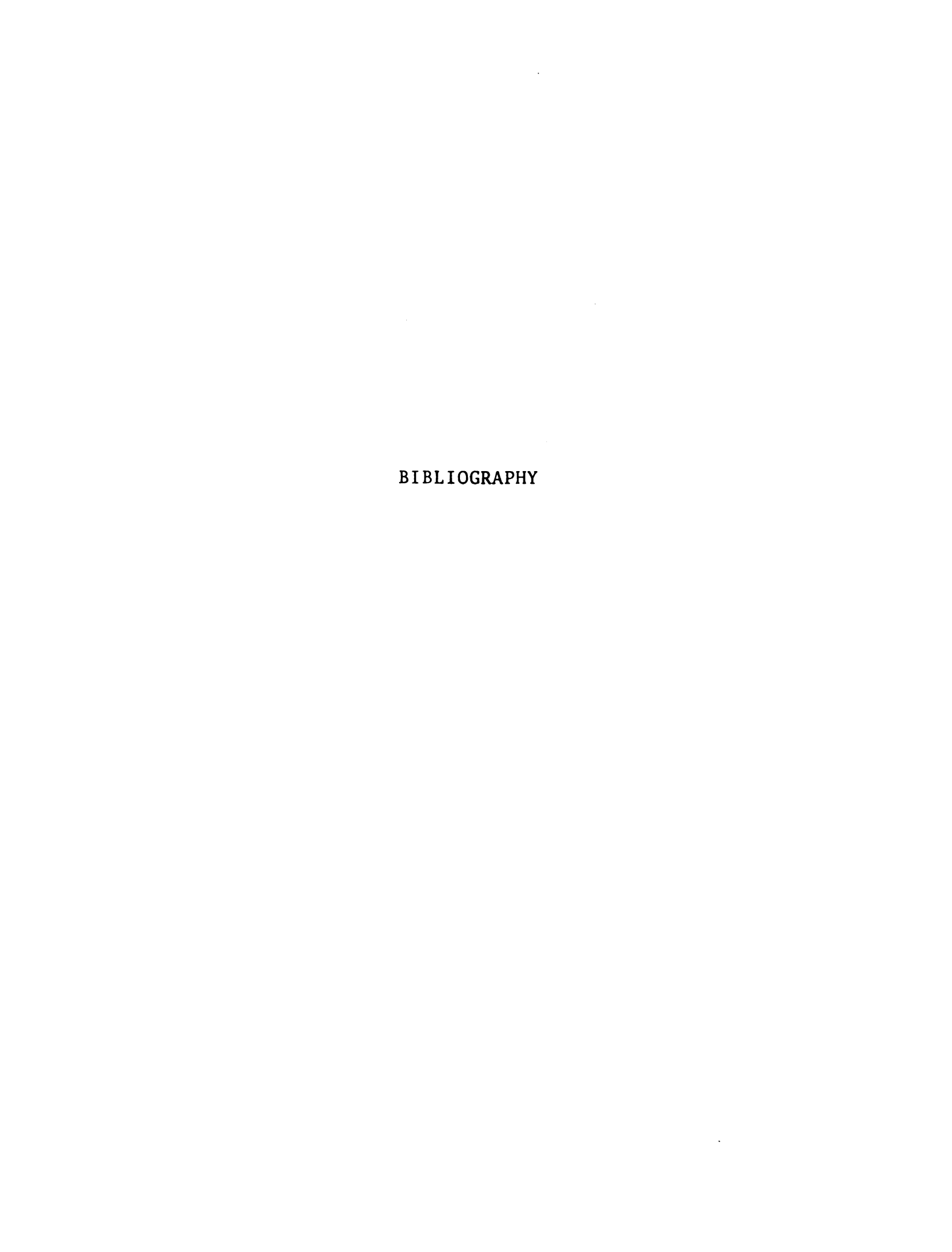
1) To date, no heteronuclear alkalide salts have been characterized conclusively. A good candidate is the compound $(Ba^{++}C222)(Na^{-})_2$. The complexation constant of barium in C222 is much larger than for sodium or potassium. The results of this work show that Na^{-} can be formed in a solid by evaporation of an ammonia solution. The synthesis would consist of reacting an ammonia solution of $(Ba^{++}C222)$ and $2e^{-}_{solv}$ as

$$(Ba^{++}C222) + 2e_{solv}^{-} + 2Na \rightarrow (Ba^{++}C222)(Na^{-})_{2}.$$

The ammonia could be evaporated quickly and at low temperatures, both of which would contribute to minimizing decomposition.

Additional samples should have characterizations made on the same sample. Single crystals for studies such as x-ray structure and conductivity would be extremely useful. Other electride systems remain to be more fully characterized, such as (Li⁺C211)e⁻ and systems similar to (Ba⁺⁺C222)(e⁻)₂ which have lanthanide cations inside the cryptand.

- 3) The negative Weiss constant for the Cs-18C6 R=0.5 electride suggests that the system may order antiferromagnetically or ferrimagnetically at low temperatures (104).
- 4) The optical spectrum of Na-C221 could be done, and this combination is an excellent choice for alkalide salts using a cryptand other than C222. Another attractive system is Cs-C322.



BIBLIOGRAPHY

- 1. W. Weyl, Ann. Phys. 197, 601 (1863).
- 2. G. Lepoutre and M. J. Sienko (eds.), "Metal-Ammonia Solutions, Colloque Weyl I", W. A. Benjamin (New York) 1964.
- 3. J. J. Lagowski and M. J. Sienko (eds.), "Metal-Ammonia Solutions", Butterworths (London) 1970.
- 4. J. Jortner and N. R. Kestner (eds.), "Electrons in Fluids", Springer-Verlag (New York) 1973.
- 5. J. Phys. Chem. 79 (26) 1975.
- 6. J. Phys. Chem., in press.
- 7. G. Lepoutre and J. P. Lelieur, ref. 3, p. 247.
- 8. R. A. Ogg, J. Am. Chem. Soc. 68, 155 (1946).
- 9. J. Jortner, J. Chem. Phys. 30, 829 (1959).
- 10. G. A. Kenney-Wallace, Acc. Chem. Res. 11, 433 (1978).
- 11. J. L. Dye, ref. 3, p. 1.
- 12. M. Gold, W. L. Jolly, and K. S. Pitzer, J. Am. Chem. Soc. 84, 2264 (1962).
- 13. J. V. Acrivos and K. S. Pitzer, J. Phys. Chem. <u>66</u>, 1693 (1962).
- 14. J. P. Lelieur, P. Damay, and G. Lepoutre, ref. 5, p. 2879.
- 15. E. Huster, Ann. Phys. 33, 477 (1938).
- 16. S. Freed and N. Sugarman, J. Chem. Phys. <u>11</u>, 354 (1943).
- 17. C. A. Hutchison, Jr., and R. C. Pastor, Rev. Mod. Phys. 25, 285 (1953); J. Chem. Phys. 21, 7959 (1953).

- 18. A. Demortier and G. Lepoutre, C. R. Acad. Sci. Paris 268, 453 (1969).
- 19. A. Demortier, M. DeBacker, and G. Lepoutre, J. Chim. Phys. 69, 380 (1972).
- 20. R. R. Dewald and J. L. Dye, J. Phys. Chem. <u>68</u>, 121 (1964).
- 21. I. Hurley, T. R. Tuttle, Jr., and S. Golden, J. Chem. Phys. 48, 2818 (1968).
- 22. S. Matalon, S. Golden, and M. Ottolenghi, J. Phys. Chem. 73, 3098 (1969).
- G. W. A. Fowles, W. R. McGregor, and M. C. R. Symons,
 J. Chem. Soc., 3329 (1957).
- 24. M. C. R. Symons, J. Chem. Phys. <u>30</u>, 1628 (1959); Quart. Rev. 13, 99 (1959).
- L. R. Dalton, J. D. Rynbrandt, E. M. Hansen, and J. L. Dye, J. Chem. Phys. 44, 3969 (1966).
- 26. M. G. DeBacker and J. L. Dye, J. Phys. Chem. 75, 3092 (1971).
- 27. J. L. Dye, M. G. DeBacker, J. A. Eyre, and L. M. Dorfman, J. Phys. Chem. 76, 839 (1972).
- 28. L. J. Gilling, J. G. Kloosterboer, R. P. H. Rettschnick, and J. D. W. van Voorst, *Chem. Phys. Lett.* 8, 457, 462 (1971).
- 29. G. Gabor and K. H. Bar-Eli, J. Phys. Chem. <u>75</u>, 286 (1971).
- 30. M. Fisher, G. Ramme, S. Claesson, and M. Swarc, Chem. Phys. Lett. 9, 309 (1971).
- 31. A. Gaathon and M. Ottolenghi, Israel J. Chem. 8, 165 (1970).
- 32. D. Huppert and K. H. Bar-Eli, J. Phys. Chem. 74, 3285 (1970).
- 33. S. H. Glarum and J. H. Marshall, J. Chem. Phys. <u>52</u>, 5555 (1970).
- 34. R. R. Dewald and J. L. Dye, J. Phys. Chem. 68, 128 (1964).
- 35. R. R. Dewald and K. W. Browall, J. Phys. Chem. 74, 129 (1970).

- 36. T. R. Tuttle, Jr., Chem. Phys. Lett. 20, 371 (1973).
- 37. K. D. Vos and J. L. Dye, J. Chem. Phys. 38, 2033 (1963).
- 38. K. Bar-Eli and T. R. Tuttle, Jr., J. Chem. Phys. 40, 2508 (1964).
- 39. V. A. Nicely and J. L. Dye, J. Chem. Phys. 53, 119 (1970).
- 40. L. R. Dalton, M. S. Thesis, Michigan State University, 1966.
- 41. B. Bockrath and L. M. Dorfman, J. Phys. Chem. 77, 1002 (1973).
- 42. J. W. Fletcher and W. A. Seddon, J. Phys. Chem. 79, 3055 (1975).
- 43. J. L. Dye, ref. 4, p. 77.
- 44. C. J. Pedersen, J. Am. Chem. Soc. 89, 2495 (1967).
- 45. C. J. Pedersen, J. Am. Chem. Soc. 89, 7017 (1967); 90, 3299 (1968).
- 46. B. Dietrich, J.-M. Lehn, and J.-P. Sauvage, Tetrahedron Lett., 2885, 2889 (1969).
- 47. E. Kauffmann, J.-M. Lehn, and J.-P. Sauvage, *Helv. Chim. Acta* 59, 1099 (1976).
- 48. G. W. Gokel and H. D. Durst, Synthesis, 168 (1976).
- 49. A. C. Knipe, J. Chem. Ed. 53, 618 (1976).
- 50. J.-M. Lehn, Pure Appl. Chem. 49, 857 (1977).
- 51. J.-M. Lehn, Acc. Chem. Res. 11, 49 (1978).
- 52. R. M. Izatt and J. J. Christensen (eds.), "Progress in Macrocyclic Chemistry", Vol. 1, Wiley-Interscience (New York) 1979.
- 53. J. L. Dye, M. G. DeBacker, and V. A. Nicely, J. Am. Chem. Soc. 92, 5226 (1970).
- 54. J. L. Dye, M.-T. Lok, F. J. Tehan, R. B. Coolen, N. Papadakis, J. M. Ceraso and M. G. DeBacker, Ber. Bunsenges. Phys. Chem. 75, 659 (1971).
- 55. J. Lacoste, F. Schué, S. Bywater, and B. Kaempf, J. Polym. Sci. Polym. Lett. Ed. 14, 201 (1976).

- 56. J. M. Ceraso and J. L. Dye, J. Chem. Phys. $\underline{61}$, 1585 (1974).
- 57. J. L. Dye, C. W. Andrews, and S. E. Matthews, J. *Phys. Chem.* 79, 3065 (1975).
- 58. M. S. Greenberg, R. L. Bodner, and A. I. Popov, J. Phys. Chem. 77, 2449 (1973).
- 59. M. Herlem and A. I. Popov, J. Am. Chem. Soc. <u>94</u>, 1431 (1972).
- 60. R. H. Erlich and A. I. Popov, J. Am. Chem. Soc. 93, 5620 (1971).
- 61. R. H. Erlich, E. Roach, and A. I. Popov, J. Am. Chem. Soc. 92, 4989 (1970).
- 62. J. M. Ceraso, Ph.D. Dissertation, Michigan State University, 1975.
- 63. J. L. Dye, J. M. Ceraso, M.-T. Lok, B. L. Barnett, and F. J. Tehan, J. Am. Chem. Soc. 96, 608 (1974).
- 64. F. J. Tehan, B. L. Barnett, and J. L. Dye, J. Am. Chem. Soc. 96, 7203 (1974).
- 65. The synthetic procedure and other aspects of alkali metal anion salts are patented: U.S. Pat. 4, 107, 180. Inventors are J. L. Dye, J. M. Ceraso, F. J. Tehan, and M.-T. Lok. Patent is assigned to U.S. Government.
- 66. M.-T. Lok, Ph.D. Dissertation, Michigan State University, 1973.
- 67. F. J. Tehan, Ph.D. Dissertation, Michigan State University, 1973.
- 68. J. L. Dye, C. W. Andrews, and S. E. Matthews, J. Phys. Chem. 79, 3065 (1975).
- 69. W. L. Jolly, "The Synthesis and Characterization of Air-Sensitive Compounds", Prentice Hall (Englewood Cliffs, New Jersey) 1970.
- 70. B. Dietrich, J.-M. Lehn, J. P. Sauvage, and J. Blanzat, Tetrahedron 29, 1629 (1973).
- 71. G. W. Gokel, D. J. Cram, C. L. Liotta, H. P. Harris, and F. L. Cook, J. Org. Chem. 39, 2445 (1974).
- 72. R. N. Green, Tetrahedron Lett., 1793 (1973).

- 73. N. A. McNeal and A. M. Goldman, *Phys. Rev. Lett.* 38, 445 (1977).
- 74. L. H. Feldman, R. R. Dewald, and J. L. Dye, Adv. Chem. Ser. 50, 163 (1965).
- 75. E. C. Ashby and R. D. Schwartz, *J. Chem. Ed.* 51, 65 (1974).
- 76. D. F. Shriver, "The Manipulation of Air-Sensitive Compounds", McGraw-Hill (New York) 1969, ch. 8.
- 77. R. C. Douthit, Ph.D. Thesis, Michigan State University, 1959.
- 78. L. N. Mulay, ch. 7 in A. Weissberger and B. W. Rossiter, "Physical Methods of Chemistry", Vol. I, John Wiley and Sons (New York) 1972.
- 79. D. A. Zatko and G. T. Davis, III, Rev. Sci. Instrum. 43, 818 (1972).
- 80. J. C. Thompson, "Electrons in Liquid Ammonia", Clarendon Press (Oxford) 1976.
- 81. T. A. Beckman and K. S. Pitzer, J. Phys. Chem. 65, 1527 (1961).
- 82. W. A. Seddon, J. W. Fletcher, and R. Catterall, Can. J. Chem. <u>55</u>, 2017 (1977).
- 83. W. A. Seddon, J. W. Fletcher, F. C. Sopchyshyn, and R. Catterall, Can. J. Chem. <u>55</u>, 3356 (1977).
- 84. Two probe, packed powder conductivity study by M. R. Yemen, unpublished results.
- 85. H. Aulich, L. Nemac, and P. Delahay, J. Chem. Phys. 61, 4235 (1974).
- 86. T. A. Patterson, H. Hotop, A. Kasdan, D. W. Norcross, and W. C. Lineberger, *Phys. Rev. Lett.* 32, 189 (1974).
- 87. E. Mei, A. I. Popov, and J. L. Dye, J. Am. Chem. Soc. 99, 6532 (1977).
- 88. J.-M. Lehn and J. P. Sauvage, J. Am. Chem. Soc. <u>97</u>, 6700 (1975).
- 89. M. F. Fox and E. Hayon, J. Chem. Soc., Faraday Trans. I, 72, 1990 (1976).
- 90. R. Payan, Ann. Phys. (Paris) 4, 543 (1969).

- 91. M. H. Cohen, J. Jortner, and J. C. Thompson, J. Chem. Phys. 63, 3741 (1975).
- 92. D. Moras and R. Weiss, Acta Crystallogr. Sect. B 29, 396 (1973).
- 93. H. J. Hesse, W. Fuhs, G. Weiser, and L. Von Szentpaly, Chem. Phys. Lett. 41, 104 (1976).
- 94. T. Shida, S. Iwata, and T. Watanabe, J. Phys. Chem. <u>76</u>, 3683 (1972).
- 95. J. J. Markham, "F-Centers in Alkali Halides", Academic Press (New York) 1966.
- 96. J. E. Willard, J. Phys. Chem. 79, 2966 (1975).
- 97. I. M. Kolthoff, Anal. Chem. 51, 1R (1979).
- 98. J. L. Dye, M. R. Yemen, M. G. DaGue, and J.-M. Lehn, J. Chem. Phys. 68, 1665 (1978).
- 99. J. L. Dye, M. G. DaGue, M. R. Yemen, J. S. Landers, and H. L. Lewis, ref. 6, in press.
- 100. M. G. DaGue, J. S. Landers, H. L. Lewis, and J. L. Dye, Chem. Phys. Lett., in press.
- 101. R. A. Levy, Phys. Rev. 102, 31 (1956).
- 102. F. J. Dyson, Phys. Rev. <u>98</u>, 349 (1955).
- 103. G. Feher and A. F. Kip, Phys. Rev. 98, 337 (1955).
- 104. E. A. Bourdreaux and L. N. Mulay (eds.), "Theory and Application of Molecular Paramagnetism", John Wiley (New York) 1976.